Late Quaternary environment of Central Yakutia (NE' Siberia): Signals in frozen ground and terrestrial sediments

Spätquartäre Umweltentwicklung in Zentral-Jakutien (NO-Sibirien): Hinweise aus Permafrost und terrestrischen Sedimentarchiven

---

Steffen Popp

Steffen Popp
Alfred-Wegener-Institut für Polar- und Meeresforschung
Forschungsstelle Potsdam
Telegrafenberg A43
D-14473 Potsdam

Diese Arbeit ist die leicht veränderte Fassung einer Dissertation, die im März 2006 dem Fachbereich Geowissenschaften der Universität Potsdam vorgelegt wurde.

Contents

Abstract

Central Yakutia represents one of earth's most continental climate regions with severe winters and temperate summers in a periglacial setting with widespread and thick permafrost. During the late Quaternary, the landscape along the western margin of the Verkhoyansk Mountains was sculptured by repeated glaciations, fluvial activity and periglacial processes. So far, the chronology of the glaciations and environmental changes are poorly understood. In the scope of a joint Russian-German cooperation, field work was conducted on selected sites across Central Yakutia in order to collect new data on palaeoenvironmental change. The research strategy followed a multidisciplinary approach, comprising the evaluation of remote-sensing data and luminescence dating (RWTH Aachen, Germany), palaeopedological analysis (Bayreuth University, Germany), as well as sedimentological, geocryological, limnogeological studies and pollen analysis (AWI Potsdam, Germany; Melnikov Permafrost Institute and Yakutsk State University, Yakutsk, Russia). This thesis concentrates on three different aspects of environmental change:

Ice-rich permafrost deposits and their isotopic composition were studied at four sites in the western Verkhoyansk foreland. The isotopic composition of ice wedges generally reflects the palaeoclimatic winter conditions. During the late Pleistocene, ice wedges formed under stable severe conditions at around 41 ka, 20 ka to 13 ka ^{14}C BP. The climatic favourable early to mid-Holocene is isotopically reflected between 8.5 and 4.5 ka ^{14}C BP. Towards the late Holocene and sub-recent times, a climatic deterioration is recorded, shown by lighter isotopic composition of ice wedges, which developed between 1.2 ka and 0.7 ka ^{14}C BP.

Provenance analysis of late Quaternary deposits were conducted on tributaries of the Aldan and Lena Rivers in Central Yakutia. Cluster analysis revealed distinct heavy-mineral assemblages that serve as the basis for palaeoenvironmental studies. Thus, relatively high proportions of amphibole, orthopyroxene and garnet as well as pedogenic clay minerals point to sediment provenance from the wide catchment area of the Lena and Aldan Rivers. In contrast, the three other clusters are dominated by stable heavy minerals with varying amounts of clinopyroxene, apatite and garnet as well as high percentages of illite and chlorite that are indicative of source rocks of the Verkhoyansk Mountain area. Basically, morainic deposits reveal the local mountain source signal that is overprinted by the Lena-Aldan signal in the oldest moraines by reworking processes. Alluvial sediments in the Verkhoyansk foreland show a clear Lena source signal in the middle Pleistocene, related to a stream course closer to the mountains during those times. Loess-like cover sediments are characterised by dominant Lena provenance with increasing proportions of local sediments from nearby mountain sources towards the mountain valleys. Aeolian sands in an alluvial terrace section at the mountain margin, covering the time between 30 ka and 10 ka BP, reflect temporarily dominant inputs of aeolian materials from the Lena plains.

A new high-resolution lake status record of Lake Satagay from Central Yakutia reflects climate-driven hydrological changes in a typical thermokarst lake environment. The sedimentary lake record spans the last 7500 years of the mid- to late Holocene. The downcore variability in the composition of organic matter and the assemblages of fossil

bioindicators give evidence of climate-driven and interrelated changes in biological productivity, lacustrine trophic states, and lake-level fluctuations. The lake status record reveals a long-term trend towards lake-level lowering in the course of climate deterioration after 4.2 cal. ka BP and progressive sediment infill. This long-term trend is overprinted by short-term fluctuations at centennial time scales with high lake levels and decreased biological productivity during cool climate spells with reduced evaporation, as also observed in modern thermokarst lakes of Central Yakutia. The short-term climate spells are related to sun-spot variations and are coherent with a 350-yr cycle of solar activity, which represents a multiple of the prominent 88-yr Gleissberg solar cycle. The short-term cycles were most pronounced during the mid-Holocene climate transition between 6.5 and 4.2 cal. ka BP, following the regional climate optimum and heralding late Holocene climate deterioration. The Lake Satagay record shows that climate instability during the mid-Holocene climate transition is of global significance.

Zusammenfassung

Zentraljakutien gehört zu den kontinentalsten Regionen der Erde, charakterisiert durch sehr kalte Winter und kurze warme Sommer sowie der Existenz des tiefgründigen und kontinuierlichen Permafrostes. Während des Spätquartärs war die Region am westlichen Rand des Werchojansker Gebirges wiederholt von Gletschervorstößen, fluvialer Aktivität und periglazialen Prozessen beeinflusst. Jedoch ist sowohl die Chronologie der Gebirgsvergletscherungen als auch die Klima- und Landschaftsentwicklung dieser kaltkontinentalen Region nur wenig bekannt. Im Rahmen eines russisch-deutschen Verbundprojektes wurden an verschiedenen Stellen Zentraljakutiens Feldarbeiten durchgeführt, um neue Daten zur Paläoumwelt-Entwicklung zu sammeln. Das interdisziplinäre Methodenspektrum umfasste die Auswertung von Fernerkundungsdaten und Lumineszenzdatierungen (RWTH Aachen), bodenkundliche Untersuchungen (Universität Bayreuth) sowie sedimentologische, geokryologische und limnogeologische Untersuchungen und Pollenanalysen (AWI Potsdam, Melnikow Permafrost Institut Jakutsk, Staatliche Universität Jakutsk). Im Rahmen dieser Arbeit wird auf drei verschiedene Aspekte der Umweltentwicklung eingegangen:

An vier Lokalitäten im westlichen Gebirgsvorland wurde eisreicher Permafrost und die isotopische Zusammensetzung des Grundeises untersucht. Paläoklimatisch gesehen reflektiert die Zusammensetzung der stabilen Wasserisotope in Eiskeilen die herrschenden Winterbedingungen zur Zeit der Eiskeilbildung. Das Isotopensignal zeigt für das Spätpleistozän um 41 000 ^{14}C Jahre v.H. und zwischen 20 000 und 13 000 ^{14}C Jahren v.H. (^{14}C = Radiokarbonalter; v.H. = vor heute) sehr kalte und stabile Winter an. Das Früh- und Mittelholozän zwischen 8500 ^{14}C Jahren und 4500 ^{14}C Jahren v.H. ist anhand der Isotopenzusammensetzung als wärmerer Zeitabschnitt identifiziert worden. Im späten Holozän bis in historische Zeiten zwischen 1200 ^{14}C Jahren und 700 ^{14}C Jahren v.H. verschlechterten sich die Winterbedingungen wieder, ausgedrückt durch ein „kaltes“ Isotopensignal.

An spätquartären Sedimenten entlang zweier Nebenflüsse von Lena und Aldan wurden Herkunftsanalysen durchgeführt. Mit Hilfe der Clusteranalyse wurden bestimmte Schwermineralassoziationen identifiziert, welche die Basis für die Paläoumwelt-Rekonstruktion entlang des Gebirgsrandes in Zentraljakutien darstellen. Die relativ hohen Anteile von Amphibol (Hornblende), Orthopyroxen, Granat sowie quellfähigen Tonmineralen in einem Cluster können dem ausgedehnten Einzugsgebiet von Lena und Aldan zugeordnet werden. Im Gegensatz dazu spiegeln die anderen drei Cluster die Herkunftsregion des Werchojansker Gebirges wider, dominiert durch Zirkon, Turmalin, Klinopyroxen, Apatit und Granat sowie durch Illit und Chlorit. Die Moränenablagerungen sind grundsätzlich durch ein lokales Herkunftssignal der Gebirgsregion gekennzeichnet, welches in den älteren Moränen durch eingearbeitetes Sedimentmaterial aus dem Lena-Aldan Einzugsgebiet überprägt worden ist. Flussablagerungen im Gebirgsvorland zeigen ein klares Lena-Signal im Mittelpleistozän, das auf einen Flussverlauf östlich des heutigen Lenatals hinweist. Lössähnliche Deckschichten sind durch ein vorherrschendes Lena-Herkunftssignal charakterisiert, welches durch zunehmende Anteile lokaler Sedimentquellen in Richtung der Gebirgstäler modifiziert wird. Äolische Sande in einer spätweichselzeitlichen Flussterrasse (30 000 – 10 000 Jahre v.H.) am Gebirgsrand verweisen auf kurzzeitige verstärkte Winderosion und Verlagerung von Sedimentmaterial aus dem Lenaflusstal in Richtung Gebirge während des letzten globalen Hochglazials.

Ein hochauflösendes Sedimentarchiv aus dem Satagaj See in Zentraljakutien liefert Hinweise für klimatisch gesteuerte hydrologische Änderungen in einem typischen Thermokarstsee-System. Das Sedimentarchiv reicht bis 7500 Jahre ins Mittelholozän zurück. Die Variabilität in der Sedimentzusammensetzung und der Vergesellschaftung fossiler Bioindikatoren im Sedimentkern wird als Reaktion der biologischen Produktivität, des Nährstoffangebotes und des Seewasserspiegels auf klimatische Veränderungen interpretiert. Die Proxy-Daten zeigen einen Langzeittrend der allmählichen Wasserspiegelabsenkung und Verlandung des Sees im Zuge einer zunehmenden Klimaverschlechterung an, beginnend um 4200 Jahre v.H. (kalibrierte ^{14}C Jahre) an. Dieser Langzeittrend wird von kurzfristigen Seespiegelschwankungen in multiplen 100-Jahresrhytmen überprägt. Hohe Seespiegel sind an klimatisch kühlere Phasen mit geringerer biologischer Produktivität und geringerer Verdunstung gebunden und umgekehrt. Die kurzzeitigen Klimaschwankungen können mit Sonnenfleckenzyklen in Verbindung gebracht werden und zeigen eine Kohärenz mit einem 350-Jahreszyklus, welcher annähernd das Vierfache des bekannten solaren Gleißbergzyklus (88-Jahre) darstellt. Diese Zyklizität war besonders im Mittelholozän zwischen 6500 und 4200 Jahren v.H. ausgeprägt, also am Übergang vom postglazialen Klimaoptimum zur spätholozänen Klimaabkühlung. Das Sedimentarchiv des Satagaj Sees liefert einen Beitrag zur globalen Bedeutung der klimatischen Instabilität im Verlauf des mittelholozänen Klimaumschwungs.

List of Figures

List of Tables

Acknowledgements

The doctoral thesis was part of the research project “Jungquartäre Klima- und Landschafts- entwicklung im Werchojansker Gebirge und in der Zentraljakutischen Tiefebene”, funded by the Deutsche Forschungsgemeinschaft through grant Hu378/12-1 and -2.

I would like to express my sincere gratitude to my supervisors Prof. Dr. Hans-Wolfgang Hubberten and PD Dr. Bernhard Diekmann (AWI Potsdam) for their guidance, support and the opportunity to use the infrastructure of the institute. In particular during field work, I benefited from Bernhard’s broad knowledge of Quaternary geology and sedimentology and enjoyed his great repertoire of guitar music.

Many thanks go to the great partners of the project, Prof. Dr. Frank Lehmkuhl (RWTH Aachen) and Prof. Dr. Wolfgang Zech (University of Bayreuth) and to the other PhD student in the project, my colleague and friend Georg Stauch (RWTH Aachen). Despite the great distance between Aachen and Potsdam, the frequent phone-based discussions with Georg stimulated the clarification of some ambiguous field-work interpretations.

In Yakutsk, many Russian colleagues became good friends of mine and were involved in the preparation and successful conduction of field work and the time-consuming sample handling afterwards, namely Andrei Prokopiev and Innokenty “Kesha” Belolyubsky from the Diamond and Precious Metal Geology Institute, Igor

Syromyatnikov and Valentin Spektor from the Permafrost Institute, and Ludmilla Pestryakova from the Yakutsk State University. Thank you all!

For fruitful discussions, the friendly atmosphere, and many helping hands, I thank the experienced AWI scientists, Dr. Christine Siegert, Dr. Hanno Meyer, Dr. Lutz Schirrmeister, and Dr. Andrei Andreev. In particular, Christine was unresting in finding and translating Russian literature and to teach me the special secrets of periglacial research in general and Yakutian climate and permafrost in all details.

Special thanks go to the laboratory staff at AWI Potsdam for the instruction and support in analytical work, namely Ute Bastian, Antje Eulenburg, Martin Buchholz, Heiko Baschek, and Rita Fröhlking from AWI Bremerhaven. The following people gave me constructive advices and shared their special expertise to bring me forward to new ideas: Thomas Kumke in statistical data treatment, Wolf-Dieter Hermichen by his broad geoscientific knowledge, Dörthe Handorf helped me with statistical time-series analysis, and Helga Kemnitz (GFZ Potsdam) instructed me in REM analysis.

Beyond scientific matter, I want to acknowledge the administration and technical staff at AWI Potsdam. My special thank is dedicated to Sandy Schneider for her diligent way in handling library issues and to Gerald Müller for his careful preparation of field campaigns and diverting stories during coffee breaks. I thank all the AWI PhD students for the great time and atmosphere among the young researchers. I will never forget the nice outdoor “Dok Meetings” at the volleyball yard during summer time and the humorous conversations in the atmospheric pubs of Potsdam. With positive feelings, I remember Nadja Hultzsch, who shared the office with me and never refused to have some coffee and cookies with me, while we jointly suffered from our scientific difficulties and unpleasant private strokes.

Finally and most important, I want to acknowledge and honour my family and “girls” at home, my wife Jana and our daughter Finia. They both gave me great support by their patience and appreciation during the accomplishment of the thesis.

1. Introduction

The high latitudes of the northern hemisphere are sensitive regions to climatic change. Current changes in the global climate system contribute to the observed warming of the Arctic that is amplified by several positive feedbacks, including atmospheric variability causing surface-temperature anomalies, changes in ice and snow radiation (albedo effect), and permafrost degradation (e.g. Chapman and Walsh, 1993; Overpeck et al., 1997; Serreze et al., 2000; Moritz et al., 2002; Hinzman et al., 2005; Chapin III et al., 2005). Climatic changes in Arctic regions, in turn, influence the environment at lower latitudes by changes in freshwater runoff, affecting the global thermohaline circulation, and impacts on the atmospheric circulation pattern as well as carbon-dioxide and methane concentrations (e.g. Jones et al., 1998; McCabe et al., 2001; Peterson et al., 2002; ACIA, 2004). In order to estimate and predict responses and implications of the Eurasian Arctic environment to the current global warming, numerous palaeoclimatic studies were conducted in the Russian high latitudes in the scope of the QUEEN project (Quaternary Environment of the Eurasian North). Important outcomes of terrestrial research in the framework of QUEEN were the detailed reconstruction of the ice-sheet extent in northern Eurasian and related ice-dammed lakes in northern Eurasia (e.g. Svendsen et al., 2004; Mangerud et al., 2004), as well as the reconstruction of the late Pleistocene periglacial environment (e.g. Hubberten et al., 2004). Furthermore, related research dealt with detailed palaeoclimatic reconstructions using lake sediments and ice-rich permafrost sequences on Taymyr Peninsula (e.g. Hahne and Melles, 1999; Kienel et al., 1999; Siegert et al., 1999; Kienast et al., 2001; Andreev et al., 2002a, 2003), and on Bykowsky Peninsula, Laptev Sea coast (e.g. Andreev et al., 2002b; Meyer et al., 2002a; Schirrmeister et al., 2002; Siegert et al., 2002).

Since all terrestrial studies predominantly focussed on the coastal lowlands around the Arctic Ocean and on western Siberia, the late Quaternary environment of the hinterland across northeastern Siberia remains poorly understood. Central Yakutia represents the most continental region of the northern hemisphere in climatic terms and sets up the linkage between two different regions of intense palaeoclimatic research, the Lake Baikal and the Laptev Sea coast. The extended lowlands are drained by the Lena River and its tributaries (Fig. 2.1), which contribute significant quantities of freshwater and sediment to the Arctic Ocean (Alabyan et al., 1995). Environmental changes in the hinterland therefore have large influence on the freshwater discharge and sediment supply to the Arctic shelf regions. Periglacial processes, such as frost heaving, ice segregation, and the thawing of permafrost (thermokarst) largely contribute to sediment erosion, surface transport, and the hydrological regime. The stability of the permafrost environment, and thus also the intensity of periglacial processes, is closely related to the regional temperature and precipitation pattern (Gavrilova, 1993; Pavlov, 1994). Currently, the southern and central parts of Yakutia experience the strongest increase in air temperatures over northern Eurasia (Pavlov and Ananjeva, 2004). During the Pleistocene, the periglacial environment of Central Yakutia was affected by regional glaciations and fluvial activity. In particular, the western foreland of the Verkhoyansk Mountains is characterised by fluvial and glacial deposits, which partly

interfinger with each other. This interaction as well as the occurrence of varved sediments (Kind, 1975; Kolpakov, 1986) gave rise to the assumption of presumably ice-dammed rivers or pro-glacial lakes that rapidly discharged to the Laptev Sea. This supposition is based on an oxygen-isotope record of marine sediments revealing an outburst of large amounts of freshwater into the Laptev Sea at 13 ka BP (Spielhagen et al., 2005). However, the origin of the freshwater signal remains speculative owing to the lack of well-dated terrestrial records. Moreover, the previous reconstruction of Pleistocene glaciations, as documented in up to ten terminal-moraine stages (Kind et al., 1971; Kind, 1975; Kolpakov, 1979), is partly contradicted by new findings on the timing and extent of glaciations in northwestern Eurasia (e.g. Mangerud et al., 2002; Svendsen et al., 2004) and from Chukotka in the Russian Far East (e.g. Glushkova, 2001; Brigham-Grette et al., 2003). In addition, comprehensive palaeoclimatic data, as available for northern Yakutia with interdisciplinary approaches (e.g. Meyer et al., 2002a; Schirrmeister et al., 2002; Siegert et al., 2002), are sparse for the central Yakutian lowlands. Available studies mainly focus on single key localities, such as Mamontova Gora at the lower Aldan River banks (Fig. 2.1) (e.g. Markov, 1973; Baranova, 1979; Péwé et al., 1977; Péwé and Journaux, 1983). This section comprises Neogene and Pleistocene sediments with mammal fossils and large ice wedges, which provides information on the general trend of palaeoclimatic conditions. However, the major handicap of almost all previous studies, in particular of Russian reports, is the lack of definite age constraints or detailed palaeoclimatic implications.

In the view of these uncertainties, a joint Russian-German cooperation was initiated, dealing with the late Quaternary environment in the Verkhoyansk Mountains and the lowlands of Central Yakutia. The basic approach comprised multidisciplinary research, under the application of remote-sensing data and related geomorphological fieldwork as well as luminescence dating (RWTH Aachen, Germany), palaeopedological analysis (University of Bayreuth, Germany), as well as sedimentological, geocryological, limnogeological studies and pollen analysis (AWI Potsdam, Germany; Melnikov Permafrost Institute and Yakutsk State University, Yakutsk, Russia). The glaciation history of the Verkhoyansk Mountain range is dealt with in a PhD-thesis, in the scope of which first results are already presented (Stauch et al., 2005, in press).

The overall objective of this thesis is to gain new insights into the palaeoenvironment of Central Yakutia during the late Pleistocene and Holocene. Reconstructions were derived from various proxy records with different methodical approaches. Ground ice serves as a palaeoclimatic archive for winter conditions during the late Quaternary (e.g. Meyer et al., 2002a, 2002b). In addition, sediment samples of different facies and stratigraphic units were collected for provenance and palaeoenvironmental analyses. In contrast to these spatially extended studies, temporal high-resolution palaeoclimatic research was focussed on a sediment core retrieved from a thermokarst lake. The respective sections of this thesis represent independent but successive case studies that provide new results from a subarctic region with only few up-to-date palaeoclimatic data.

The thesis comprises the following objects:

- the use of the frozen ground as palaeoclimatic archive with respect to geocryological characteristics (ice textures and ice content) and massive ground ice,
- the reconstruction of relative winter conditions by analysing the stable-isotope composition (hydrogen and oxygen isotopes) of ice wedges,
- the utilisation of AMS radiocarbon age constraints for detailed palaeoclimatic implications,
- the provenance and distribution of different sediment units for palaeoenvironmental reconstructions, including the correlation of terminal-moraine stages, by means of heavy-mineral analysis and clay-mineral content,
- the reconstruction of Holocene climatic variations by high-resolution analysis of organic-rich lacustrine sediments based on carbon-content determination and its isotope ratio, as well as by means of bioindicators,
- the integration and comparison of the new findings into the context of the former knowledge of environmental change.

The thesis comprises three research articles that were designed for submission to international peer-reviewed journals. The first manuscript (Chapter 3) is published in *Permafrost and Periglacial Processes*, the second one (Chapter 4) is accepted for publication, while the last manuscript (Chapter 5) represents a final draft for submission. Owing to the article structure, overlapping sections and statements may occur within the thesis. In order to introduce the study area with its special characteristics, Chapter 2 (Climate and Regional Setting) was added to provide more detailed background information on geology, geomorphology, climate, and permafrost features. Chapter 3 discusses newly-obtained data on the isotopic composition of late Pleistocene and Holocene ice wedges in Central Yakutia, their age constraints, and the resulting palaeoclimatic implications. The findings of provenance analyses of late Pleistocene and recent sediments by means of heavy minerals and clay mineralogy are presented in Chapter 4. The third research article deals with organic-rich deposits of a thermokarst lake that provides a proxy record of climatic variability during the middle and late Holocene, as described in Chapter 5. A synthesis of the three research articles is given in Chapter 6, including the outline of the basic findings as well as an outlook for further palaeoenvironmental research in Central Yakutia.

2. Regional Setting and Climate

Approximately a quarter of the global surface and nearly two third of Russia are affected by perennially frozen ground (Ershov, 1995). The Sakha Republic (Yakutia), which stretches from the tundra lowlands along the coast of the Arctic Ocean to the northern foothills of the Stanovoy Mountains east of Lake Baikal, is completely underlain by continuous permafrost. The study area focuses on the central parts of Yakutia, along the middle and lower reaches of Lena River. The term 'Central Yakutia' is commonly referred to the central Yakutian lowland, stretching along the great rivers Lena, Aldan, and Vilyuy (Fig. 2.1). This lowland is characterised by relatively uniform geomorphological, hydrological and climatic parameters. With the exception of the Verkhoyansk Mountains and its foreland, the study area is situated within the limits of Central Yakutia, extending between 62° and 66°N and 122° and 135°E. Hence, the term 'Central Yakutia' will be used synonymous for the area under investigation. The latter encloses several relief elements, determined by the different geological units (Fig. 2.1). In the northeast of the study area, the western crests of the Verkhoyansk Mountains rise up to 2000 m above sea level. Adjacent to the mountains, the fluvioglacial accumulation plain (the Verkhoyansk Foreland) extends gently inclined to the Lena and Aldan valleys. Remains of both fluvial terraces and glacial deposits characterise the erosive-accumulated relief of the Verkhoyansk Foreland (Rusanov et al., 1967). The uppermost topographic level in the Verkhoyansk Foreland and in Central Yakutia is related to the Neogene denudation plain. The basement of the denudation plain is formed by Palaeozoic sedimentary rocks south of Yakutsk, changing into Mesozoic sedimentary rocks and Cenozoic sediments north of Yakutsk towards the Verkhoyansk Mountain range (Soloviev, 1973a). Incised into the denudation plain, Lena and Aldan Rivers and their tributaries have modelled different elevated terraces in Central Yakutia. These terraces are part of an alluvial plain, located between 400 m and 50 m above sea level in the study area. The terrace bodies are composed of varieties of Quaternary fluvial and covering loess-like sediments (e.g. Soloviev, 1973a; Péwé and Journaux, 1983). In the northwest, the study area is characterised by extending lowlands along the lower reaches of Vilyuy River.

2.1 Tectonic Setting and Geology

The territory of Yakutia extends across two major geotectonic provinces with diverse stratigraphic and lithological inventory: the Siberian Platform to the west and the Verkhoyansk-Kolyma Orogen to the east (Fig. 2.2). The Siberian Platform is a Precambrian craton of complex structure, extending from the Yenisei River in the west to the Lena and Aldan Rivers in the east. The Verkhoyansk-Kolyma Orogen resulted from the collision of the North Asia Craton with the Kolyma-Omolon Microcontinent along the eastern margin of the Siberian Platform in Mesozoic times (Oxman, 2003; Parfenov, 1991). The study area is situated on the suture of these two blocks, traced by the Lena and Aldan River valleys. The regional geology may be briefly described as follows, according to Parfenov (1991, 1997), Dolginow and Kropatschjow (1994), Chain and Koronovskii (1995), and Oxman (2003):

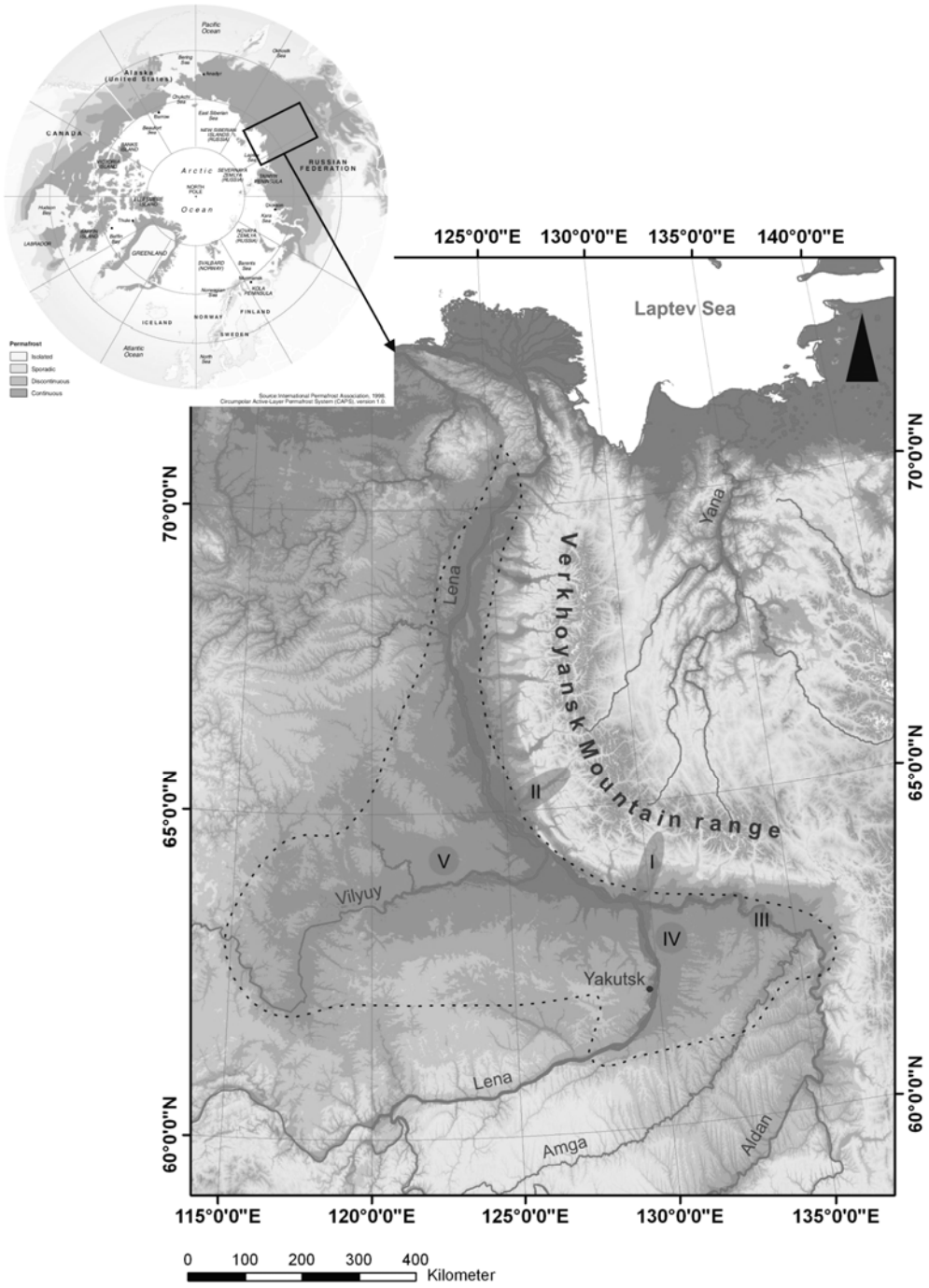

Fig. 2.1: Overview of the area under investigation with the respective studied sections indicated by the Roman numerals: I – Tumara River, II – Dyanushka River, III – Mamontova Gora, IV – Lake Syrdakh and Ulakhan Surdakh, V – Lake Satagay. The dotted line encloses the region referred to as Central Yakutia (according to the Atlas of Yakutia, 1981).

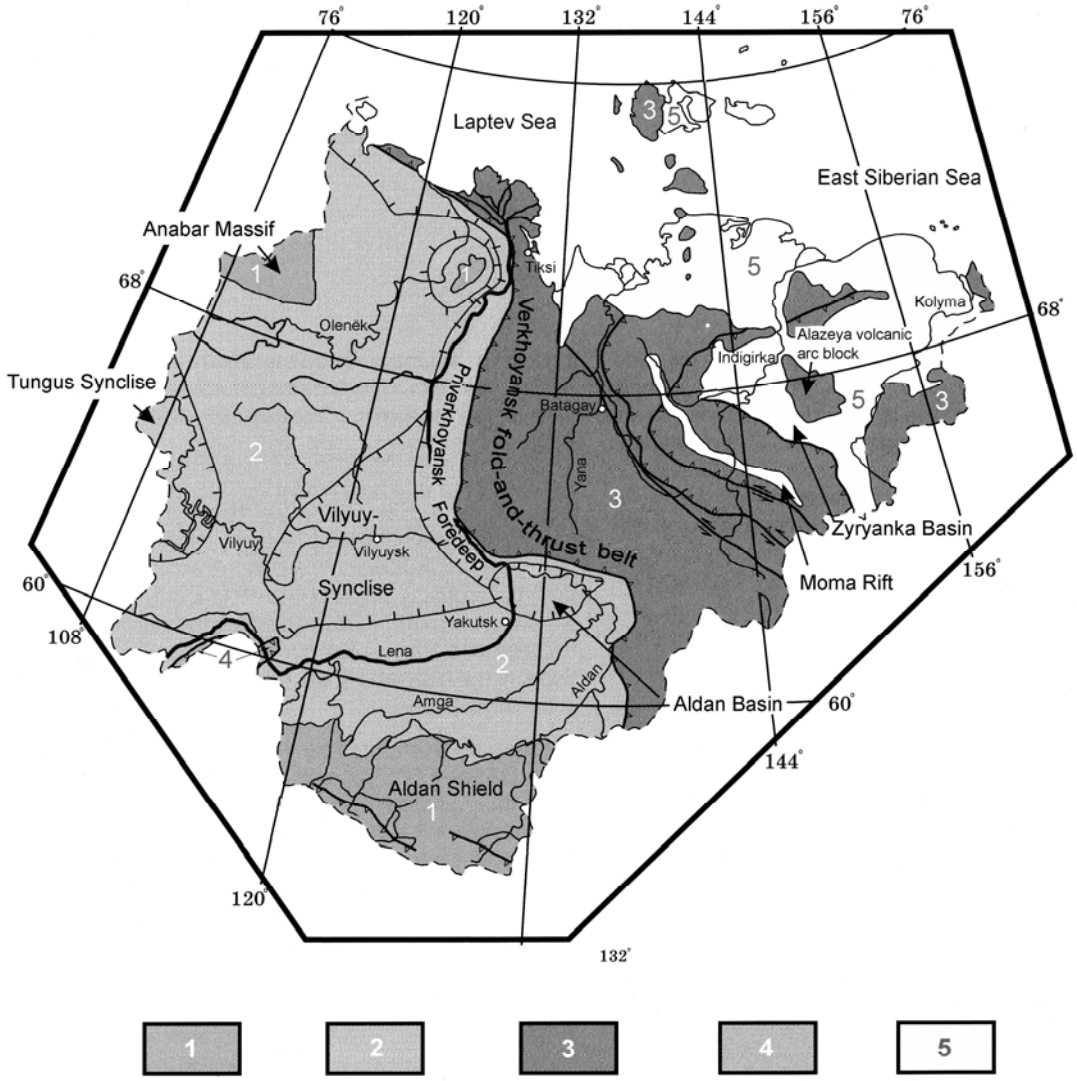

Fig. 2.2: Geotectonic map of Yakutia (after Parfenov, 1997): 1-basement rocks of the Siberian Platform, 2-sedimentary cover of the Siberian Platform, 3-Verkhoyansk-Kolyma orogenic region, 4-fragments of Palaeozoic Baikal-Patom fold-and-thrust belt, 5-main Cenozoic basins.

The Archaean and Palaeoproterozoic crystalline basement of the Siberian Platform is exposed south of the study area in the headwaters of the Lena and Aldan Rivers. By dipping to the north towards the Vilyuy River, the basement rocks become successive covered by carbonate and clastic series of Riphean to Cenozoic age. At the lower Vilyuy River, the sedimentary rocks reach a thickness of 10 km and more. To the east, the Verkhoyansk Mountains (the Verkhoyansk fold-and-thrust belt, Fig. 2.2) extend along of Lena and Aldan Rivers, which consist mainly of clastic sedimentary sequences of Riphean to Mesozoic age with inclusions of carbonates and volcanic rocks. Granitoid plutons in the central and eastern parts of the Verkhoyansk-Kolyma Orogen (Fig. 4.2) intruded during the tectonic deformation, which occurred in the late Jurassic and Cretaceous. Cenozoic sediments are widely distributed in the sedimentary basin of the lower Vilyuy River, to which the Priverkhoyansk Foredeep (the Verkhoyansk

Foreland), and the Aldan Basin at the lower reaches of Aldan River belongs (Fig. 2.2, 4.2). In particular, the Aldan Basin contains several hundred metres of sediment successions of Neogene to late Pleistocene age (e.g. Markov, 1973; Péwé et al., 1977; Baranova, 1979).

Quaternary sediments are widespread in the central Yakutian lowlands, comprising fluvial, glacial and loess-like deposits that almost completely cover the Cenozoic sediments. Numerous fluvial terraces have developed along Lena and Aldan Rivers and their tributaries during the Pleistocene (Alekseev, 1961; Rusanov et al., 1967; Soloviev, 1973a; Péwé and Journaux, 1983). In general, the following main terrace units were discriminated: Neogene to late Pleistocene aggradation-denudation plains (80 to 200 m above the modern Lena level), middle Pleistocene terrace complexes (40 to 80 m above the modern Lena level), and late Pleistocene to Holocene terrace complexes (15 to 25 m above the modern river levels). In the Verkhoyansk Foreland, fluvial-terrace sequences may contain reworked glacial material that originated from middle and late Pleistocene mountain glaciations. According to the Russian stratigraphy (Katasonov, 1963; Kind et al., 1971; Kind, 1975; Kolpakov, 1979), the greatest glacier advances reached far into the Lena valley, and were tentatively related to the Samorov Stage (Saalian, time equivalent to MIS 6) and the Zyryan Stage (Early Weichselian, time equivalent to MIS 4). The younger terminal moraines of the Zhigansk Stage (Middle Weichselian, time equivalent to late MIS 3) and Sartan Stage (Late Weichselian, time equivalent to MIS 2) were mostly placed within the mountains or at the mountain margins. New age constraints, however, report on very limited glaciations during the middle and late Weichselian (Stauch et al., 2005, in press). Loess-like sediments are widely distributed in variable thickness between 0.5 and 30 m, often modified by periglacial processes (Soloviev, 1973a; Péwé and Journaux, 1983).

2.2 Climate and Permafrost

The climatic situation of Central Yakutia is commonly described as highly continental. Continentality matters great seasonal contrasts, expressed by the mean January and July temperatures of -41 °C and +18°C, respectively, as well as by low annual precipitation of around 250 mm (Agriculture Atlas of the Republic Sakha (Yakutia), 1989). These severe seasonal conditions demonstrate the extreme climatic situation of Central Yakutia. Major factors leading to the extreme weather are the huge land mass of the Asian continent with its associated atmospheric circulation and the remoteness and inaccessibility of the region with respect to maritime humid air masses. With the exception of the northern access to the Arctic Ocean, whose influence is relative week due to its low surface temperatures, Central Yakutia is effectively debarred from the influx of maritime air masses by the surrounding mountains in the east and south.

During the winter, moisture advection by the Westerlies is prevented by a relatively steady high-pressure area (Siberian High), which is centred over northern Mongolia, deflecting humid air masses northwards. This, in turn, leads to increased radiation over the continent because of little cloudiness, promoting the establishment of the Siberian High (Franz, 1973). This situation gives rise to an extreme cooling of the lower strata of the atmosphere, which is accentuated further by temperature inversion in basin-like formations, such as the Yakutian Basin and intra-mountainous basins of Oymyakon and

Verkhoyansk. Along with the severe cold, very little precipitation occurs. Occasionally, cyclones from the Sea of Okhotsk reach Central Yakutia during the cold season, leading to temporary temperature rise and snowfall (Gavrilova and Atlasova, 1969; Cherdonova, 1993).

In summer, low-pressure areas are distributed over the continent due to the high insolation and the heating of air masses (Franz, 1973). The pressure drop from western Eurasia towards east facilitates the transport of Atlantic maritime air across the continent. During the summer months, the atmospheric moisture content over eastern Siberia is relatively high, leading to increased precipitation (Kuznetsova, 1997). In contrast to the winter, an increased influx of cyclones from the Transbaikal region, the Sea of Okhotsk and the Kara Sea region to Central Yakutia is remarkable, resulting in more unsteady weather conditions (Gavrilova and Atlasova, 1969; Cherdonova, 1993).

Evidently, the annual precipitation pattern is related to the influence of cyclones and anticyclones in northeast Siberia. Hence, the precipitation is particularly low in winter months and concentrates in the warm season from June to August. The evaporation, however, is equivalent up to four times, in dry years even up to ten times the amount of precipitation in summer (Gavrilova, 1973), leading to increased aridity. Thawing of the upper permafrost table and the soil-water content above the frozen ground provides moisture needed for the vegetation cover. The low precipitation in winter results in a low snow cover, ranging between 20 to 60 cm in the lowlands and up to 80 cm in the mountains (Agriculture Atlas of the Republic Sakha (Yakutia), 1989). Despite the snow cover, which may be thinned out or incomplete in places due to wind drifting or sublimation processes, the severe cold with absolute minimum temperature of -60°C and more is able to penetrate into the ground, promoting permafrost conditions.

Permafrost

The permafrost table in the lowlands of Central Yakutia is 400 to 700 m thick, increasing in depth within the central Verkhoyansk Mountains up to 1000 m (Agriculture Atlas of the Republic Sakha (Yakutia), 1989). In summer, commonly the upper 0.5 to 2.0 m of the ground is unfrozen. The thickness of the so-called active layer mainly depends on substrate, exposition and vegetation covers. According to the way of freezing, epigenetic and syngenetic permafrost deposits are distinguished. Epigenetic permafrost describes frozen sediments and rocks that have been affected by the lowering permafrost table clearly after their deposition. In contrast, syngenetic permafrost developed by rising of the permafrost table that transfer the accumulated sediments roughly contemporaneous into the frozen state (International Permafrost Association, 1998). Syngenetic permafrost deposits are mostly enriched in segregated ice due to migration of moisture during freezing. The formation of segregated ice causes a marked excess of moisture in frozen deposits in relation to non-frozen ground (French, 1996). Depending on the initial water content of the sediment and the extent of water migration during freezing, distinct types and arrangements of cryostructures will be formed (e.g. Katasonov, 1975; Murton and French, 1994).

Massive ice bodies can be enclosed in both epigenetic and syngenetic permafrost deposits. One of the most prominent features is wedge ice, widely distributed across the Russian and Canadian Arctic. The contraction of the ground during freezing opens frost

cracks that are predominately filled with snow melt in spring. If the frost crack reaches the perennially frozen ground underneath the active layer, the shaped ice vein will be stored. By repeating this process, an ice wedge forms, composed of several single ice veins. The oldest well-dated ice wedges are known from Ice Complex deposits at the Laptev Sea coast, revealing an age of 200 ka (Meyer et al., 2002b). The term ‘Ice Complex’ is referred to Pleistocene ice-rich deposits of various lithology with large syngenetic ice-wedges that form the typical polygonal pattern on the surface (e.g. Romanovskii, 1993; Gavrilova et al., 2003).

The local thawing of near-surface layers of permafrost deposits, in particular of the Ice Complex, is referred to as thermokarst, which is related to a thermal disturbance on the surface. The loss of ground ice results in the formation of depressions that are mostly occupied by ponds and lakes. The accumulated water in the depression accelerates the processes of thermokarst owing to its thermal storage capacity, leading to enlargement of the thermokarst depression. The term ‘alass’ is referred to distinct a depression with steep sides and a flat bottom, which hosts a thaw lake. By dissection or by lowering of the water level, thermokarst processes are slowed or stopped and the lake deposits are transferred into the frozen state again. More in detail, the development of thermokarst depressions and alasses are described in Soloviev (1959), Czudek and Demek (1970) and Soloviev (1973b).

3. Palaeoclimate signals as inferred from stable-isotope composition of ground ice in the Verkhoyansk Foreland, Central Yakutia

S. Popp, B. Diekmann, H. Meyer, C. Siegert, I. Syromyatnikov, H.-W. Hubberten.
Reprint from **Permafrost and Periglacial Processes 17, p. 119-132, 2006**;

Abstract

Ice-rich permafrost deposits and their isotopic composition were studied at four sites in the western foreland of the Verkhoyansk Mountains, Central Yakutia. The isotopic composition of ice wedges formed in alluvial and loess-like sediments generally reflects the palaeoclimate of winter conditions. The middle Weichselian Ice Complex developed around 41 ka ^{14}C BP during a period with colder winters than today. Similarly severe conditions are reflected in the late Weichselian Ice Complex from around 20 ka to 13 ka ^{14}C BP. The transition to the Holocene is characterised by increases of 5 ‰ and 35 ‰ in δ^{18}O and δD, respectively. This warming is documented in wedge ice, which grew between 8.5 and 4.5 ka BP. Towards the late Holocene and sub-recent times, a climatic deterioration is recorded, reflected by lighter isotopic composition of ice wedges, which developed between 1.2 ka and 0.7 ka ^{14}C BP.

3.1 Introduction

The landscape of Yakutia in northeast Siberia is strongly influenced by the existence of permafrost (Soloviev, 1973b; Katasonov, 1975). The region's extreme continental periglacial setting gave rise to the development of permafrost that attains a thickness of 400 m or more. Continuous permafrost has existed since at least the beginning of the middle Pleistocene with reliable ages for old permafrost conditions between 366 and 267 ka obtained from deposits at the archaeological site Diring-Yuryakh south of Yakutsk (Waters et al., 1997). The oldest dated permafrost horizon at this site contains large primary infill sand wedges that provide evidence of an extremely cold continental climate during the period of their formation.

During the last glacial period, the so-called Ice Complex was formed, composed of polygonal ice-wedge systems hosted in ice-rich soils and sediments, which had been syngenetically transformed into permafrost (Soloviev, 1959). Deposits of the Ice Complex are widespread in the coastal lowlands of Yakutia (e.g. Schirrmeister et al., 2002) and in the non-glaciated lowlands of Central Yakutia (Katasonov, 1975; Romanovskii, 1985). In contrast to the lowlands, the Verkhoyansk Mountain range (Fig. 3.1) was affected by regional glaciations during the late Pleistocene (Kind et al., 1971; Kind, 1975). Several glacial advances reached the western foreland, as documented by morainic arcs and associated glaciofluvial deposits. These prevented continuous ground-ice development and Ice Complex formation (Kolpakov, 1979). Ice-wedge growth took place in periglacial areas during those periods when glaciers were restricted to high elevations or had completely disappeared.

The spatial and temporal distribution of ice-rich permafrost documents distinct episodes of ice-wedge formation between the stages of major glacial recession. At present, only small remnants of glacial ice exist at elevations above 1800 m a.s.l. in the northern Verkhoyansk Mountains and in the Suntar-Khayata Ridge (Koreysha, 1989), while ice wedges are actively developing on the plains.

Ice wedges mainly form during spring, when meteoric waters released by snow melt enter thermal-contraction cracks that opened during the late winter (Mackay, 1983; Romanovskii, 1985). Repeated cracking leads to lateral ice-wedge growth in epigenetic wedges and the resultant ground ice is younger than the host sediment. Where prolonged sediment accumulation occurs, ice wedges tend to grow vertically. In this mode, vertical ice accretion and enrichment of dispersed ice in the adjacent sediments proceed more or less syngenetically with the accumulation of fine-grained loess-like material (clayey silts and fine sand) deposited by aeolian, fluvial, lacustrine and slope processes (Mackay, 1990; French, 1996).

Previous work has demonstrated the potential for ice wedges to archive palaeoclimatic information within their stable-isotope signatures. For example, stable-oxygen isotope signals in ice wedges have been used as indicators of changes in palaeo-winter temperature (e.g. Michel, 1982; Mackay, 1983; Vaikmäe, 1989; Vasil'chuk, 1991). However, studies by Meyer et al. (2002a, 2002b) dealing with the palaeoclimatic development of the coastal region of northeast Siberia during the late Pleistocene, have shown that palaeoenvironmental reconstruction requires knowledge of site-specific characteristics, such as slope aspect, surface relief, vegetation cover and regional climate conditions to enable full understanding of the variations in hydrogen and oxygen isotope signals in ice wedges. In this study, we present stable-isotope data from ice wedges of Weichselian and Holocene ages from the foreland of Verkhoyansk Mountains, as well as from Central Yakutia, and discuss their palaeoclimatic implications.

3.2 Study area and sites

The study area in Central Yakutia stretches along the Lena and Aldan Rivers in the southwestern foreland of the Verkhoyansk Mountains (Fig. 3.1). Fieldwork was conducted at *Mamontova Gora* (63°N/134°E), a key location for Quaternary stratigraphy in Central Yakutia on the left bank of Aldan River, 325 km upstream of the Aldan-Lena confluence. The Ice Complex, which is exposed at this location, is distributed across the entire Lena-Amga interfluve area, developed on terrace plains of various elevations and ages (Péwé and Journaux, 1983). On the so-called Tyungyulyu terrace of late Weichselian age (equivalent to MIS 2), large ice wedges of the Ice Complex were sampled in the upper part of steep banks adjacent to two thermokarst lakes, the *Ulkakhan Surdakh Alas* and the *Syrdakh Alas* (62°30'N/131°E). Other sections were studied along the Tumara River (64°N/130°E), a tributary of the Aldan, and the Dyanushka River (65°N/126°E), a tributary of the Lena. At least four glacial advances shaped the basins of the Tumara and Dyanushka Rivers and left distinct morainal belts in front of the mountains (Kolpakov, 1979).

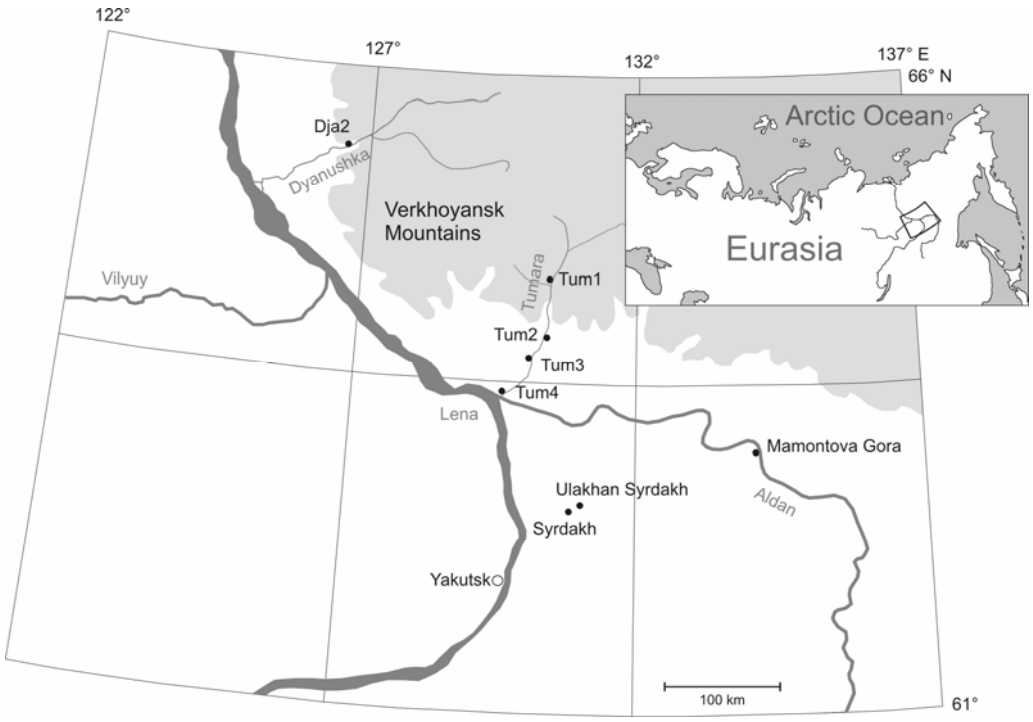

Fig. 3.1: Map of the study area in Central Yakutia. The black dots mark the locations of the studied ice-wedge sections.

The study area is characterised by a strong continental climate. Data from the meteorological station in Yakutsk reveal low mean annual precipitation (222 mm) and a mean annual air temperature from 1985-1993 of -8.7°C (RIHMI-World Data Centre: http://www.meteo.ru/index_e.html). Mean January temperature and precipitation are -37.6°C and 10 mm, respectively, while corresponding July values are 19.3°C and 33 mm, pointing to long severe winters and short warm summers. The distribution of annual precipitation, with its main period in summer between June and September, means that thick insulating snow cover does not form in winter and its absence promotes permafrost and ice-wedge formation.

3.3 Material and methods

Host sediments were described, sampled and the gravimetric ice contents were determined. Single ice-wedge exposures were examined at four sites in peat and sand along the Tumara River and at one site in sandy sediments at Dyanushka River (Fig. 3.1). The ice wedges examined at the Ice Complex at *Mamontova Gora* and on the Tyungyulyu terrace are hosted in loess-like sediments.

Sampling of ice was performed along horizontal and vertical transects across the wedges, using an ice screw or chain saw, depending on the size of the wedge, according to the method of Meyer et al. (2002a). Samples for stable oxygen and hydrogen isotopes were collected at 10-cm intervals, thawed in sample bags, and then stored in 30-ml polyethylene bottles.

The isotopic composition of ground ice was measured with a Finnigan MAT Delta-S mass spectrometer in the laboratory of the Alfred Wegener Institute for Polar and Marine Research in Potsdam, following the equilibration technique developed for ^{18}O

by Epstein and Mayeda (1953). The data are presented as permil difference relative to the standard V-SMOW (Vienna Standard Mean Ocean Water) with an internal 1-σ error of better than 0.8 ‰ and 0.1 ‰ for δD and $\delta^{18}O$, respectively (Meyer et al., 2000). Results are displayed in $\delta^{18}O$-δD scatter diagrams, relative to the Global Meteoric Water Line (GMWL), which delineates the temperature-dependent isotopic composition of fresh natural waters, defined as $\delta D = 8\ \delta^{18}O + 10$ ‰ SMOW (Craig, 1961). The linear regression of precipitation data for a particular sampling site is known as Local Meteoric Water Line (LMWL). Slope and intercept of the LMWL are parameters that characterise the $\delta^{18}O$-δD relationship and give information on the evolution of precipitation and the influence of secondary evaporation processes (Dansgaard, 1964). The deuterium excess value (defined as *d* excess = $\delta D - 8\delta^{18}O$) is an indicator for non-equilibrium fractionation processes (Dansgaard, 1964) and gives information on the origin of vapour masses, since the *d* excess is controlled by humidity in the source region (Merlivat and Jouzel, 1979). Thus, the winter precipitation resulting from an air mass yields a site-specific signature of its history, which is stored within glacier ice (Johnsen and White, 1989), and may also account for variations in the isotopic composition of ground ice as discussed below.

3.4 Dating of ice wedges

With one exception, the ages of the sampled ice wedges were estimated by accelerator mass spectrometry (AMS) ^{14}C dating of plant remains found within the ground ice and in the surrounding sediments (Table 3.1). Wood macrofossils at the *Mamontova Gora* site were dated by conventional radiocarbon method. The measurements were carried out at the Leibniz Laboratory in Kiel, Germany. In order to get reliable ages by AMS, only the leached tissue of the organic material was dated, with the exception of plant remains that were found within the ice wedges that contained few organic materials. The organic remnants of reed, roots and wood in bulk sediments were picked out under a microscope.

Dating ice wedges is difficult because of the diachronic growth of the ice body within a sediment sequence, and possible sources of error owing to the presence of redeposited slope material as well as infiltration, migration and storage of young water containing modern ^{14}C. Dating of the host sediments mostly provides a maximum age for the enclosed ground ice, i.e. the ground ice is no older than the host sediments and, more likely, is younger than them. Organic matter obtained from the ice gives an age marker of one moment in time during the entire wedge development, if redeposition and contamination of the material transported into the thermal contraction crack can be excluded. The best age constraint, however, is given when both the host sediments and the ice wedge are dated or at least the age of the sediments is known from other studies.

Table 3.1: AMS radiocarbon ages of organic remains from host sediments and ground ice. The sample from Mamontova Gora was dated by the conventional radiocarbon method. Data without calibrated ages are out of the range of calibration data sets or contain uncertainties, preventing the calibration.

Site	Lab. Number	^{14}C yr BP	cal. yr BP 2-σ range	Organic matter source
Mam. G.	KI-5183	41230	Not available	Host sediments
Ulakh. Syr.	KIA 26364	13110 ± 285	16466 - 14410	Ground ice
	KIA 26365	3755 ± 30	4184 - 4072	Ground ice
Syrdakh	KIA 26367	21710 ± 680	Not available	Ground ice
Tum1	KIA 19144	8539 ± 44	9557 - 9469	Host sediments
Tum2	KIA 19724	770 ± 22	715 - 666	Host sediments
Tum3a	KIA 19727	2340 ± 25	2362 - 2314	Ground ice
	KIA 25983	16420 ± 400	20661 - 18522	Ground ice
Tum3	KIA 20724	40420 ± 1440	Not available	Host sediments
Tum3	KIA 20725	39710 ± 1185	Not available	Host sediments
Tum4	KIA 19725	1200 ± 23	1179 - 1057	Host sediments
	KIA 25984	475 ± 60	565 - 428	Ground ice
Dja2	KIA 24041	13980 ± 60	17267 - 16295	Ground ice
	KIA 24042	14620 ± 150	18125 - 16936	Host sediments

3.5 Results

In this section, ground-ice exposures studied are described in terms of their field appearance, their depositional environments, the datable material that constrains their ages (Fig. 3.2), and the stable-isotope values for the ice wedges (Table 3.2).

Mamontova Gora

This exposure extends about 12 km along the Aldan riverbank and is situated about 325 km upstream of the Aldan-Lena confluence (Fig. 3.1). It consists of two main geomorphologic units, marked by an 80 m high and a 50 m high terrace level, respectively (Baranova, 1979). The upper part of both terrace sections is composed of greyish and brownish silt of middle and late Weichselian age (equivalent to MIS 3 and 2), respectively (Péwé and Journaux, 1983). Ice wedges up to 5 m wide were sampled within the silts of the lower terrace. Their syngenetic origin is indicated by layered cryostructures in the host sediments that turn upward adjacent to the wedge owing to the ice growth (Fig. 3.2a). A piece of wood from the sediments somewhat above the ice samples yielded a radiocarbon age of 41230 a BP. This age fits in well to with previous published results from this site, suggesting that ice-wedge growth took place roughly between 46700 ± 1500 ^{14}C a BP and 34020 ± 1500 ^{14}C a BP (Péwé and Journaux, 1983). The isotopic composition of the ice averages -30.5 ‰ for $\delta^{18}O$ and -237 ‰ for δD. The mean *d* excess value amounts to 7.6 ‰. There is particularly low variability in the stable isotope composition, less than 2 ‰ for $\delta^{18}O$ and 16 ‰ for δD.

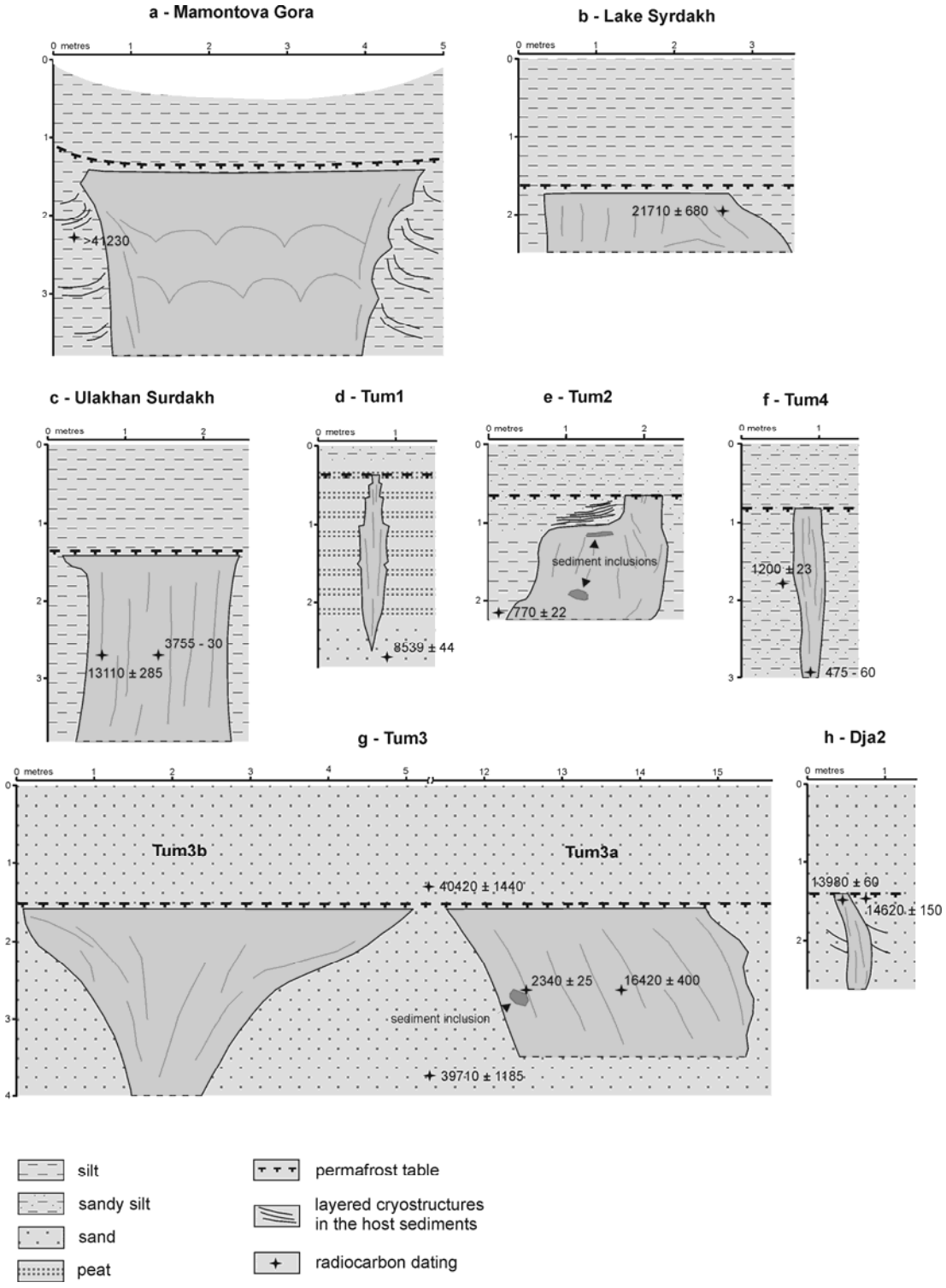

Fig. 3.2: Sketches of the sampled ice wedges and the related radiocarbon ages (^{14}C a BP).

Table 3.2: Stable isotope data ($\delta^{18}O$, δD and d excess minima, mean and maxima) as well as the standard deviation, slope and intercept of all sampled ice wedges of the study area. The recent precipitation was sampled in Yakutsk. Samples of river water apply to Tumara and Dyanushka Rivers during field work in summers 2002 and 2003.

site	N	$\delta^{18}O$ (‰) min	$\delta^{18}O$ (‰) mean	$\delta^{18}O$ (‰) max	$\delta^{18}O$ (‰) s.d.	δD (‰) min	δD (‰) mean	δD (‰) max	δD (‰) s.d.
Mam.G.	18	-31.31	-30.52	-29.37	0.61	-243.1	-236.6	-227.5	4.8
Ulakh.Syr.	24	-31.99	-31.30	-30.50	0.40	-252.1	-245.6	-238.2	3.9
Syrdakh	23	-31.16	-30.79	-30.42	0.20	-247.9	-244.5	-241.9	1.7
Tum1	22	-27.57	-25.94	-24.43	0.94	-211.0	-199.4	-187.9	7.1
Tum2	21	-29.26	-28.33	-27.27	0.48	-222.5	-215.7	-207.6	3.5
Tum3a	24	-29.59	-28.13	-27.09	0.77	-228.2	-219.1	-210.6	5.1
Tum3b	22	-29.04	-28.68	-27.47	0.35	-223.7	-221.3	-211.3	2.7
Tum4	20	-29.85	-27.64	-24.96	1.20	-226.6	-210.9	-190.8	9.1
Dja2	15	-24.09	-22.36	-21.74	0.58	-181.7	-171.5	-167.5	3.6
River water	5	-21.25	-20.84	-20.58	0.28	-160.6	-158.4	-156.3	1.9
Recent precipitation									
rain	35	-22.06	-12.15	-5.09	3.70	-177.4	-105.5	-68.1	24.9
snow	38	-43.12	-32.56	-20.92	6.57	-336.6	-252.1	-168.8	50.6

site	N	d (‰) min	d (‰) mean	d (‰) max	d (‰) s.d.	slope	intercept	r^2
Mam.G.	18	6.4	7.6	8.9	0.6	8.02	8.09	0.98
Ulakh.Syr.	24	3.2	4.5	6.0	0.8	9.60	53.32	0.98
Syrdakh	23	0.9	1.8	3.1	0.6	7.99	1.34	0.90
Tum1	22	7.1	8.2	9.7	0.8	7.48	-5.43	0.99
Tum2	21	8.7	11.0	13.2	1.0	7.06	-15.51	0.94
Tum3a	24	3.6	6.0	8.7	1.4	6.53	-35.50	0.97
Tum3b	22	6.8	8.2	9.2	0.7	7.41	-8.84	0.94
Tum4	20	8.9	10.2	12.5	0.9	7.56	-1.99	0.99
Dja2	15	5.7	7.5	11.0	1.6	5.91	-39.38	0.91
River water	5	7.3	8.4	10.1	1.3	-	-	-
Recent precipitation								
rain	35	-32.3	-8.3	8.3	10.4	6.34	-28.46	0.89
snow	38	-8.1	8.3	16.9	5.7	7.66	-2.90	0.99

Lake Syrdakh and Ulkakhan Surdakh

These two sites are very similar and thus are described together. Both sampled ice wedges grew in loess-like deposits that cover the Tyungyulyu terrace. These sediments were dated to around 19 ka BP close to the permafrost table at *Lake Syrdakh* (Katasonov, 1979). The results of dating organic matter enclosed in the ground ice suggest a late Weichselian age for the sediments. The sampled material in the ground ice at *Lake Syrdakh* provides an age of 21710 ± 680 ^{14}C a BP (Fig. 3.2b). At site *Ulkakhan Surdakh*, organic material in the ice date to 13110 ± 680 ^{14}C a BP at the margin and to 3755 ± 30 ^{14}C a BP in the middle (Fig. 3.2c). Non-parallel, lenticular cryostructures, a moderate gravimetric ice content (30 %) and palaeosoils characterise the silty sediments. At *Ulkakhan Surdakh*, the top of the exposed ice wedge is approximately 2.1 m in width and 2.3 m in length. The whole ice wedge, however, probably extends more than 10 m into the ground, to at least the level of the thermokarst

lake below. At site *Lake Syrdakh*, the exposed ice wedge is around 3 m wide and 0.8 m long, but the true extent is probably similarly great.

The mean isotopic composition of the ice is -31.3 ‰ for $\delta^{18}O$ and -246 ‰ for δD at site *Ulkakhan Surdakh* and -30.8 ‰ and -245 ‰ for $\delta^{18}O$ and δD, respectively, at *Lake Syrdakh* (Table 3.2). These values, as well as the low variability of the data, are comparable to the isotopic record at site *Mamontova Gora*, but differ by lower mean *d* excess values of 1.8 ‰ and 4.5 ‰, respectively.

Tumara River

Ice wedges were exposed at four sites along the Tumara riverbanks (Fig. 3.1). Site *Tum1* is situated within a broad glacially carved valley in the mountains. The ice wedge developed within a two-meter thick peat deposit overlying river gravel (Fig. 3.2d). The 0.4 m wide and 1.8 m long wedge likely penetrated epigenetically into the basal sands, and grew then syngenetically with the peat accumulation. Organic remains from the basal sands were dated to 8539 ± 44 ^{14}C a BP. This age is the absolute maximum age for the ice. The isotopic composition is relatively enriched, showing mean values of -25.9 ‰ and -199 ‰ for oxygen and hydrogen, respectively. The mean *d* excess value amounts to 8.2 ‰ with low variability.

Sites *Tum2* and *Tum4* exhibit syngenetic ice wedges of different sizes. The first one is up to 1.3 m wide whereas the second is only 0.2 m wide (Fig. 3.2e, f). The visible lengths of about 2 m for both ice wedges show a transition zone to the host sediments with an ice-rich matrix and for site *Tum2*, layered ice structures. Both ice wedges formed on flood plain terraces of the Tumara and Aldan Rivers. The ice bodies are embedded in mainly silty sediments with high gravimetric ice content (46-175 %). The growth of *Tum2* appears to have been affected by rapid accumulation of overbank deposits with higher sand content, resulting in a narrow width in the upper part of the ice wedge. The wedge at *Tum4* shows a constant width. The host sediments were dated at both sites, providing an age of 770 ± 22 ^{14}C a BP for *Tum2* (Fig. 3.2e) and an age of 1200 ± 23 ^{14}C a BP for *Tum4* (Fig. 3.2f). Additionally, organic matter enclosed in the ice shows an age of 475 ± 60 ^{14}C a BP for the ice wedge *Tum4*. The mean isotopic composition of both wedges is around -28 ‰ for $\delta^{18}O$ and -214 ‰ for δD with a mean d excess value of 11 ‰ and 10 ‰, respectively (Table 3.2).

In contrast to the other *Tum* sites, *Tum3* is situated approximately 20 m above the river within a retrogressive thaw slump more than 30 m in diameter. This thaw slump is underlain by basal till, acting as an impermeable bed for the overlying ice-bearing sandy deposits. Several ice wedges with widths of up to 5 m were exposed, of which two were sampled at this site (*Tum3a and Tum3b*). Radiocarbon dating of the sandy sediments resulted in an age around 40 ka BP at both 1.2 m and 3.9 m depths (Fig. 3.2g). At least one of these two samples was likely biased by refrozen slope material or other thaw-freeze related processes. Infrared stimulated luminescence (IRSL) dating nearby the ice wedges, however, provided an age of 48500 ± 3900 a BP (Stauch et al., in press), constraining the age of the host sediments as middle Weichselian. Dating of organic matter in the ice resulted in contradictory ages of 2340 ± 25 ^{14}C a BP at the left margin near a sediment inclusion and 16420 ± 400 ^{14}C a BP in the middle part of *Tum3a* (Fig. 3.2g). The mean isotopic composition of around -28 ‰ for $\delta^{18}O$ and -220 ‰ for δD

closely agrees with the isotopic signal in the late Holocene ice wedges *Tum2* and *Tum4*. On the other hand, the *d* excess differs by lower values of 6.0 ‰ and 8.2 ‰ in comparison with the late Holocene ice (Table 3.2).

Dyanushka River

The ice wedge exposed at site *Dja2* is 0.3 m in width and >1.2 m in length and is enclosed in alluvial sediments. The sediment sequence is about 10 m thick and forms the upper part old terrace step above the modern Dyanushka River valley floor, overlying basal diamicton. The terrace surface exhibits a pattern. Curved and layered cryostructures and ice-rich matrix (40–52 %) characterise the permafrost deposits. Syngenetic growth of the wedge is evident from the dating results. Organic matter from the upper part of ice wedge *Dja2* is dated to 13980 ± 60 ^{14}C a BP and the nearby sediments yield an age of 14620 ± 150 ^{14}C a BP (Fig. 3.2h). The ice wedge has a relatively heavy mean isotopic composition of -22.4 ‰ and -172 ‰ for δ^{18}O and δD, respectively, with a mean *d* excess value of 7.4 ‰ (Table 3.2).

3.6 Discussion

In general, melting of snow and its refreezing in thermal contraction cracks is accepted as the main reason for recent ice-wedge formation (e.g. Mackay, 1983; Vaikmäe, 1989; Vasil'chuk, 1992; Lauriol et al., 1995). The isotopic signal in ice wedges therefore is strongly related to the stable-isotope composition of winter precipitation. The isotopic composition of both winter and summer precipitation at a given site is the result of various processes. The initial formation of a vapour-bearing air mass over the oceans by evaporation and advection towards the continent is accompanied by significant isotopic fractionation in terms of the rain-out effect, which is described by the Rayleigh model (snow amounts to -32.6 ‰ for δ^{18}O and -252 ‰ for δD with a relatively large variability of more than 20 ‰ and 160 ‰, respectively (Table 3.2).

During snowmelt in spring, the isotopic signal in the melt changes through time. The initial snowmelt is highly depleted in comparison with the average snowpack and the snow becomes enriched in oxygen and hydrogen stable isotopes. The progressive melting results in the enrichment of ^{18}O and D in both the snowmelt and the residual snow pack (Taylor et al., 2001). Sub-recent ice wedges younger than 700 years (*Tum2 and Tum4*) show enriched mean isotopic compositions in comparison with Dansgaard, 1964). As a result, the moisture reaching Yakutia by the Westerlies is depleted in δ^{18}O and δD values in comparison with the initial vapour mass (Kurita et al., 2004), known as the continental effect. Seasonal variations in the stable-isotope content of precipitation are attributed to the temperature-depended fractionation processes (Jouzel et al., 1997). Intra-seasonal variations in the isotopic composition may be related to mixing of different air masses labelled by different isotopic ratios and the additional contribution of recycled water from the land surface. The latter process in particular influences the summer precipitation (Fig. 3.3), modifying the isotopic ratio of rain in eastern Siberia (Kurita et al., 2003). In contrast, winter precipitation in Yakutia is not significantly altered by kinetic fractionation processes, as suggested by a mean *d* excess value of 8.9 ‰ and a slope value of 7.6, which closely agree with the GMWL (Fig. 3.3).

The mean isotopic composition of the sampled the average snow amounts to -32.6 ‰ for $\delta^{18}O$ and -252 ‰ for δD with a relatively large variability of more than 20 ‰ and 160 ‰, respectively (Table 3.2). This may be the result of filling the frost-cracks during a later stage of snowmelt (Lauriol et al., 1995). However, the lack of isotopic data in recent ice veins, which could refer to distinct average winter precipitation, makes this interpretation difficult to prove.

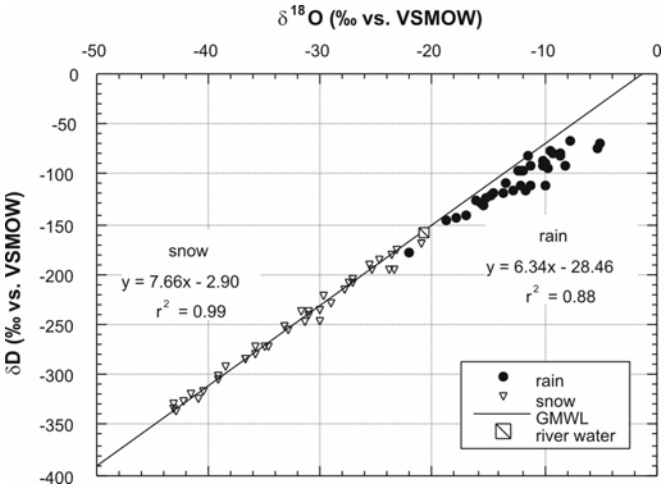

Fig. 3.3: $\delta^{18}O$-δD diagram for snow, rain and river water in Central Yakutia. The rain samples were collected in summer 1997 (June-August) and the snow samples reflect the winter 1997/98 (November-April) in Yakutsk. The square represents the mean isotopic composition of waters from Tumara and Dyanushka Rivers, sampled during field work in summers 2002 and 2003.

The freezing of the snowmelt in the frost-crack represents a reverse fractionation process, with exchange occurring between the water and the ice. The first ice is enriched in ^{18}O and D and with continued freezing, both the ice and the remaining water gradually become depleted in ^{18}O (Clark and Fritz, 1997). Non-equilibrium fractionation is negligible when the freezing rate is faster than 2 mm per hour (Michel, 1982). Apparently, the considered processes predominantly follow the Rayleigh distillation with no significant kinetic fractionation as shown by the isotopic composition in most of the ice wedges (Table 3.2). In particular the isotopic compositions of Holocene ice wedges closely agree with the GMWL (Fig. 3.4). Kinetic fractionation that might have occurred is likely related to sublimation and metamorphism of the snowpack during winter as well as to the additional contribution of waters of different origin. Other processes, such as vapour diffusion within the ice, which would result in a smoothing of isotope gradients with time (Jean-Baptiste et al., 1998), can be excluded for the young ice wedges. Even in late Pleistocene ice wedges, this process is of minor importance as discussed by Meyer et al. (2002a). Furthermore, water migration at the interface of ice and sediment may occur, which results in mixing effects between wedge ice and segregated ice (Meyer et al., 2002a). Therefore, we excluded the data points of the marginal ice-wedge samples from the scatter plots (Fig. 3.4), to avoid false interpretations.

In conclusion, the major shifts in the mean isotopic composition among the ice wedges reflect different condensation temperatures of precipitation that are basically controlled by the ambient air temperature and therefore provide a signal of palaeo-winter temperatures. The variability in the isotopic data thus would indicate climatic changes for particular periods of the past. The character of variations among the isotopic compositions is illustrated in Fig. 3.5, which shows three groups that comprise the Pleistocene ice wedges, the Holocene ice wedges and one outlier, respectively.

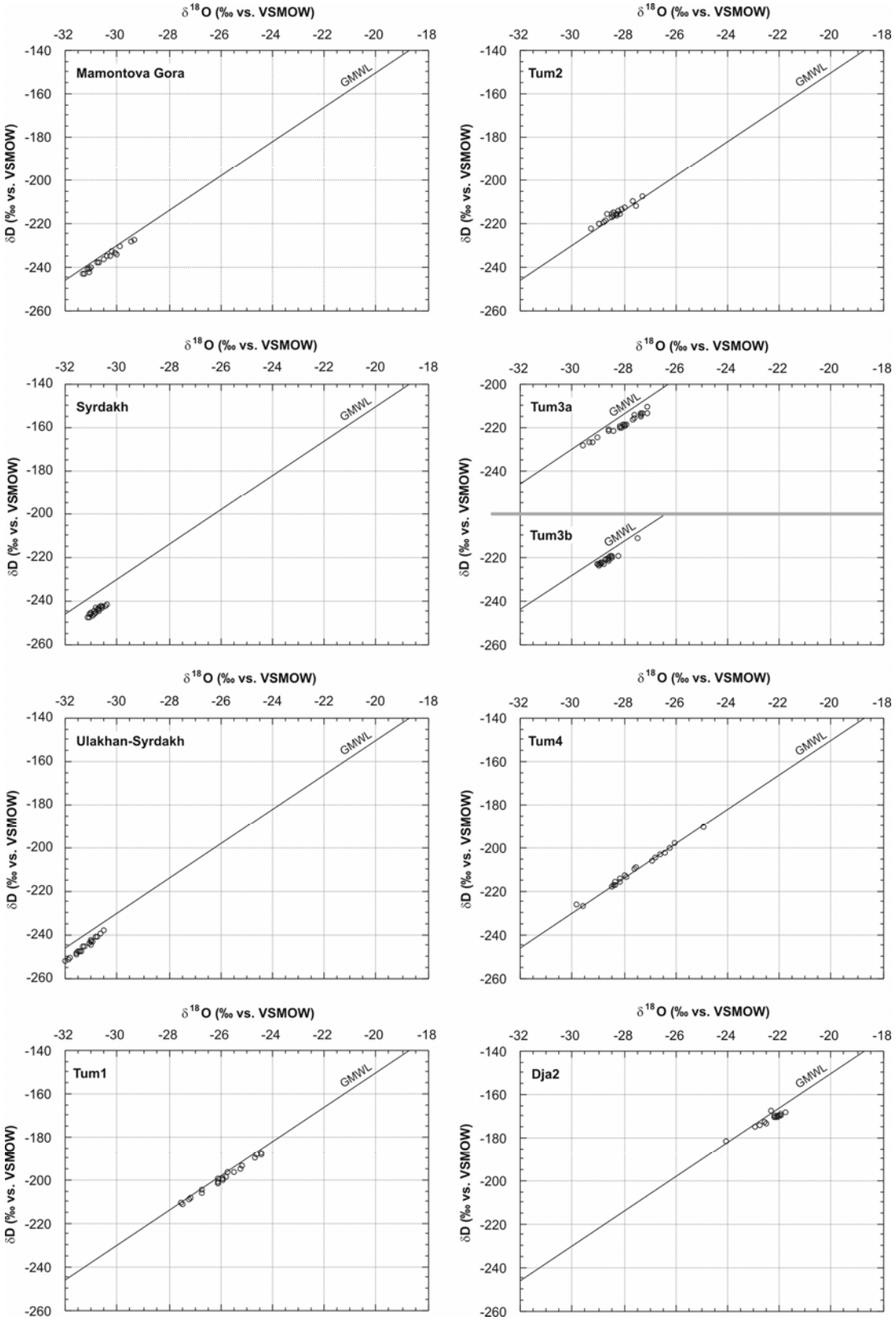

Fig. 3.4: $\delta^{18}O$-δD diagrams for all sampled ice wedges in relation to the Global Meteoric Water Line (GMWL).

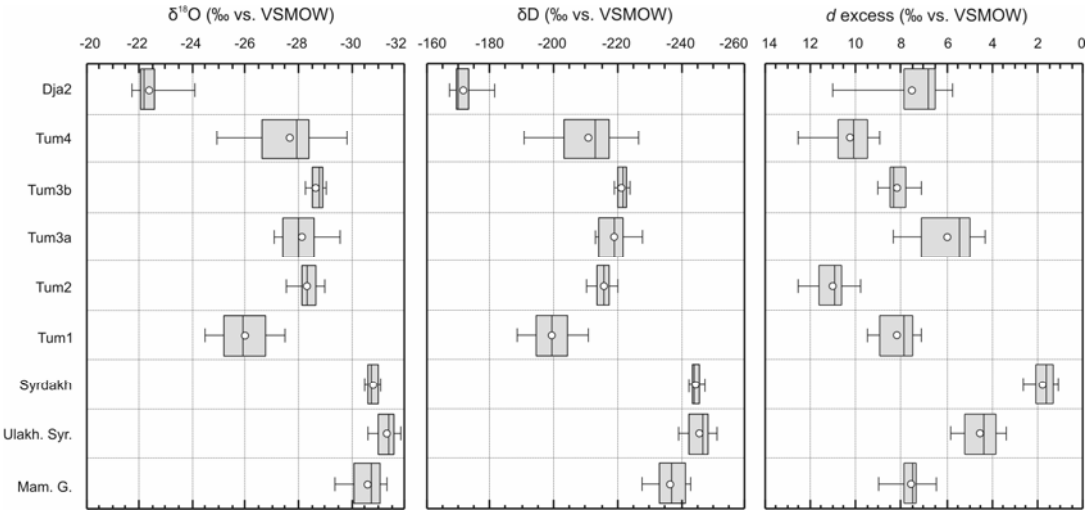

Fig. 3.5: Box plots of the isotopic composition ($\delta^{18}O$ and δD) and the *d* excess values of the ice-wedge sites. The boxes enclose 50 % of the respective data with the median value (black line therein) and the mean value (white circle therein). The bottom and the top of the boxes (right and left definitions) represent the first and the third quartiles, respectively. The lines extending from the boxes enclose 90 % of the data by marking the 0.05 and the 0.95 percentile, respectively. These limits were chosen in order to exclude extreme values and outliers from the diagrams.

In order to test weather the variability of $\delta^{18}O$ and δD among the ice-wedge sites is statistically different, an analysis of variance (ANOVA) was performed, using the software 'StatView' (version 4.5). The sites *Tum2* and *Tum4* as well as *Tum3a* and *Tum3b* were each combined into a single group because they are assumed to represent comparable environments in terms of their isotopic compositions, host sediments and ages. The results of ANOVA show that the isotopic composition among the ice wedges are significantly different, meaning that the statistical samples originate from independent populations. A multiple comparison test (Bonferroni/Dunn procedure, Table 3.3) showed that the sites and *Lake Syrdakh* and *Ulkakhan Surdakh* are not statistically different in regard to both $\delta^{18}O$ and δD values. This suggests that the 3755 ± 30 ^{14}C a BP date from the middle of the wedge at *Ulkakhan Surdakh* (Fig. 3.2c) is unlikely to be correct and probably represents contamination of the ice vein by younger organic matter by infilling or redeposition and subsequent freezing on the ice surface.

Taking only the $\delta^{18}O$ values into account, no significant differences were revealed for the sites *Mamontova Gora* and *Syrdakh* as well as for *Tum2, Tum4* and *Tum3*, respectively. The disparities in the multiple comparisons of $\delta^{18}O$ and δD values may be attributed to kinetic fractionation processes, affecting oxygen and hydrogen stable isotopes in different ways. However, the results of the ANOVA and the multiple comparison test show similarities in the isotopic data of mainly Pleistocene ice wedges as well as distinct differences in isotopic compositions between Pleistocene, middle Holocene and late Holocene ice wedges that serve as the basis for the palaeoclimatic interpretation of the data.

Table 3.3: Analysis of variance (ANOVA) for comparison of $\delta^{18}O$ and δD data among the seven ice-wedge sections (note that sites *Tum2* and *Tum4* as well as *Tum3a* and *Tum3b* are each combined into a group). Table 3.3a presents the results of ANOVA, showing that significant differences between the sampled sites do exist (indicated by the P-value of <.0001). Table 3.3b exhibits the result of the multiple comparison test (Bonferroni/Dunn procedure) that reveals which sites are different at the level of significance of 5 %. The statistically significance difference is indicated, if the P-value ranges below 0.0024. Only three sites underlined do not fulfil the latter criterion in reference to the $\delta^{18}O$ variable.

a)

Source of variation	d.f.	Sum of squares	Mean squares	F-value	P-value
Sites $\delta^{18}O$	6	1093.943	182.324	364.591	<.0001
residual	182	91.014	.500		
Sites δD	6	81014.343	13502.390	500.413	<.0001
residual	182	4910.809	26.982		

b)

	Bonferroni/Dunn for $\delta^{18}O$			Bonferroni/Dunn for δD		
Sites	Mean Diff.	Crit. Diff.	P-value	Mean Diff.	Crit. Diff.	P-value
Dja2, Mam.G.	8.157	.762	<.0001	65.090	5.596	<.0001
Dja2, Syrdakh	8.423	.723	<.0001	73.075	5.312	<.0001
Dja2, Tum1	3.581	.730	<.0001	27.926	5.359	<.0001
Dja2, Tum2, 4	5.629	.658	<.0001	41.899	4.830	<.0001
Dja2, Tum3	6.028	.648	<.0001	48.651	4.759	<.0001
Dja2, Ulakh.Syr.	8.894	.717	<.0001	74.152	5.268	<.0001
Mam.G., Syrdakh	.266	.686	.2336	7.985	5.037	<.0001
Mam.G., Tum1	-4.576	.693	<.0001	-37.164	5.087	<.0001
Mam.G., Tum2, 4	-2.527	.616	<.0001	-23.191	4.526	<.0001
Mam.G., Tum3	-2.129	.606	<.0001	-16.439	4.450	<.0001
Mam.G., Ulakh.Syr.	.738	.679	<.0001	9.062	4.991	<.0001
Syrdakh, Tum1	-4.842	.650	<.0001	-45.148	4.773	<.0001
Syrdakh, Tum2, 4	-2.793	.568	<.0001	-31.176	4.170	<.0001
Syrdakh, Tum3	-2.395	.556	<.0001	-24.424	4.088	<.0001
Syrdakh, Ulakh.Syr.	.472	.636	.0234	1.078	4.670	.4780
Tum1, Tum2, 4	2.049	.576	<.0001	13.972	4.230	<.0001
Tum1, Tum3	2.447	.565	<.0001	20.725	4.149	<.0001
Tum1, Ulakh.Syr.	5.314	.643	<.0001	46.226	4.724	<.0001
Tum2, 4, Tum3	.398	.468	.0094	6.752	3.438	<.0001
Tum2, 4, Ulakh.Syr.	3.265	.560	<.0001	32.254	4.114	<.0001
Tum3, Ulakh.Syr.	2.866	.549	<.0001	25.502	4.030	<.0001

3.7 Palaeoclimatic implications

The Pleistocene ice wedges are characterised by the lightest isotopic composition that reflect the coldest winter temperatures within the considered time span (Figs. 3.4 and 3.5). In particular, at the sites *Ulkakhan Surdakh* and *Syrdakh*, the isotope values of up to -32.0 ‰ and -252 ‰ for $\delta^{18}O$ and δD, respectively, reveal very severe climate conditions for the late Weichselian around 21 ka and 13 ka BP (Table 3.1). The older ground ice at *Mamontova Gora* shows a slightly warmer isotopic signal with a larger variability than the former sites that may attributed to the climatically more variable Kargin interstadial (equivalent to MIS 3) (e.g. Schirrmeister et al., 2002; Hubberten et al., 2004). The isotopic composition, however, which averages -30.5 ‰ for $\delta^{18}O$ and

-236 ‰ for δD, still indicates a very cold winter environment around 40 ka BP. The similarity of the winter conditions during the middle and late Weichselian, emphasized by the results of the ANOVA, is also reported from the Ice Complex at the Laptev Sea coast and neighbouring regions in northeast Siberia (Vasil'chuk, 1991; Meyer et al., 2002a). These results suggest severe winter conditions over wide expanses of Yakutia during that time.

Unlike the other Ice Complex sections, the site *Dja2*, which is dated to around 14 ka BP (Table 3.1), presents relatively enriched mean isotopic composition of -22.4 ‰ and -172 ‰ for $\delta^{18}O$ and δD, respectively (Figs. 3.4 and 3.5). This signature would indicate more favourable winter conditions at that time than during the postglacial warming, which is not consistent with findings from other proxy data across the Siberian Arctic, such as fossil insects, pollen records, mammals, and other isotopic data (e.g. Meyer et al., 2002a; Schirrmeister et al., 2002; Hubberten et al., 2004; Kienast et al., 2005; Sher et al., 2005). These studies reveal a pronounced continental climate with very cold winters and summers distinctly warmer than today under extremely dry conditions between 20 and 15 ka BP. These contradictions can be resolved by taken into account the probable origin of the water that fed the ice wedge. Given that the isotopic composition exhibits no strong alteration by kinetic fractionation processes (Fig. 3.4), it appears most likely that the water originated from spring flooding because the site is located on fluvial terrace deposits. Modern river water shows a similar isotopic composition of -20.8 ‰ and -158 ‰ for oxygen and hydrogen, respectively, as well as a similar range in the *d* excess values (Table 3.2). If this interpretation is correct, the lighter isotopic composition of the ice wedge would be the result of the prevailing climate conditions, affecting the surface waters. Consequently, the results from this ground ice are not comparable with the other ice-wedge data.

In comparison with the Ice Complex data, the Holocene ice wedges are characterised by an enriched isotopic composition relative to the Pleistocene ice wedges (Figs. 3.4 and 3.5), indicating warmer conditions. The oldest postglacial site is *Tum1*, showing enriched oxygen and hydrogen compositions of around 5 ‰ and 35 ‰, respectively. The age of the ice wedge at this site remains uncertain because the radiocarbon dating provides only a maximum age of 8.5 ka BP. Given the relatively warm isotopic signature of -25.9 ‰ for $\delta^{18}O$ and -199 ‰ for δD, however, we believe that the ice wedge grew during the favourable middle Holocene period. Pollen-based studies from lakes in Central Yakutia revealed a climate optimum between 6.0 ka and 4.5 ka BP (Andreev et al., 2002c). The general warming trend, however, started during the Boreal period around 8.0 ka BP in northern Yakutia and neighbouring areas (Andreev and Klimanov, 2000; Andreev et al., 2002b; Naidina and Bauch, 2001). Thus, the isotopic composition of *Tum1* may reflect postglacial climate amelioration in northeast Siberia, most likely between 8.5 ka and 4.5 ka BP.

The isotopic composition of ice wedges changed to relatively light towards the late Holocene and sub-recent time. The ground ice at the sites *Tum2* and *Tum4* is interpreted as being younger than 1.2 ka BP based on the dating results of the host sediments. The mean isotopic composition amounts to around -28 ‰ for oxygen and -214 ‰ for hydrogen (Figs. 3.4 and 3.5). These values document the climate deterioration, which started at around 4.5 ka BP according to pollen records in northern Yakutia (Andreev et

al., 2002b; Andreev et al., 2004a). Similarly light but also slightly enriched isotopic compositions of late Holocene ice wedges are reported from the Laptev Sea coast between 3.5 ka and 1.0 ka BP (Meyer et al., 2002a; Meyer et al., 2002b). Both regions demonstrate the impact of climate on the stable-isotope composition in young ground ice, even though northern and Central Yakutia differ by being in the tundra and taiga zone, respectively.

Site *Tum3* is excluded from the chronological palaeoclimatic interpretation because of the uncertain age dating of the ice. The mean isotopic composition of around -28 ‰ for oxygen and around -220 ‰ for hydrogen for both sampled ice wedges matches the late Holocene isotopic signal of *Tum2* and *Tum4* (Figs. 3.4 and 3.5) and would be consistent with the radiocarbon age of 2.3 ka BP. On the other hand, the middle Weichselian host sediments and the other age marker from the ice around 16 ka BP give inconsistent age indications.

3.8 Conclusions

The interpretations of the isotopic data support the assumption that ice wedges are basically fed by meteoric water, released during snow melt in spring and provide an isotopic signal of winter precipitation. Secondary kinetic fractionation processes play a subordinate role, whereas the contribution of surface waters, which possibly diluted the snow melt water and biased the primary precipitation signal, had an significant influence on the isotopic composition of some wedges.

The ice wedges with mostly unaltered isotope signals indicate that pronounced variations in winter conditions occurred over the past 40000 years. The middle Weichselian, around 41 ka BP, was characterised by cold and severe winter conditions in Central Yakutia. Similar and even colder conditions are indicated for the late Weichselian Ice Complex around 21 ka and 13 ka BP. The early Holocene showed a winter climate optimum, as indicated by isotope signals in the ice, dating to a maximum of 8.5 ka BP. The late Holocene was characterised by a deterioration of winter conditions in Central Yakutia, indicated by “cold” isotopic signals in ice wedges younger than 1000 years. Variations of winter temperatures were consistent with parallel changes in summer temperatures, as indicated by pollen records from Central Yakutia, which reflect warm-season climate conditions.

The palaeoclimatic interpretation of isotopic composition of ice wedges in Central Yakutia is a promising technique but requires more detailed information on boundary conditions that control the depositional environment of the host sediments as well as accurate age determinations.

Acknowledgements

Field work was carried out together with German and Russian partners within the scope of the DFG project: “Late Quaternary development of climate and environment of the Verkhoyansk Mountains and the central lowland of Yakutia” (Le730/10-1& Hu378/12-1). For fruitful collaboration, the authors are grateful to their colleagues F. Lehmkuhl and G. Stauch from RWTH Aachen, W. Zech from Bayreuth University, Germany, as well as I. Belolyubsky from the Diamond and Precious Metal Geology Institute,

Yakutsk, and V. Spektor from the Permafrost Institute SB RAS, Yakutsk. Furthermore we would like to thank L. Schirrmeister for additional information on the Mamontova Gora site and sampling as well as A. G. Lewkowicz, I. D. Clark and the anonymous reviewer for their helpful comments, which improved the previous version of the manuscript.

4. Sediment provenance of late Quaternary morainic, fluvial, and loess-like deposits in the southwestern Verkhoyansk Mountains (eastern Siberia) and implications for regional palaeoenvironmental reconstructions

S. Popp, I. Belolyubsky, F. Lehmkuhl, A. Prokopiev, C. Siegert, V. Spektor, G. Stauch, B. Diekmann.
Accepted for publication.

Abstract

Provenance analysis of late Quaternary deposits from tributaries of the Aldan and Lena Rivers in Central Yakutia was performed by analysis of heavy minerals and clay mineralogy. Cluster analysis revealed one assemblage, which is characterised by relatively high proportions of amphibole, orthopyroxene and garnet as well as pedogenic clay minerals, reflecting a sediment provenance from the wide catchment area of the Lena and Aldan Rivers. In contrast, the three other clusters are dominated by stable heavy minerals with varying amounts of clinopyroxene, apatite and garnet as well as high percentages of illite and chlorite that are indicative of source rocks of the Verkhoyansk Mountains. Glacial moraines reveal the local mountain source signal that is overprinted by the Lena-Aldan signal in the oldest moraines by reworking processes. Alluvial sediments in the Verkhoyansk Foreland show a clear Lena source signal through intervals of the middle and late Pleistocene, related to a stream course closer to the mountains at that time. Loess-like cover sediments are characterised by the dominant Lena provenance with increasing proportions of local mountain sources towards the mountain valleys. Aeolian sands in an alluvial terrace section at the mountain margin covering the time between 30 ka and 10 ka BP reflect temporarily dominant inputs of aeolian materials from the Lena Plains.

4.1 Introduction

The Verkhoyansk Mountains of Central Yakutia (eastern Siberia) are situated in one of the earth's extreme continental settings around the 'cold pole' of the northern hemisphere. Strong seasonal climate gradients and longlasting periglacial conditions since about 2.5 myr have given rise to widespread and deep-reaching permafrost (Velichko and Nechaev, 2005). During the Quaternary glacial-interglacial climate cycles, the Yakutian landscape was sculptured by cryogenic processes, fluvial and aeolian activity, and lake formation. Local glaciations affected the Verkhoyansk Mountains and its foreland (e.g. Rusanov et al., 1967; Kind et al., 1971; Kind, 1975; Kolpakov, 1979; Péwé and Journaux, 1983; Zamoruyev, 2004).

The present paper focuses on sedimentological provenance studies of morainic, fluvial and loess-like sediments exposed along the tributaries of Lena and Aldan Rivers at the southwestern margin of the Verkhoyansk Mountains (Fig. 4.1), whose regional glaciation history and permafrost palaeoenvironment is being investigated by a joint

Russian-German research project (Stauch et al., 2005; Stauch et al., in press; Popp et al., 2006).

By using clay mineralogy and heavy-mineral analyses, the purpose of the study is to outline the mineralogical inventory of the different genetic sediment types and to discuss their origin in terms of palaeoenvironmental changes. The basis of our interpretations is provided by the mineralogical composition of recent fluvial sands that are supposed to reflect the average detrital source signals in the respective modern sedimentary catchment areas. Mineral assemblages from glacial tills and glaciofluvial outwash sediments of morainic arcs were investigated to constrain the palaeo-catchment areas of former glaciers in the Verkhoyansk Mountains and are tested for their potential as a stratigraphic tool for the correlation of distinct morainic stages observed between the studied river outcrops. Furthermore, detrital source signals in aquatic deposits of ancient river terraces that interfinger with glacial deposits are helpful to give insights into postulated displacements of the course of the Lena in the past (e.g. Kolpakov, 1986; Grigoriev et al., 1989; Alekseev and Drouchits, 2004).

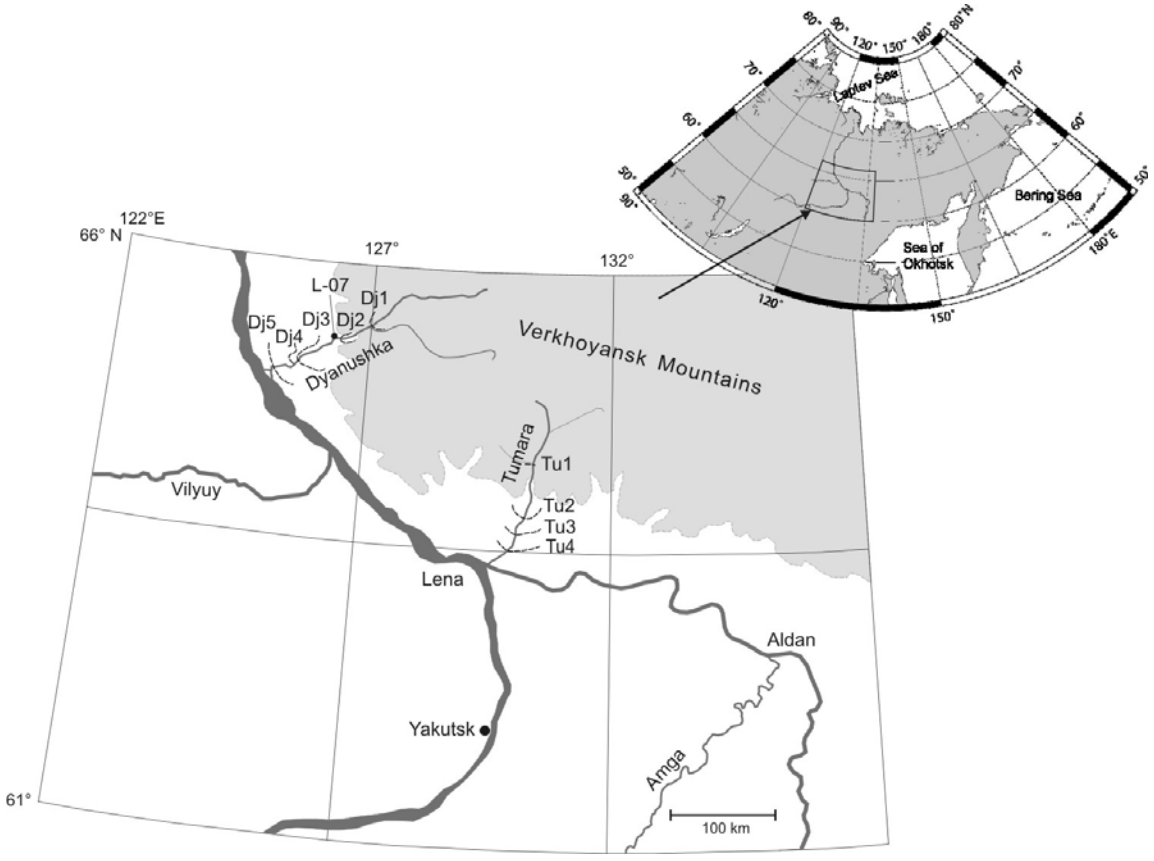

Fig. 4.1: Map of the study area in Central Yakutia, NE Siberia. The dotted lines delineate the terminal-moraine stages along Tumara and Dyanushka Rivers, according to Stauch et al. (in press).

4.2 Regional geology

The area of study stretches from the Verkhoyansk Mountains across the southwestern Verkhoyansk Foreland to the Lena and Aldan streams in Central Yakutia (Fig. 4.1). Field work took place in 2002 and 2003 along the Tumara River (64°N/130°E), a tributary of the Aldan, and along the Dyanushka River (65°N/126°E), a tributary of the Lena (Fig. 4.1). Both rivers originate in the Verkhoyansk Mountains and pass the glacially and periglacially formed foreland. The area is situated in the continuous permafrost zone, climatically characterised by a strong seasonal temperature gradient. Mean January and July temperatures of -41°C and +19°C, respectively, and a low mean annual precipitation of around 250 mm for the station in Yakutsk (Agriculture Atlas of the Republic Sakha (Yakutia), 1989) characterise the cold continental climate, presumably promoting physical weathering processes.

4.2.1 Prequaternary geology

Yakutia lies at the boundary of two major geotectonic provinces with diverse stratigraphic and lithological successions that influence the mineralogical inventory of modern river sediments in the area (Behrends et al., 1999; Peregovich et al., 1999): the Siberian Platform to the west and the Verkhoyansk-Kolymian Orogen to the east.

Crystalline basement rocks of the Siberian Platform are exposed on the Anabar Massif in the northwestern part of Yakutia and on the Aldan Shield in southeastern Yakutia (Fig. 4.2). The Aldan Shield represents the headwater region of the Aldan River and comprises Archaean metamorphic series with schist, gneiss, granulite, gabbro, amphibolite and metabasalt (Chain and Koronovskii, 1995). The Lena River originates in the southern margin of the Siberian Platform, around Lake Baikal, where crystalline rocks of the Trans-Baikal-Highlands comprise Proterozoic metamorphic rocks of green schist facies, amphibolite facies, clastic-carbonate series, and granitoids (Dolginow and Kropatschjow, 1994). In western Yakutia, flood-basalt successions form the upper parts of the Siberian Platform, uplifted during the Palaeozoic-Mesozoic transition. The Riphean to Cenozoic sedimentary cover rocks of the eastern margin of the Siberian Platform form the Yakutian lowland basin along the middle and lower courses of the Aldan and Lena Rivers, reaching a maximum thickness of up to 15 km in the Vilyuy Basin (Chain and Koronovskii, 1995).

The Verkhoyansk Mountains on the eastern margins of the Aldan and Lena Rivers are the topographic expression of the approximately 200 km wide Verkhoyansk fold-and-thrust belt (Fig. 4.2). It resulted from the collision of the North Asia Craton with the Kolyma-Omolon Microcontinent along the eastern margin of the Siberian Platform in Mesozoic times (Oxman, 2003; Parfenov, 1991). The lower stratigraphic units of the mountain belt are primarily composed of Riphean and Palaeozoic clastic rocks and carbonate series with inclusions of basic and intermediary tuffs and dykes. These units are overlain by continental to shallow marine sandstones, siltstones, and shales of Carboniferous to middle Jurassic age that are exposed along the Tumara and Dyanushka Rivers (Chain and Koronovskii, 1995; Parfenov, 1991). Granitoid intrusions occur in the eastern part of the Verkhoyansk fold-and-thrust belt and farther east within other geotectonic provinces of the Verkhoyansk-Kolymian Orogen (Oxman, 2003). To the

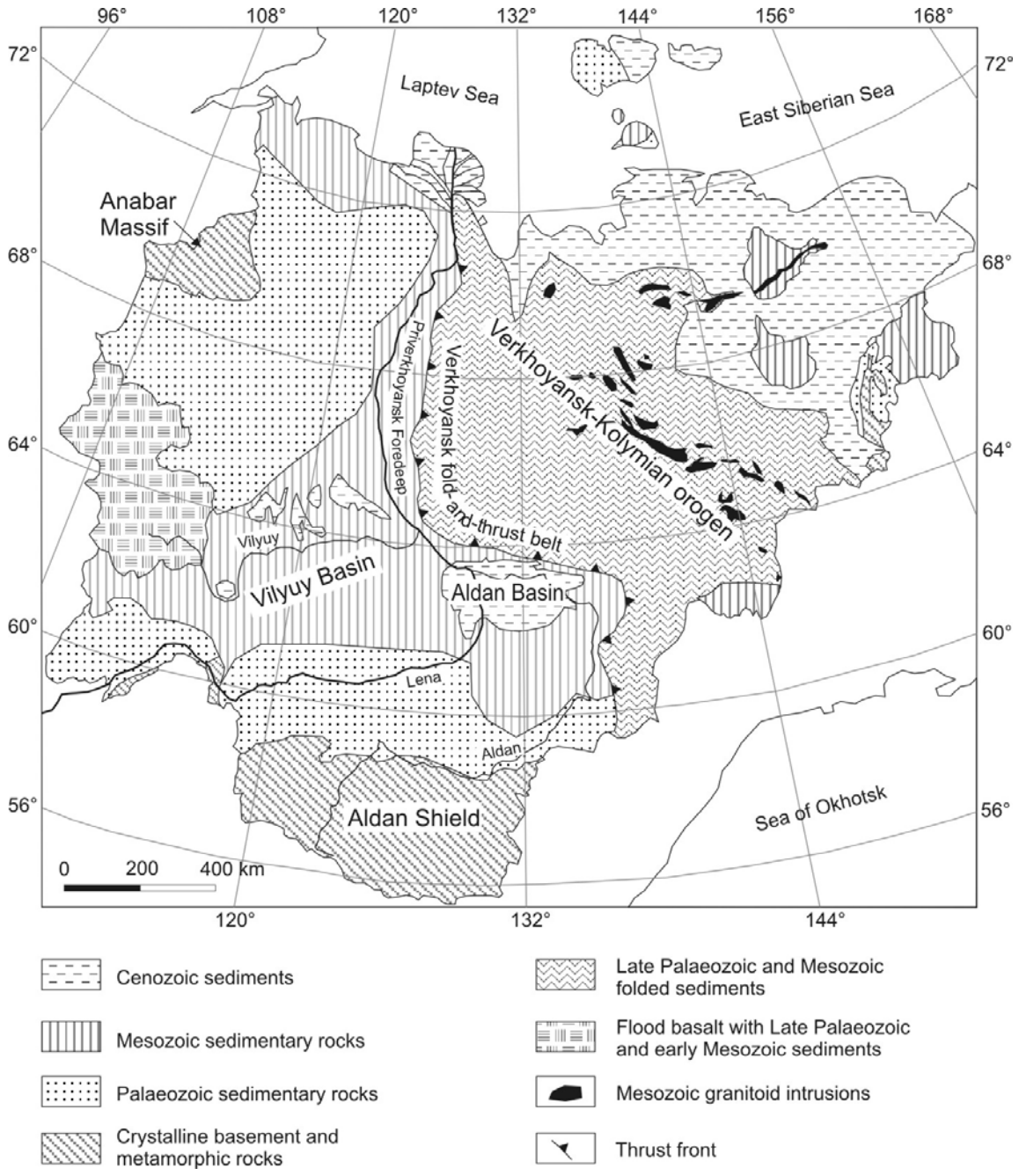

Fig. 4.2: Generalized geological map of the Sahka Republic (Yakutia) (after Sedenko *et al.* 2001).

west and southwest, the Verkhoyansk fold-and-thrust belt is bordered by the Priverkhoyansk Foredeep, a molasse basin that was filled with Cretaceous coal-bearing deposits, which were partly deformed and folded in the course of orogenesis of the Verkhoyansk Mountains (Parfenov, 1991).

Between the late Cretaceous and the Miocene, the area was subject to denudation, the formation of weathering crusts in the mountain areas as well as in the Lena-Aldan lowlands, where these processes prevailed during the Palaeogene (Rusanov et al., 1967; Chain and Koronovskii, 1995). By the end of the Palaeogene, the Aldan Basin

developed as an intra-continental tectonic depression along the lower Aldan River on the Priverkhoyansk Foredeep (Fig. 4.2) and was filled with several hundred metres of coal-bearing sands of Neogene age (Katasonov and Soloviev, 1969; Baranova, 1979; Grigoriev et al., 1989).

4.2.2 Quaternary geology of the Verkhoyansk Foreland

By the end of the Neogene, the Verkhoyansk Foreland, which includes the Priverkhoyansk Foredeep, was a plain of several tens of kilometres width. Periodic uplift along the foothills of the Verkhoyansk Mountains increased the erosional gradients between the mountains and the river basins of the Lena and Aldan streams (Kolpakov, 1984). At the same time, a cooling trend heralded the onset of the Pleistocene cold-continental climate. At least since the beginning of the middle Pleistocene, continuous and deep-reaching permafrost has been widespread in Yakutia (Fradkina et al., 2005).

During the Pleistocene, numerous fluvial terraces have developed in the Verkhoyansk Foreland along the Lena and Aldan Rivers and their tributaries (Table 4.1) (Alekseev, 1961; Rusanov et al., 1967; Soloviev, 1973; Péwé and Journaux, 1983). The older terraces usually comprise a pre-Quaternary basement that is covered by coarse alluvial sediments. The alluvial sediments of the middle terraces are in places intercalated with glacigenic sediments derived from the Verkhoyansk Mountains. The late Pleistocene terraces include redeposited morainic material between fluvial sands and gravel. Fluvial sediments of Holocene age make up the lowest terrace levels. The petrographic composition of the distinct alluvial sediments in the Verkhoyansk Foreland suggests that the Lena flowed eastward of the present course, about 50 km closer to the Verkhoyansk Mountains during the middle and late Pleistocene (Kind, 1975; Grigoriev et al., 1989; Alekseev and Drouchits, 2004).

Table 4.1: Classification of different terrace levels in Central Yakutia, according to the Russian literature (citation see text).

Terrace level (above modern river level)	Stratigraphy
80 – 200 m	Early Pleistocene – Neogene
40 – 80 m	Middle Pleistocene
15 – 25 m	Holocene – late Pleistocene

During the Quaternary, the Verkhoyansk Mountains were affected by several glaciations, as documented by well-preserved morainic arcs and till deposits in the Verkhoyansk Foreland (Katasonov, 1963; Kind et al., 1971; Kind, 1975; Kolpakov, 1979). According to the latter authors, glacier advances occurred in the middle Pleistocene and repeatedly during the early to late Weichselian (Table 4.2).

Most terraces and glacial deposits are covered by loess-like sediments with variable thickness between 0.5 m and 30 m (Katasonov, 1963; Péwé and Journaux, 1983). The origin of this so-called mantle loam has been a matter of debate for a long time, involving weathering, fluvial and lacustrine hypotheses. Péwé and Journaux (1983) and Kolpakov (1986), however, concluded that the silty deposits are primarily of aeolian origin, but in many places were modified by secondary slope processes, such as gelifluction and frost creep. Sediments may include high amounts of intergranular

ground ice due to migration of moisture into the ground towards the permafrost table. Massive ground ice also occurs in the sediments that have formed by repeated cracking of the ground and filling the thermal-contraction cracks with snowmelt during spring (Mackay, 1983, Romanovskii, 1985). During the Pleistocene, these processes resulted in the syngenetical accumulation of ice-rich sediments with large polygonal ice-wedge systems (Ice Complex or Yedoma), which are widely distributed in the lowlands of Yakutia (e.g. Gavrilov et al., 2003).

Table 4.2: Exposed glacial deposits along Tumara (Tu) and Dyanushka (Dj) Rivers (numbered from the youngest to the oldest), the related prevalent Russian stratigraphy, and the newly obtained IRLS dating results (citation see text).

Moraines	Russian stratigraphy	New age constrains
Tu1 / Dj1	Sartan (Late Weichselian, MIS 2)	> 50 ka
Tu2 / Dj2	Sartan (Late Weichselian, MIS 2)	?
Tu3 / Dj3	Sartan (Late Weichselian, MIS 2)	~87 ka
Tu4 / Dj4	Zhigansk (Middle Weichselian, MIS 3)	≥100 ka
- / Dj5	Not exposed	~135 – 140 ka

4.3 Material and methods

Outcrop

Samples were taken from outcrops along the riverbanks of Tumara and Dyanushka Rivers, as well as from modern Lena River sediments. Four sediment types have been differentiated, comprising (1) modern fluvial sands that are representative source indicators for the different catchment areas, (2) fluvial sand and gravel of river terraces ranging in age from Neogene to early Holocene, (3) loess-like sediments, and (4) morainic deposits. In this study, we deal with a total number of 83 samples, containing 12 samples of modern fluvial sands, 21 samples of morainic deposits, 36 samples of older river terraces (26 samples belong to the profil L-07), and 14 samples of loess-like deposits. The specifications of the studied samples are compiled in Table 4.3.

Sampling of medium and fine-grained fluvial sands has been performed on sand bars along the river courses. Older fluvial sediments were sampled from terraces at different elevations above the river level. A geological map of the area (Prokopiev et al., 1994) shows middle and late Pleistocene terraces cropping out along the rivers. The middle Pleistocene terraces were sampled at the lower river courses of Tumara and Dyanushka Rivers (up to 50 m above the river level). The late Pleistocene terraces comprise terrace levels of global Last Glacial Maximum (gLGM) age (10–20 m altitude above the modern valley floor) and a late glacial to early Holocene age (approximately up to 15 m in altitude) at the middle and lower courses of the Dyanushka River (Katasonov, 1963; Rusanov et al., 1967; Katasonov and Solovyev, 1969; Grigoriev et al., 1989). The late glacial to early Holocene terrace was sampled in detail, comprising an eight-meter thick sand profile (L-07) with marked colour changes in front of the mountain margin from a steep bank at Dyanushka River (Fig. 4.1).

Morainic deposits comprise both glacial diamictons and glaciofluvial outwash sands and gravels, which were sampled along riverbanks and in thermokarst pits at locations, shown in Fig. 4.1. Samples were taken from the sand- to clay-sized matrix of the sediments.

Table 4.3: Specifications of studied samples. Information on the geological formation and age assignments are adopted from the geological map and after Kind (1975), the latter marked by the *symbol. The second age[1)] column presents newly obtained age data according to Stauch et al. (in press) and radiocarbon dating results (this study), marked by the #symbol.

Geological Unit/ Sediment type	Sample No.	Formation according to the geological map	Age	Age [1)]	Coordinates Northing/Easting
Modern fluvial sands					
Tumara River	Di-02/07/19_02	recent fluvial sand	-	-	64°35'N/130°38'E
Tumara River	Di-02/07/21-04	recent fluvial sand	-	-	64°26'N/130°43'E
Tumara River	Di-02/07/25-01	recent fluvial sand	-	-	64°21'N/130°26'E
Tumara River	Di-02/07/26_02	recent fluvial sand	-	-	64°07'N/130°23'E
Dyanushka R.	Di-03/08/17-01	recent fluvial sand	-	-	65°31'N/127°06'E
Dyanushka R.	Di-03/08/19-03	recent fluvial sand	-	-	65°27'N/126°58'E
Dyanushka R.	Di-03/08/19-04	recent fluvial sand	-	-	65°27'N/126°58'E
Dyanushka R.	Di-03/09/05-01	recent fluvial sand	-	-	65°01'N/125°06'E
Lena River	Di-02/07/14_01	recent fluvial sand	-	-	62°02'N/129°44'E
Lena River	Di-03/09/07-03	recent fluvial sand	-	-	64°60'N/124°58'E
Lena River	Di-03/09/07-04	recent fluvial sand	-	-	64°60'N/124°58'E
Aldan River	Di-02/08/07_01	recent fluvial sand	-	-	63°27'N/129°35'E
Morainic deposits					
Diamicton Tu1	Di-02/07/25_02	Sartansk Horizon	28-18 ka BP	>53 ka BP	64°19'N/130°24'E
Glaciofluvial outwash Tu2	TUM-M1-W_Graukies_O	Segemdin Stadial (Sartan)	~15 ka BP *	-	63°51'N/130°18'E
Diamicton Tu3	Di-02/07/31_01	lower Sartan Stadials	26-19 ka BP *	~87 ka BP	63°49'N/130°17'E
Diamicton Tu3	Di-02/07/31_02	lower Sartan Stadials	26-19 ka BP *	~87 ka BP	63°49'N/130°17'E
Diamicton Tu3	Di-02/07/31_07	lower Sartan Stadials	26-19 ka BP *	~87 ka BP	63°49'N/130°17'E
Diamicton Tu3	Di-02/08/01_02	lower Sartan Stadials	26-19 ka BP *	~87 ka BP	63°47'N/130°10'E
Glaciofluvial outwash Tu3	Di-02/07/31_04	lower Sartan Stadials	26-19 ka BP *	≤87 ka BP	63°49'N/130°17'E
Diamicton Tu4	Di-02/08/03_01	Zhigansk Stadial	33-30 ka BP *	>100 ka BP	63°42'N/130°10'E
Diamicton Tu4	Di-02/08/03_03	Zhigansk Stadial	33-30 ka BP *	>100 ka BP	63°42'N/130°10'E
Diamicton Dj1	Di-03/08/19-01	Sartan Horizon	28-18 ka BP	>40 ka BP	65°27'N/126°58'E
Diamicton Dj1	Di-03/08/19-02	Sartan Horizon	28-18 ka BP	>40 ka BP	65°27'N/126°58'E
Diamicton Dj2	Di-03/08/23-03	Sartan Horizon	28-18 ka BP	-	65°20'N/126°28'E
Diamicton Dj2	Di-03/08/24-03	Sartan Horizon	28-18 ka BP	-	65°21'N/126°16'E
Diamicton Dj3	Di-03/08/30-07	lower Sartan Stadials	26-19 ka BP *	<92 ka BP	65°09'N/125°33'E
Diamicton Dj4	Di-03/08/30-12	Zhigansk Stadial	33-30 ka BP *	>100 ka BP	65°05'N/125°30'E
Diamicton Dj4	Di-03/08/30-13	Zhigansk Stadial	33-30 ka BP *	>100 ka BP	65°05'N/125°30'E
Diamicton Dj4	Di-03/08/30-14	Zhigansk Stadial	33-30 ka BP *	>100 ka BP	65°05'N/125°30'E
Diamicton Dj5	Di-03/09/04-05	Samarov Horizon	Mid-Pleistocene	140-135 ka	65°01'N/125°06'E
Diamicton Dj5	Di-03/09/04-06	Samarov Horizon	Mid-Pleistocene	140-135 ka	65°01'N/125°06'E
Diamicton Dj5	Di-03/09/04-04	Samarov Horizon	Mid-Pleistocene	140-135 ka	65°01'N/125°06'E
Diamicton Dj5	Di-03/09/04-03	Samarov Horizon	Mid-Pleistocene	140-135 ka	65°01'N/125°06'E
Terrace deposits					
Pleistocene sand on Neogene	Di-02/08/04_09	Tustakh Facies	upper Eopleistocene	>100 ka BP	63°37'N/129°58'E
Pleist. gravel on Neogene	Di-02/08/04_05	Tustakh Facies	upper Eopleistocene	>100 ka BP	63°37'N/129°58'E
Neogene sand	Di-02/08/04_01	Mamontovy Khayata Horizon	middle Miocene	-	63°37'N/129°58'E
Pleistocene sand	Di-03/08/22-07	Sartan Horizon	28-18 ka BP	≥17 ka BP #	65°21'N/126°37'E
Loess-like silt	L07-1 / 0-10	Sartan - Early Holocene	11-9 ka BP	-	65°20'N/126°14'E
Loess-like silt	L07-1 / 40-45	"	"	-	"

Table 4.3 (Continued)

Geological Sediment type	Sample No.	Formation according to the geological map	Age	Age [1)]	Coordinates Northing/Easting
Loess-like silt	L07-1 / 95-100	Sartan - Early Holocene	11-9 ka BP	-	65°20'N/126°14'E
Fluvial sand	L07-1 / 155-160	"	"	~11 ka BP #	"
Fluvial sand	L07-1 / 170-175	"	"	~13 ka BP #	"
Fluvial sand	L07-1 / 200-205	"	"	-	"
Fluvial sand	L07-1 / 225-230	"	"	-	"
Fluvial sand	L07-1 / 270-275	"	"	-	"
Fluvial sand	L07-1 / 320-325	"	"	-	"
Fluvial sand	L07-1 / 340-345	"	"	-	"
Fluvial sand	L07-1 / 355-360	"	"	~10.7 ka BP #	"
Fluvial sand	L07-1 / 385-390	"	"	-	"
Fluvial sand	L07-1 / 430-435	"	"	-	"
Fluvial sand	L07-1 / 465-470	"	"	-	"
Fluvial sand	L07-1 / 510-515	"	"	-	"
Fluvial sand	L07-1 / 525-535	"	"	~44 ka BP #	"
Fluvial sand	L07-1 / 535-545	"	"	-	"
Fluvial sand	L07-1 / 545-555	"	"	-	"
Fluvial sand	L07-1 / 555-560	"	"	-	"
Fluvial sand	L07-1 / 575-580	"	"	~14 ka BP #	"
Fluvial sand	L07-1 / 610-615	"	"	-	"
Fluvial sand	L07-1 / 650-655	"	"	-	"
Fluvial sand	L07-1 / 700-705	"	"	-	"
Fluvial sand	L07-1 / 740-745	"	"	-	"
Fluvial sand	L07-1 / 780-785	"	"	~37 ka BP	"
Fluvial sand	L07-1 / 800-810	"	"	~9.5 ka BP #	"
Fluvial sand	L09-1 / 265-270	Segemdin Stadial (Sartan)	~15 ka BP *	<14 ka BP #	65°10'N/125°42'E
Fluvial sand	L09-1 / 165-170	Segemdin Stadial (Sartan)	~15 ka BP *	<14 ka BP #	65°10'N/125°42'E
Sand, silty L12	Di-03/09/01_02	Sartan - Early Holocene	11-9 ka BP	-	65°03'N/125°27'E
Gravel, sandy L14	Di-03/09/04_20	Tobol H., Bestyakhsker Facies	middle Pleistocene	>100 ka BP	65°01'N/125°06'E
Sand, silty L14	Di-03/09/04_23	Tobol H., Bestyakhsker Facies	middle Pleistocene	>100 ka BP	65°01'N/125°06'E
Sand L14	Di-03/09/04_26	Tobol H., Bestyakhsker Facies	middle Pleistocene	>100 ka BP	65°01'N/125°06'E
Loess-like deposits					
Silt, sandy Tu1	Di-02/07/23_02/045	Sartan Horizon	28-18 ka BP	12-9 ka BP	64°20'N/130°24'E
Silt, sandy Tu2	Tum-M1-W-1.0	Segemdin Stadial (Sartan)	~15 ka BP *	~19 ka BP	63°51'N/130°18'E
Silt, sandy Tu2	Tum-M1-W-9.2	Segemdin Stadial (Sartan)	~15 ka BP *	~27 ka BP	63°51'N/130°18'E
Silt on Neogene	P III 100	Muruktin-Kargin Horizon	49-32 ka BP	50-9 ka BP	63°37'N/129°58'E
Silt Dj1	Di-03/08/19-07	Sartan Horizon	28-18 ka BP	11 ka BP	65°27'N/126°58'E
Silt Dj1	Di-03/08/19-08	Sartan Horizon	28-18 ka BP	11 ka BP	65°27'N/126°58'E
Silt Dj1	Di-03/08/19-09	Sartan Horizon	28-18 ka BP	11 ka BP	65°27'N/126°58'E
Silt Dj2	Di-03/08/23-04	Sartan Horizon	28-18 ka BP	10 ka BP	65°20'N/126°28'E
Silt Dj2	Di-03/08/23-05	Sartan Horizon	28-18 ka BP	10 ka BP	65°20'N/126°28'E
Silt Dj3	Di-03/08/30-09	above lower Sartan Stadials	<19 ka BP	~27 ka BP	65°08'N/125°33'E
Silt Dj4	Di-03/08/31-03	above Zhigansk Stadial	<30 ka BP	32-13 ka BP	65°04'N/125°31'E
Silt Dj4	Di-03/08/31-04	above Zhigansk Stadial	<30 ka BP	32-13 ka BP	65°04'N/125°31'E
Silt Dj5	Di-03/09/03-01	Muruktin-Kargin Horizon	49-32 ka BP	-	65°01'N/125°06'E
Silt Dj5	Di-03/09/03-05	Muruktin-Kargin Horizon	49-32 ka BP	-	65°01'N/125°06'E

Loess-like sediments were sampled in the immediate vicinity of the morainic deposits from fresh outcrops and dug holes, avoiding sections that were strongly modified by soil-forming processes.

Laboratory

After disaggregation and removal of organic matter of bulk samples in 10% hydrogen peroxide solution, wet-sieving at 63 µm was performed in order to separate silt and clay from sand and gravel. Further grain size separations were achieved by Stokes' law settling procedure in 'Atterberg' tubes (silt and clay) and dry-sieving in whole Phi-steps with 'Sonic shifter' (sand and gravel). In this paper, the grain-size data are only discussed as far as they are needed for the interpretation of sediment provenance.

Heavy-mineral analysis was conducted on the very fine sand fraction (63-125 µm). Sample preparation and analysis followed standard procedures outlined in relevant text books (Boenigk, 1983; Mange and Maurer, 1991). The heavy minerals were obtained by density separation in a centrifuge, dispersed in sodium metatungstate solution (density of 2.89 g cm^{-3}). For optical identification under a polarization microscope, the heavy fraction was mounted with Meltmount (refraction index = 1.68). Per sample, we tried to count at least 100 translucent grains, which was not always achieved owing to a lot of weathered grains. We are aware that this relatively low number of grains may be of low statistical confidence. However, empirical studies have revealed that the statistical error produced by counting only 100 grains still ranges below the compositional variability of natural samples from distinct geological sections (Boenigk, 1983). Approximately one third of the studied samples present less than 100 counts, the average grain number of two third of the samples amounts to 150. The counting results are expressed as frequency grain percentages (Figs. 4.3 to 4.6).

The clay fraction was analysed with an X-ray diffraction device (Philips PW 1830). Step scan measurements were run with CoK_{α} radiation (40 kV, 40 mA) from 2-18°2θ in a 0.02° 2θ/s mode for air-dried samples. Additionally, glycolated samples were analysed from 2-40°2θ in 0.02° 2θ/s and 0.005° 2θ/s mode in order to differentiate between expandable clay minerals (mainly smectite), chlorite and the kaolinite-chlorite double peak. The semi-quantitative evaluation of the X-ray diffractograms followed techniques adopted from marine studies, which are explained in detail elsewhere (e.g. Biscaye, 1965; Ehrmann et al., 1992; Petschick et al., 1996; Kuhn and Diekmann, 2002). Mineral proportions are calculated from weighted peak areas, and the relative abundance of the clay-mineral groups in the clay fraction is summed to 100% using standard weighting factors (Biscaye, 1965): the 17-Å peak area *1 for smectite, the 10-Å peak area *4 for illite, and the 7-Å peak area *2 for kaolinite and chlorite subdivided in proportion to the relative areas of their 3.57-Å and 3.54-Å peaks, respectively. Relative analytical precision is 6-9% for major clay components and 8-14% for minor clay components (Ehrmann et al., 1992).

4.4 Results

Heavy-mineral assemblages

Heavy-mineral grains appear in typical shapes, as described in petrographic text books (Boenigk, 1983; Mange and Maurer, 1991). Fluvial and glacial samples from the Verkhoyansk Mountain area, however, contain a lot of oxidized and weathered grains that are hard to identify.

We carried out a conventional joining cluster analysis to define heavy-mineral assemblages (Swan and Sandilands, 1995). A similarity matrix based on Euclidian distance calculations and Ward's linkage method was applied for sample clustering, following routines of the commercial 'STATISTICA' software. The cluster analysis was used to obtain specific associations and key species of the observed heavy-mineral spectra. Only unaltered translucent heavy minerals were used for this statistical approach. The results show that the heavy-mineral inventory of the various sediment types can be pooled to distinct assemblages, even though the genesis of the sediments is different. Four different clusters can be distinguished (Fig. 4.3). In the following description of the clusters, we refer to mean heavy-mineral percentages.

Cluster 1: This cluster is clearly dominated by the stable heavy minerals zircon, tourmaline and rutile (ZTR, ~60%), followed by apatite (~15%) and clinopyroxene (~9%). The assemblage comprises modern fluvial sands of the Tumara and Dyanushka Rivers as well as four samples from the L-07 sand sequence. Furthermore, loess-like deposits at the Tu1 and Dj1 moraines, morainic deposits of the Tu2 moraine and Pleistocene gravel from the lower reaches of Tumara River are also related to this cluster.

Cluster 2: This assemblage differs from the previous cluster by a high percentage of garnet (~29%) and a lower amount of stable heavy minerals (ZTR, ~28%). With exception of a higher amount of amphibole (~10%), the remaining heavy minerals occur in similar abundance as in Cluster 1. Only morainic deposits of the Tu1 and Tu3 moraines characterise the assemblage.

Cluster 3: The key minerals of this cluster are apatite (~34%), ZTR (~30%), and clinopyroxene (~17%), associated with epidote (~10%). Modern fluvial sand samples from the Tumara and Dyanushka Rivers are included. Other related sediment types are morainic deposits of the Tu4, Dj1, and Dj2 moraines, loess-like deposits of the Tu2 and Dj2 moraines, as well as almost the complete sample set from the L-07 sand profile. Some samples of this sequence as well as morainic deposits of the Dj1 and Dj2-moraine, loess-like deposits at Dj2-moraine and a modern sand sample of Dyanushka River present a high percentage of clinopyroxene (29-40%).

Cluster 4: In contrast to the previous clusters, this assemblage is defined by high amounts of hornblende (~38%) and the frequent presence of orthopyroxene (~8%) as well as low proportions of apatite (~5%) and stable heavy minerals (~6%). Another key mineral is garnet (~13%). Cluster 4 is shared by various sediment types, comprising modern Lena sands, the old morainic deposits along the Tumara and Dyanushka (Tu4, Dj3-Dj5), as well as Neogene and younger overlying fluvial and loess-like sediments from the lower reaches of the Tumara River.

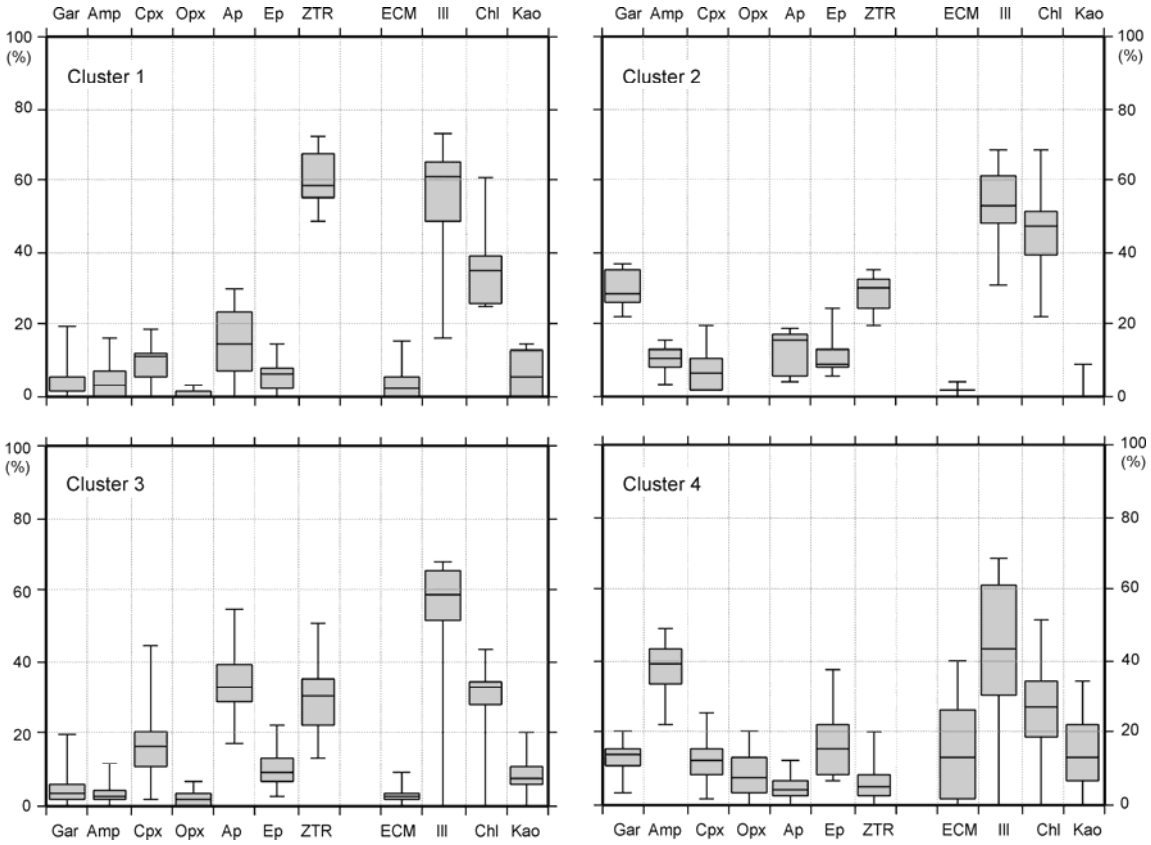

Fig. 4.3: Compositional variations of heavy-mineral assemblages as inferred from the cluster analysis in comparison with the respective clay-mineral composition. The boxes enclose 50% of the data with the median value of the mineral displayed as a line. The top and the bottom of the box mark the limit of ±25% of the mineral population. The extending lines mark the minimum and maximum values of the populations. Abbreviations: gar = garnet, amp = amphibole, cpx = clinopyroxene, opx = orthopyroxene, ap = apatite, ep = epidote, ZTR = zircon+tourmaline+rutile, KAST = kyanite+andalusite+staurolite+ titanite, ECM = expandable clay minerals, ill = illite, chl = chlorite, kao = kaolinite.

Clay mineralogy

The clay-mineral spectrum of the studied sediments is mostly dominated by illite (25-60%) and chlorite (20-50%) with low amounts of kaolinite (<20%) and expandable clay minerals (<25%). In comparison with the inferred heavy-mineral clusters, the increased amounts of kaolinite and expandable clay minerals are generally associated with the sediment types of Cluster 4, whereas the sediment types of the other clusters are barren or only include trace amounts of both clay minerals and cannot be clearly distinguished in terms of clay mineralogy. However, a rough regional differentiation of clay-mineral provinces is indicated by the absence of kaolinite and expandable clay minerals in most deposits along the middle and upper reaches of Tumara, whereas ubiquitous amounts of both appear along the Dyanushka. Highest amounts of the two clay minerals always appear in sediments of the Verkhoyansk Foreland situated close to the Lena River.

4.5 Data interpretation and discussion

The interpretation of heavy-mineral assemblages and the clay mineralogy of the Quaternary fluvial, glacial, and aeolian sediments in the Verkhoyansk Mountains and its

foreland indicate their provenance from two different geological provinces. The sediments basically consist of mixtures of detrital material derived from the local sources of the Verkhoyansk Mountain range and supra-regional material, which originates from the vast catchment area of the Aldan and Lena streams and shows signs of multiple recycling. In the following sections, we will explain the mineralogical source indicators and discuss the provenance signals of the different genetic sediment types in respect to palaeoenvironmental conditions.

4.5.1 Sediment provenance

Verkhoyansk Area

Dominant sediment supply from the Verkhoyansk Mountains is indicated by the heavy-mineral assemblages of clusters 1 to 3 and by the dominance of illit and chlorite clay minerals (Fig. 4.3). High concentrations of the stable heavy minerals zircon, rutile and tourmaline are considered as recycled components of the Siberian craton that were redeposited and mechanically enriched at the former continental margin of the craton during the Paleozoic to Mesozoic. Today, these deposits comprise the highly indurated sandstone and shale sequences of the Verkhoyansk Mountains.

The high percentages of apatite in Cluster 3 may point to source signals from either magmatic intrusions (granitoids), which are locally present in the Dyanushka hinterland, or more likely from apatite-bearing calcareous concretions, which are frequently hosted in Triassic sedimentary rocks. The latter possibility can also explain the appearance of carbonate particles in the deposits of the Dj1 moraine.

Clinopyroxene can be related to the presence of volcanic dykes and porphyrites, intercalated in some stratigraphic units of the Verkhoyansk Mountains. The high abundance of garnet in Cluster 2 is most likely related to sediment provenance from garnet-rich Jurassic rocks that are widely distributed along the mountain margin at Tumara River (Kossovskaya et al., 1960). The chlorite- and illite- dominated clay-mineral composition of Quaternary sediments derived from the Verkhoyansk Mountain range is consistent with the high diagenetic consolidation of the exposed clastic series. The presence of small amounts of kaolinite and expandable clay minerals in some Quaternary sediments of the Dyanushka area points to the local erosion of Tertiary soil remnants in the hinterland (Rusanov et al., 1967; Chain and Koronovskii, 1995).

Lena-Aldan catchment area

Sediment supply from the large catchment area of the Aldan and Lena streams is indicated by the heavy-mineral assemblage of Cluster 4 with high amounts of amphibole (green hornblende), pyroxene, and garnet as well as relatively high abundances of kaolinite and expandable clay minerals (Figs. 4.3, 4.4). The Precambrian crystalline rocks of the Aldan Shield and the Trans-Baikal-Highlands are considered as primary source rocks of the heavy-mineral inventory of Aldan and Lena Rivers. The metamorphic source areas also account for epidote in the Lena and Aldan sediments. A distinction of Aldan and Lena provenance is given through higher proportions of orthopyroxene in Aldan sediments and different geochemical compositions of amphibol

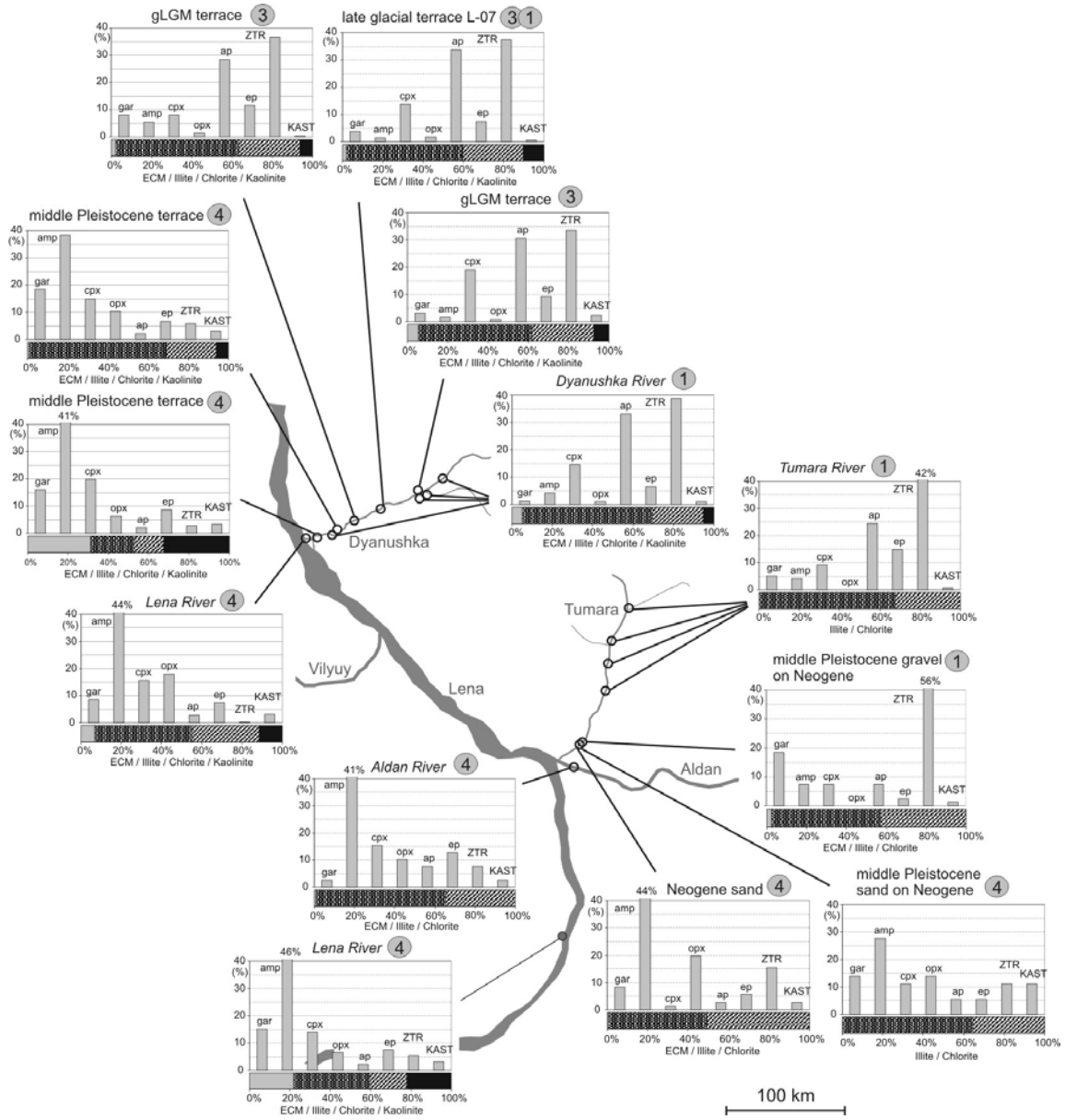

Fig. 4.4: Provenance signature (heavy minerals and clay mineralogy) of modern fluvial sands of Lena, Aldan, Tumara and Dyanushka Rivers and Quaternary alluvial as well as Neogene sediments. The circles indicate the sample position and the numbers above the diagrams refer to the respective heavy-mineral cluster of the sample. Abbreviations: gar = garnet, amp = amphibole, cpx = clinopyroxene, opx = orthopyroxene, ap = apatite, ep = epidote, ZTR = zircon+tourmaline+rutile, KAST = kyanite+andalusite+staurolite+titanite, ECM = expandable clay minerals.

and garnet (Hoops, 1999). The second largest tributary farther downstream, the Vilyuy River, provides abundant pyroxene to the Lena River (Hoops, 1999).

A distinctive feature of the sediments derived from Lena and Aldan sources are increased proportions of kaolinite and expandable clay minerals. Since the Quaternary climate conditions have not been favourable for the genesis of pedogenic clay minerals, the increased amounts of kaolinite and expandable clay minerals in modern river sands and terrace deposits point to the intermittent storage and recycling of late Mesozoic and

Cenozoic sediments in the central Yakutian denudation-accumulation plains. In particular, the coal-bearing clastic series and Neogene "Red Sands" are often associated with kaolinite and expandable clay minerals, which may be reworked in Quaternary sediments (Alekseev et al., 1990).

4.5.2 Source signals of the morainic deposits

The mineralogical composition of morainic deposits along the Tumara and Dyanushka Rivers is heterogenous in space and time (Fig. 4.5). Along the Tumara River, the moraines (Tu1-Tu4) are primarily composed of heavy-mineral assemblages of clusters 1 and 2 and are almost barren of kaolinite and expandable clay minerals, being consistent with dominant glacigenic sediment supply from the Verkhoyansk Mountains. In comparison with modern fluvial sands of the Tumara River, however, the moraines of the Tumara area generally include increased portions of garnet. The enrichment of garnet may be both the result of glacial erosion of underlying garnet-bearing Cenozoic sediments of Lena-Aldan origin in the Verkhoyansk Foreland and a secondary feature, explained by selective transport processes and multiple sediment recycling of glacial sediments, which has been observed frequently (Gravenor, 1979; Diekmann and Wopfner, 1996; Diekmann and Kuhn, 1999). In the study area, multiple recycling actually is indicated by the presence of abundant rounded and striated glacial clasts in the morainic sediments.

However, the assumption of erosion and reworking of the underlying Cenozoic sediments does not sustain because of only little amounts of amphibole and orthopyroxene in the moraines Tu1 to Tu3 (Fig. 4.5). Moreover, the fact that garnet is less dominant in Dyanushka than in Tumara moraines argues against a primary secondary garnet enrichment. Most likely, the enrichment of garnet in the Tumara moraines is thus related to the glacial erosion of nearby upper Jurassic rocks cropping out widely in the low hills along the mountain margin (Kossovskaya et al., 1960), whereas the garnet signal in modern river sands of Tumara is only evident in a sample in the immediate vicinity of the Jurassic outcrops.

Generally, the mineralogical composition of the morainic deposits along the Dyanushka River is less uniform than of those along the Tumara River. The Dj1 and Dj2 moraines, which are situated within the Verkhoyansk Mountains, clearly document sediment provenance from the adjacent mountains, as indicated by clay mineralogy and the heavy-mineral assemblages of Cluster 3. In contrast, the morainic deposits and basal tills of the foreland (Dj3-Dj5) exhibit mineralogical source signals of Lena-Aldan provenance with abundant hornblende, orthopyroxene and kaolinite, which are very likely reworked from older underlying sediments.

In summary, an important finding is that the mineral composition does not allow a correlation of the morainic deposits of distinct glacial stages between Dyanushka and Tumara areas, as defined by Stauch et al. (2005).

4.5.3 Source signals of the loess-like deposits

Loess-like deposits along the studied rivers exhibit spatial differences in sediment provenance (Fig. 4.5). Covering the younger moraines in the Tumara and Dyanushka

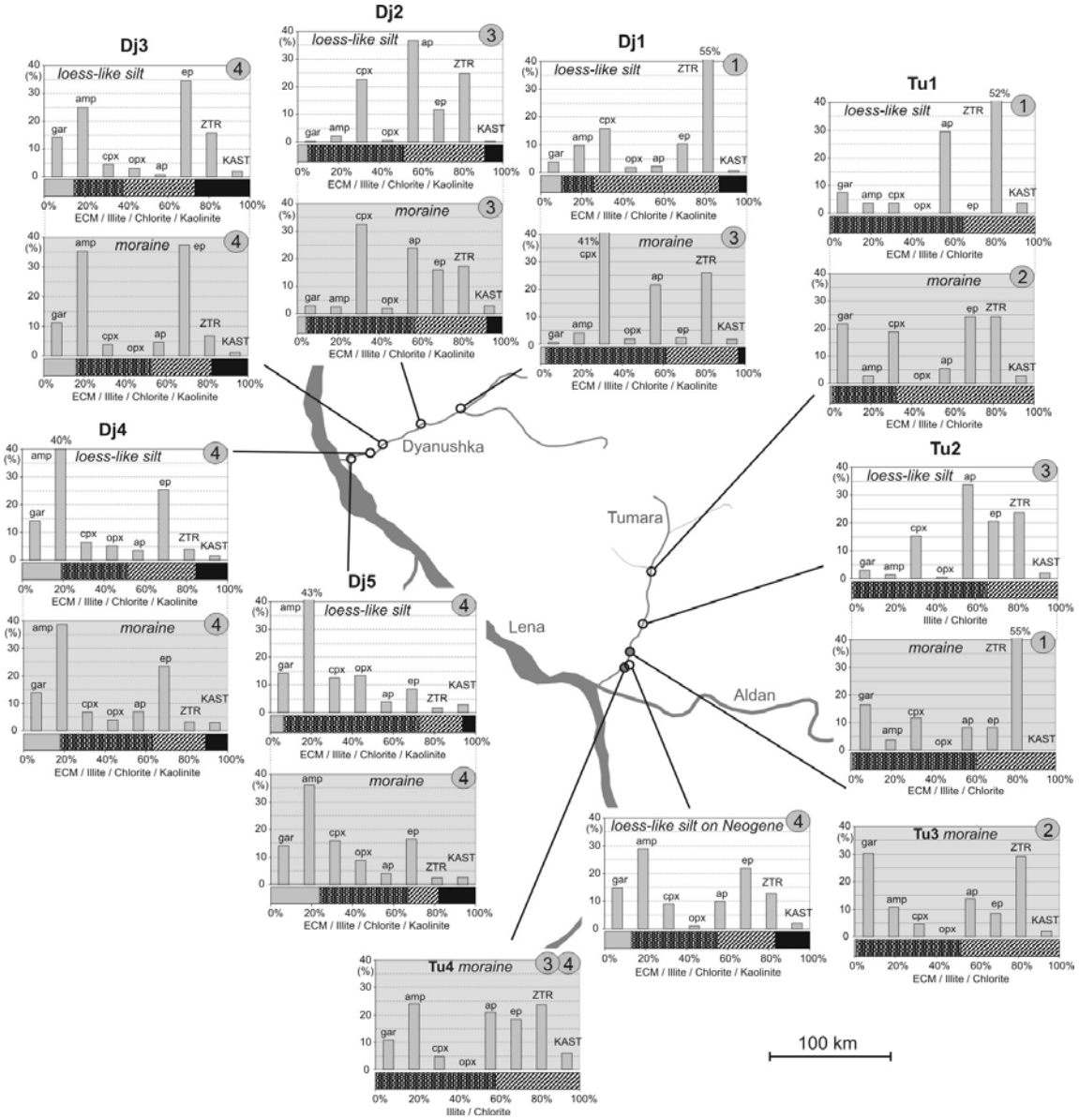

Fig. 4.5: Provenance signature (heavy minerals and clay mineralogy) of morainic deposits (grey shaded diagrams) and loess-like sediments along Tumara and Dyanushka Rivers. The circles indicate the sample position of both the morainic and the loess-like sediments, with the exception of the "Tu3" and "Tu4" moraines and "loess-like silt on Neogene", which are displayed in single diagrams. The reference to the respective cluster is given by the encircled number in the diagrams. The abbreviations for the mineral names are valid as used in Figure 4.4.

areas (Dj1, Dj2, Tu1, Tu2), the heavy-mineral assemblages of the clusters 1 and 3 and the clay mineralogy with low concentrations of kaolinite and expandable clay minerals are consistent with nearby sediment sources from the mountain areas. Closer to the Aldan and Lena Rivers, loess-like sediments mantling the older moraines and the Lena terraces show increased percentages of Lena-Aldan indicator minerals, such as hornblende, garnet and significant proportions of orthopyroxene as well as kaolinite and expandable clay minerals. Given a dominant aeolian origin of the Weichselian loess-like sediments (Péwé and Journaux, 1983), the marked differences in sediment

provenance possibly point to local sediment sources and short-distance transport of the dust components.

The deposition of loess-like sediments took place during a time of stronger aridity and sparser vegetation cover than today, as revealed by a pollen record of a loess sequence at the lower Tumara River (Müller et al., 2004). At that site, a steppe-like environment with shrubby tundra communities existed between 50 and 30 ^{14}C ka BP, while the most severe climate conditions and the lowest vegetation covers are documented for the gLGM. Exposed fluvial accumulation plains with sand and silt surfaces are considered as major targets for aeolian deflation. According to our provenance data, the braided Lena River has been the main source for wind-blown material in the Verkhoyansk Foreland. In the Verkhoyansk Mountains, the tributaries of the Lena River form braided-river systems with additional deflation plains. The provenance signals in loess-like sediments in the mountain area along the Tumara and Dyanushka Rivers point to the mixing of subordinate wind-blown material from the Lena River with silty materials from mostly local sources in the mountain valleys. Local periglacial slope processes, which may modify the primary aeolian sediment texture have no significant impact on the provenance signature of the loess-like material.

4.5.4 Source signals of alluvial terrace deposits

In the study area, the oldest and most widely distributed terrace level is the 50 m high middle Pleistocene terrace (Rusanov et al., 1967). Along the Tumara River, this middle Pleistocene level extends from the mountain margin to the sub-recent alluvial plain of the Aldan Valley and is covered by morainic deposits (Katasonov, 1963). At the lower reaches of the Tumara River, its base comprises Neogene sands covered by interfingering sand and gravel successions of early to middle Pleistocene age. The terrace sands reveal a distinct Aldan source signal with high amounts of hornblende and orthopyroxene, whereas the gravel possibly represent glaciofluvial outwash deposits, as they show mineralogical affinities to mountain sources (Fig. 4.4).

At the Dyanushka River, the middle Pleistocene terrace is exposed along the lower riverbanks. Close to the Lena valley, the terrace sands interlock with basal tills of the Dj5 moraine stage, dated to 140 and 135 ka BP (Stauch et al., in press). Between the Dj5 and the Dj3 moraines, yellowish fluvial sands in different elevations crop out, likely related to the middle Pleistocene, or in the case of the accumulation on the Dj4 moraine, to an early Weichselian terrace level. The heavy-mineral assemblage of Cluster 4 clearly points to a Lena origin of these yellowish fluvial sands, implying a stream course closer to the mountains. A long-term displacement of the Lena-Aldan course away from the mountains to the recent pathways was already described by some Russian studies (Kolpakov, 1986; Grigoriev et al., 1989; Alekseev and Drouchits, 2004). The reason for the displacement, however, is so far not fully understood, but tectonic movements and climatic causes might have played a major role. According to the new dating results of morainic deposits in the Verkhoyansk Foreland (Table 4.2) (Stauch et al., 2005; Stauch et al., in press.), the latest fluvial sedimentation of Lena River farther east of its recent pathway is indicated for the early late Pleistocene.

The late Weichselian terrace levels of gLGM and late glacial age in the foreland, which are exposed along the lower and middle Dyanushka, generally reveal a mountain influence (high amounts of stable heavy minerals).

Indicators of environmental change in alluvial sediments

In the late glacial to early Holocene terrace, which is exposed at the Dyanushka profile L-07 (Fig. 4.6), a yellowish sand layer seems to represent a short-term event of environmental change that caused an enhanced sediment supply of Lena origin. Temporarily damming events of the Lena River caused by progressing glaciers are supposed to have taken place during the middle Pleistocene glaciations (Kolpakov, 1986; Grigoriev et al., 1989; Alekseev and Drouchits, 2004). A similar process might have taken place during late glacial times in northern Yakutia, as revealed by a freshwater event recorded in marine sediments of the Laptev Sea (Spielhagen et al., 2005). The latter authors postulate that an outstanding anomaly in a foraminiferal stable oxygen isotope record around 13 cal-ka BP gives evidence of a rapid outburst of large amounts of fresh water, which likely were linked with an ice-dammed lake in the hinterland of the Lena valley.

With regard to such a damming event, the late glacial sediment sequence of profile L-07 was studied in detail. Underlain by coarse gravel, the terrace succession is dominated by dark greyish, fluvial sands with varying proportions of silt and clay, topped by loess-like sediments with intercalated peat horizons (Fig. 4.6). Throughout the succession, sediment provenance from the adjacent Verkhoyansk Mountains prevailed, as documented by the heavy-mineral assemblages of clusters 1 and 3 as well as by dominant illite and chlorite amounts in the clay fraction. Between 5.1 and 5.6 m profile depth, however, the yellow coloured sand layer shows increased percentages of garnet, hornblende and orthopyroxene as well as kaolinite (Fig. 4.6) indicating a distinct signal of increased Lena sediment influence in this stratum.

The age of the terrace deposits, late glacial to early Holocene according to the geological map, is confirmed by the new dating results, embracing the timing of the fresh-water event in the Laptev Sea. However, the exact age for the yellowish sand layer is hard to ascertain, because of contradictory results from infrared stimulated luminescence (IRSL) datings (Stauch et al., in press) and ^{14}C ages that do not reveal a coherent age-depth relationship (Fig. 4.6). We feel certain about the dating at the silt-sand transition at 1.1 m profile depth, determined as the Pleistocene-Holocene transition around 10 ka by both radiocarbon and IRSL technique. The onset of sand accumulation at 8.0 m depth, however, is marked by two different ages. The IRSL dating results in an age around 37 ka while the radiocarbon dating gives an age of 10–9 ka, which seems to be questionable in comparison with the youngest sand layers. The old radiocarbon age of around 44 ka in the middle part of the profile has to be considered as a result of re-deposited organic material in comparison with the other obtained dating results. Taking into account the increased reliability of the IRSL data from the bottom (8.0 m, 37.3±2.3 ka BP) and the top of the sand succession (1.1 m, 9.6±1.5 ka BP), an average sedimentation rate of about 25 cm per 1000 years would account for that interval. This time frame would place the base of the yellowish sand layer at around 27 ka BP, too old to be consistent with the Laptev Sea event, even when assuming a high variability of

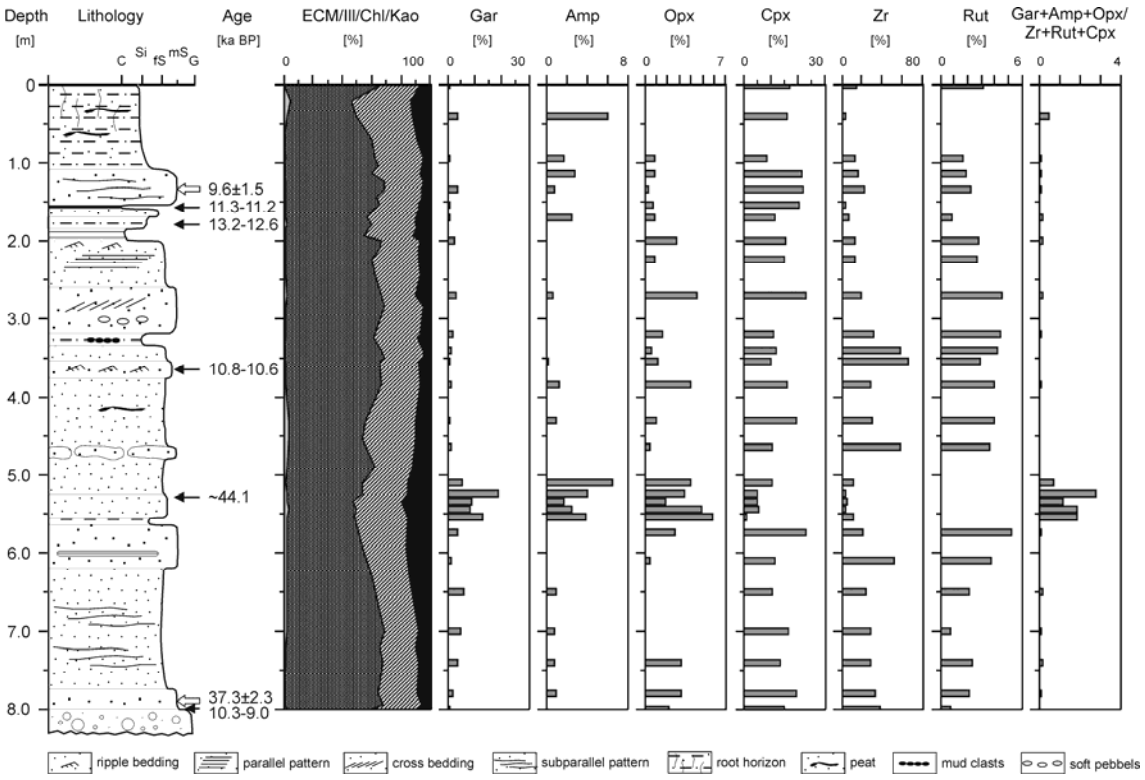

Fig. 4.6: Mineralogical composition of the sand sequence L-07 at Dyanushka River close to the mountain margin. The indicated ages were obtained from radiocarbon dating (black arrows) and infrared stimulated luminescence (IRSL, white arrows). Note the appearance of the increased proportions of garnet, amphibole and orthopyroxene between 5.1 and 5.6 m depth, which is assigned to the yellowish sand layer. The abbreviations for mineral names are valid as used in Fig. 4.4 with the exception of zr = zircon and rut = rutile. Lithological abbreviations, which are used: C = clay, Si = silt, fS = fine sand, mS = medium sand, G = gravel.

sedimentation rates that usually characterise fluvial systems. Besides, the new IRSL age constraints of glacial deposits give evidence that the study area was not affected by extensive glaciations during the last 50,000 years (Table 4.2) (Stauch et al., 2005; Stauch et al., in press).

In addition to the uncertainty of age determinations, sedimentological features do not support the existence of a dammed-up lake basin in the study area. Likewise, there are no indications of a proximal lacustrine shore facies, which should exhibit coarse transgressive beach deposits (Mangerud et al., 2001), or signs of laminated proglacial lacustrine sediments (Houmark-Nielsen et al., 2001). Furthermore, no aquatic organisms were found in the yellowish sand layer. Another strong argument against a large lake is the absence of any lacustrine sediments on terraces downstream the Dyanushka River. To date, a thick succession of lacustrine laminates of uncertain age was only found along Menkere River 300 km north of Dyanushka River (e.g. Kind, 1975; Kolpakov, 1986).

Most likely, the yellowish sand layer documents increased aeolian input of sand-sized sediments from barren fluvial deposits of the ancient Lena Valley. This is indicated by the provenance signal with increased proportions of amphibole, which is

consistent with source signals of loess-like cover sediments along Dyanushka River, revealing a still given influence of Cluster-4 mineral assemblages towards the Verkhoyansk Mountains. In addition to mineralogical evidence, the presence of frosted quartz grains and specific grain-size characteristics support the interpretation of an aeolian input. In comparison with wind-drifted Lena sand and sand-rich loess-like sediments overlying the sand sequence, the yellowish sands of the L-07 profile also show a significant maximum in the fine sand fraction, which is not revealed by both fluvial Lena sands and the grey sands of profile L-07 (Fig. 4.7).

When trusting an age of roughly 27 ka BP for the yellowish sand layer, this stratum would be placed into a period of strong aridity in Central Yakutia (Müller et al., 2004). According to IRSL datings of loess-like sediments, two major accumulation stages of aeolian sedimentation occurred in the study area between 33 and 24 ka and between 13 and 9 ka BP (Stauch et al., in press). The wind-drifted sand thus can be related to the older dry stage, while the cover sediments of the L-07 profile possibly represent the younger dry stage, which may be related to the cold and dry climate conditions of the Younger Dryas (Werner et al., 2005).

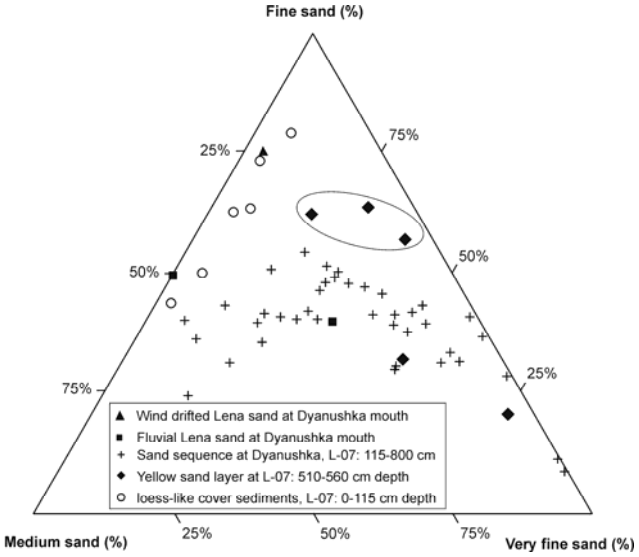

Fig. 4.7: Ternary diagram of very fine sand, fine sand and medium sand concentration of the sample set L-07 in comparison with wind-drifted material of modern Lena sand and the loess-like covering material of L-07. Three of five data points from the yellowish sand layer (encircled) show enrichment in fine sand, which is also typical for loess-like sediments and wind-drifted Lena sand.

4.6 Conclusions

Provenance analysis of Quaternary sediments is a useful tool to gain insights into palaeoenvironmental changes in the central Yakutian Verkhoyansk Mountain area and its foreland, related to glacial, fluvial, and aeolian processes. The interpretation of source signals is straightforward, because two end members basically determine the source signals that can be easily deciphered by heavy-mineral signals and clay mineralogy. Local sediment sources from the mountainous hinterland can be clearly differentiated from sediments derived from the vast catchment area of the Lena and Aldan streams. In summary, our study revealed the following findings:

• The provenance signals in morainic deposits of the stages (Tu1-Tu3, Dj1, Dj2) reflect source-rock geology in the Verkhoyansk Mountains and provide evidence for extensions of the former glacial catchment areas. Consistent with far-reaching advances to the Verkhoyansk Foreland, the old moraines (Tu4, Dj3-Dj5) include eroded materials of the Lena Basin. The spatial correlation of distinct morainic stages is not possible by petrographic means, as shown by variable provenance signals in respective moraines

exposed along the Dyanushka and Tumara Rivers. A reason for this might be different distances of glacier advance in respect to the mountain margin.

• Provenance of loess-like sediments is basically related to deflation plains of braided river systems. Thus, aeolian sediments in the foreland are characterised by a Lena-Aldan source signal, whereas mixing and local provenance increase towards the mountains.

• In the Verkhoyansk Foreland, alluvial sediments of various terraces reveal a clear Lena source signal since at least the end of the middle Pleistocene and during intervals of the late Pleistocene that relates to a stream course closer to the Verkhoyansk Mountains. Fluvial sediments of the middle to late Weichselian terrace section exposed along the Dyanushka River at the Verkhoyansk Mountain margin reveal a local mountain source signals. A yellowish sand layer in the succession of L-07 at the Dyanushka River points to a Lena influence that might be related to a late Weichselian increased mountainward aeolian sand supply from the Lena Basin, consistent with a regional dry period between 30 and 24 ka BP.

Acknowledgements

The paper is a contribution to the joint German-Russian research project “Late Quaternary climate and environment in the Verkhoyansk Mountains and the lowlands of Central Yakutia”, funded by the Deutsche Forschungsgemeinschaft (Hu 378/12). We thank our colleagues in field as well as Jana Hofmann for preliminary work on several samples and acknowledge the assistance of Ute Bastian and Martin Buchholz from the laboratory at the Alfred Wegener Institute in Potsdam.

5. Mid- to late Holocene climate change and linkages to centennial solar variability in northeastern Siberia: Evidence from a thermokarst lake status record

Manuscript by:
S. Popp, M. Gerasimova, L. Pestryakova, D. Subetto, L. Nazarova, A. Andreev, H. Meyer, R. Stein, B. Diekmann.

Abstract

A new high-resolution lake status record of Lake Satagay from Central Yakutia reflects climate-driven hydrological changes in a typical thermokarst lake environment of the extreme continental periglacial setting of northeastern Siberia. Thermokarst lakes represent highly dynamic features of permafrost landscapes across Siberia that are known to respond sensitively to climate perturbations. The sedimentary lake record spans the last 7500 years of the mid- to late Holocene. The downcore variability in the composition of organic matter and the assemblages of fossil bioindicators give evidence of climate-driven and interrelated changes in biological productivity, lacustrine trophic states, and lake-level fluctuations. The lake status record reveals a long-term trend towards lake-level lowering in the course of climate deterioration after 4.2 cal. ka BP and reduced evaporation as well as progressive sediment infill. This long-term trend is overprinted by short-term fluctuations at centennial time scales with high lake levels and decreased biological productivity during cool climate spells with reduced evaporation, as also observed in modern thermokarst lakes of Central Yakutia. The short-term climate spells are related to sun-spot variations and are coherent with a 350-yr cycle of solar activity, which represents a multiple of the prominent 88-yr Gleissberg solar cycle. The short-term cycles were most pronounced during the mid-Holocene climate transition between 6.5 and 4.2 cal. ka BP, following the regional climate optimum and heralding late Holocene climate deterioration. The Lake Satagay record shows that climate instability during the mid-Holocene climate transition is of global significance.

5.1 Introduction

Growing evidence from worldwide proxy records reveals a high variability of Holocene climate (Mayewski et al., 2004). During that time, the sun has been an important driving force of earth's climate system (Beer et al., 2000). The warming during the first half of the Holocene was triggered by the precession-driven summer-insolation maximum that led to the postglacial climate optimum between roughly 9 ka and 6 ka, followed by global climate deterioration. The maximum of the climate optimum, however, varied in space and time, and in some regions, a reverse temporal pattern of Holocene climate development with a warm late Holocene is evident (e.g. Davis et al., 2003; Kaufman et al., 2004; Mayewski et al., 2004; Kaplan and Wolfe, 2006). Superimposed on the long-term climate trends, short-term fluctuations in solar activity appear to affect the internal variability of the climate system by impacts on both atmospheric and oceanic circulation patterns (e.g. Shindell et al., 2001; Bond et al., 2001). Although the

sun-climate linkage still is a matter of debate (Rind, 2002; Carslaw et al., 2002), many proxy records reveal fluctuations of environmental conditions at decadal to millennial time scales that are apparently associated with changes in solar output. Prominent examples are the signals of IRD (ice-rafted debris) events in the North Atlantic (e.g. Bond et al., 2001), isotopic and chemical signatures from Greenland ice (e.g. O'Brien et al., 1995; Stuiver et al., 1995), oxygen-isotope records of speleothems from Ireland and Oman (McDermott et al., 2001; Neff et al., 2001) and northern-hemispheric tree-ring proxies (e.g. Esper et al., 2002; Raspopov et al., 2004). In particular, the northern-hemispheric high latitudes appear to be strongly affected by Holocene climatic changes, which are amplified by several feedback mechanisms (Overpeck et al., 1997; Serreze et al., 2000; Moritz et al., 2002). However, more detailed palaeoenvironmental records are needed to verify this notion. In contrast to Alaska, where high-resolution analysis of a lacustrine sequence revealed climatic variations at multi-centennial time scale (Hu et al., 2003), proxy records from northern Eurasia mostly document environmental changes at only low temporal resolution (e.g. Laing et al., 1999; Wolfe et al., 2000; Anderson et al., 2002; Andreev et al., 2004a). Actually, the meaning of short-term Holocene climate variability is not well established for the periglacial regions of Siberia. Clues for the presence of short-term climate perturbations arise from the reconstruction of vegetation history in eastern Siberia. However, so far these records suffer from inadequate age control (see Fradkina et al., 2005).

This study is focused on a new high-resolution lake status record of Lake Satagay from Central Yakutia, a thermokarst lake that reflects climate-driven hydrological changes in the extreme continental periglacial setting of northeastern Siberia. Thermokarst lakes represent highly dynamic features of permafrost landscapes across Siberia that are known to respond sensitively to recent climate warming and increasing precipitation (Pavlov, 1994; Agafonov et al., 2004; Smith et al., 2005). Historical data on lake-level fluctuations of thermokarst lakes in Central Yakutia during the last century are also consistent with repeated fluctuations in relative humidity (Nemichov, 1958; Bosikov, 1991, 1998). In comparison with climatic data (Gavrilova, 1993), high lake levels correspond to periods of increased annual precipitation that is related to relatively warm winters and moderate summers attributed to a enhanced cyclonic activity of the west-wind belt in eastern Siberia, such as at the beginning of the 20th century. In contrast, low levels occurred during dry periods, for example between 1935-1952 (Bosikov, 1998), with warm summers causing an two to four-time increase in evaporation rates, which are even up to seven times higher than the amount of precipitation during very dry seasons (Gavrilova, 1973). The variations in lake-level changes reveal a prominent cyclic character. Bosikov (1998) and Gavrilova (1993) report on prominent 150- to 180-year and 55-year cycles of thermokarst development in Central Yakutia and at lower frequencies in the range of 5 to 10 years. The latter 10-year oscillations in lake status roughly match a traced 11-year cycle in meteorological data (Gavrilova, 1993). The observed periodicities suggest a possible link between lake-level fluctuations and climate variability related to the original and multiple frequencies of solar activity (e.g. 11-year Schwabe cycle, 88-year Gleissberg cycle, 205-year De Vries cycle), as already postulated for Central Yakutia by Nemichov (1958). For a better understanding of the regional ancient climate history, there is need to extend the

instrumental data set back in time. The Lake Satagay provides a long-term record of lake status changes between 7.5 and 0.6 ka BP at high temporal resolution, including the final stage of the Holocene climate optimum at around 6.0 ka BP and the following mid-Holocene climate deterioration, which globally was characterised by pronounced climate instability (Steig, 1999; Yu et al., 2006; Magny et al., 2006). The reconstruction of fluctuations in lake level and trophy is derived from compositional variations of organic matter and fossil bioindicators.

5.2 Material and Methods

Lake Satagay is situated in the lowlands of the Vilyuy River area in Yakutia, Russia (64°28'N, 122°43'E, 175 m a.s.l.) (Fig. 5.1). The study site lies in the zone of continuous permafrost and is characterised by a strong continental climate regime, with very cold winters (mean January temperatures -37°C) and warm summers (mean July temperature +18°C). The majority of the low annual precipitation (around 220 mm) falls during summer. Lake Satagay represents the largest (2.9 km^2) of three chained lakes in a closed thermokarst depression, which formed through the thawing of underlying ice-reach sands of late Pleistocene age. The shape of the depression and distribution of wetlands between the lakes suggests the former presence of one big lake (Fig. 5.1). As determined in July 2003, the lake is alkaline (pH 9.0), shallow (maximum depth: 1.6 m; average depth: 0.7 m), supersaturated in oxygen (oxygen content: 26.4 mg/l; saturation: 327 %), and moderate in both transparency (Secci-depth: 0.6 m) and conductivity (270 µS/cm).

Sediment core retrieval was performed from ice cover in spring 2002, using a Russian Corer. From the 13 m long sediment core, the uppermost 1.7 m was not sampled because of strong disturbance. The basal section is composed of 18 cm peaty fine sand. The remaining part consists of green gyttja with intercalated dark gyttja horizons and layers enriched in plant remains. Nine samples of terrestrial plant macrofossils were taken for radiocarbon AMS dating (Table 5.1). The sediment core was sampled at 2-cm intervals in the lowermost meter, and at 5-cm

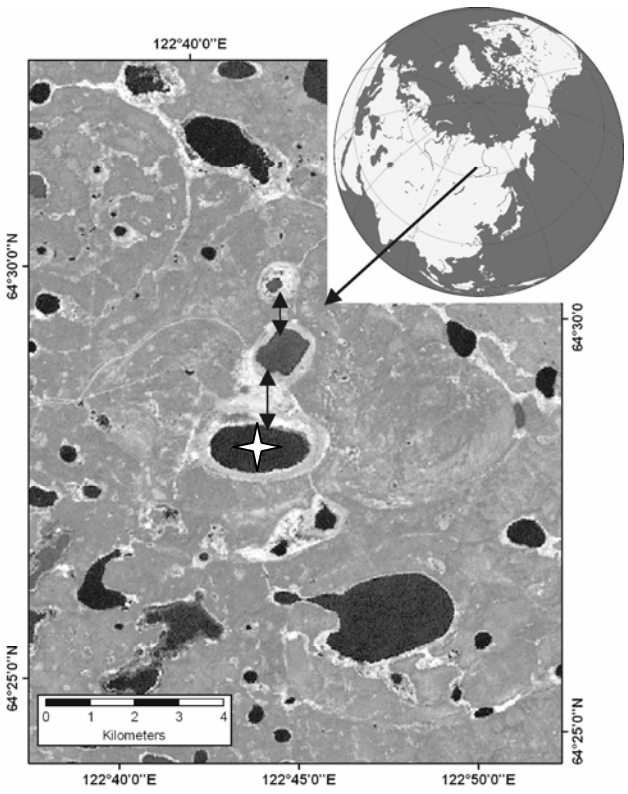

Fig. 5.1: Landsat7 ETM+ image of the Lake Satagay area from 6th June 2000. The dark areas indicate open-water conditions. The Lake Satagay basin today is occupied by a chain of three single lakes (black arrows). The studied sediment core was retrieved from the central part of the largest lake to the south (white asterisk). The bright-coloured wetland areas delineate the maximum extension of one big lake in former times.

intervals in the remaining section. The 251 samples provide an average temporal resolution of about 20 years.

The organic-rich sediments (251 samples) were analysed for their content in total organic carbon (TOC), total nitrogen (TN), as well as the stable carbon isotope ratio of bulk organic carbon. TOC and TN was measured with a 'vario EL III'-CNS-Elemental Analyzer on pulverized samples after removal of carbonate with 10%-HCL at a temperature of 80°C. The analytical precision is ±5%. Carbon stable isotope ratios ($^{13}C/^{12}C$) of the carbonate-free samples were determined with a Finnigan Delta S mass spectrometer in Ag cups after combustion to CO_2 in a Heraeus Elemental Analyzer. Analytical precision is ±0.2%. The isotope data are presented as $\delta^{13}C$ values referred to the Vienna Pee-Dee Belemnite (V-PDB) standard. For both methods, analytical accuracy was checked by parallel analysis of international standard reference materials. Selected samples were analysed with Rock-Eval Pyrolysis technique, a method which estimates hydrocarbon-bearing substances that escape from the sediment at temperatures between 200° and 600°C. The data characterize the composition of organic matter, expressed as the hydrogen index (HI, mg HC/g TOC) and the oxygen index (OI, mg CO_2/g TOC) (Meyers and Teranes, 2001). On all samples, a biogroup analysis was conducted according to the procedure of Kvasov et al. (1986). A discrete amount (0.5 cm^3) of wet sample is diluted in 25 ml water and placed on a glass-covered slide. The investigation is undertaken under an optical microscope at 280- to 400x magnification. A number of 500 individual biogenic remains were counted per slide, comprising phytoplankton, zooplankton, and macrophyte particles, expressed as frequency percentages. The data were treated statistically by a standard Varimax Principle Component Analysis (Varimax PCA), to reduce the number of variables during data evaluation. The temporal variability of all raised data was evaluated by spectral time-series analyses, using the software package AnalySeries 1.2 (Paillard et al., 1996).

5.3 Results and interpretation

Chronostratigraphy

On the basis of nine AMS-^{14}C age determinations, the sediment section was dated between around 6.4 to 0.6 ^{14}C age BP. The ^{14}C ages were calibrated to calendar ages, using the software 'CALIB rev 4.3', data set 2 (Stuiver et al., 1998) (Table 5.1). The dating sample at 10.0 m core depth resulted in a controversial age with respect to the age-depth constraints (Fig. 5.2). It therefore was rejected as an outlier from the applied age model, which was inferred from the linear interpolation between the eight age datums. The resulting age-depth correlation is reasonable and shows a gradual increase in apparent linear sedimentation rates of around 1.0 mm/yr in the basal section to around 3.0 mm/yr at around 3.5 cal. ka BP. In the younger part of the section, the sedimentation rates vary between 1.4 mm/yr and 2.5 mm/yr (Fig. 5.2).

Table 5.1: AMS radiocarbon ages of terrestrial plant remains from Lake Satagay.

Depth (m)	AMS-^{14}C yr BP	cal. yr BP	cal. yr BP 2-σ young	cal. yr BP 2-σ old	Lab. Number
3.60	670 ± 25	653	560	669	KIA 20704
6.85	2040 ± 30	1944	1923	2068	KIA 24040
8.80	3170 ± 45	3381	3322	3473	KIA 20703
10.15	1745 ± 25	1660	1566	1712	KIA 24039
11.55	3865 ± 30	4270	4225	4410	KIA 24038
12.80	4495 ± 40	5160	5036	5299	KIA 24037
13.45	4850 ± 80	5594	5449	5746	KIA 24036
14.26	5610 ± 35	6365	6306	6450	KIA 24035
14.47	6420 ± 45	7371	7271	7422	KIA 20702

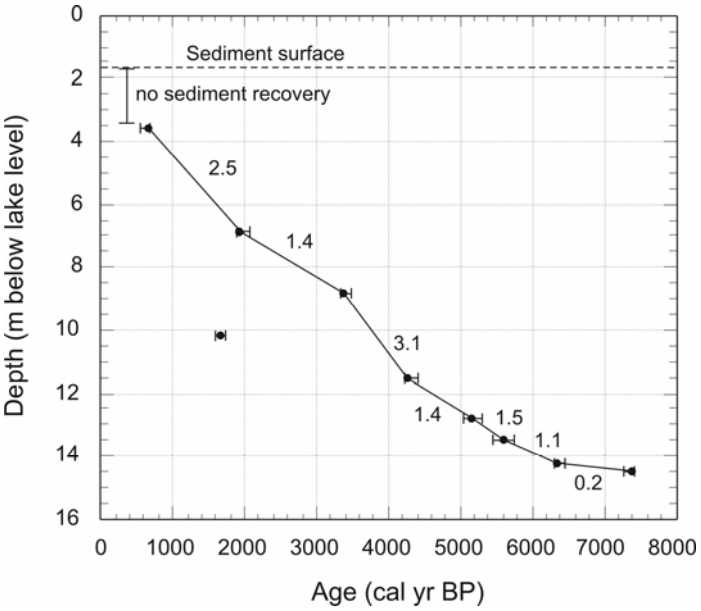

Fig. 5.2: Age-depth correlation of the Lake Satagay sediment core given in calibrated radiocarbon years BP. The age datums were determined from macroplant remains. The used age model is based on the linear interpolation between the age datums. Numbers refer to the linear sedimentation rates between the age datums given in mm/yr.

Organic matter

Throughout the sediment record, interrelated long-term and short-term variations are displayed in the TOC, TN, TOC/TN and δ^{13}C values (Fig. 5.3). The carbon and nitrogen concentrations reflect the origin of organic matter in the lacustrine sediments. Vascular plants include large proportions of carbon-rich fibres, while aquatic phytoplankton is relatively enriched in nitrogen (Meyers and Teranes, 2001). Variations in the TOC/TN ratio thus document changes in the sources of organic matter. With the exception of samples from the basal section, ratios of 11-13 dominate the organic sediments (Fig. 5.3), pointing to a mixture of vascular plants and algae material (Meyers and Lallier-Vergès, 1999; Meyers and Teranes, 2001).

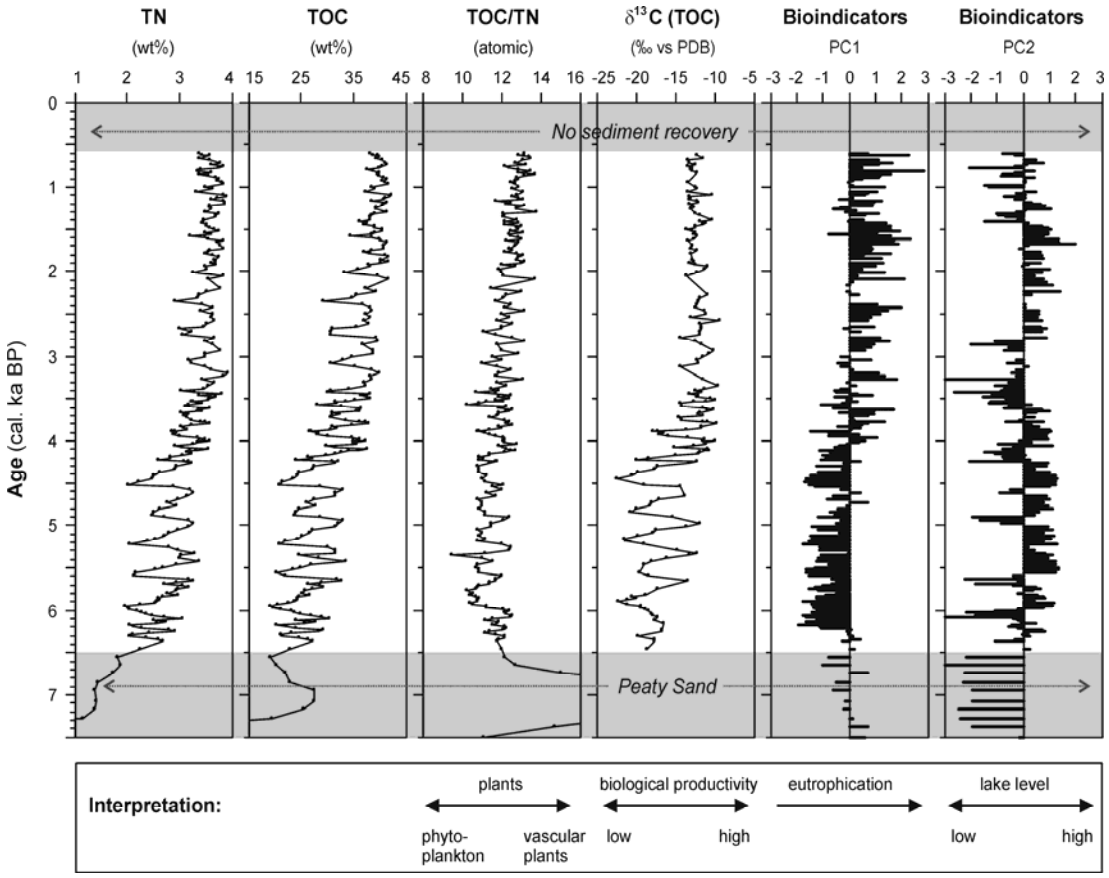

Fig. 5.3: Organic matter composition and fossil bioindicators in the lacustrine sediment record of Lake Satagay, displayed by the variability of total nitrogen (TN), total organ carbon (TOC), TOC/TN ratio, carbon-isotope ratio of bulk organic matter ($\delta^{13}C$), as well as the scores of the principal components derived from the biological group analysis and Varimax Principal Component Analysis.

High carbon-nitrogen ratios (>20) at the base of the section point to a dominant input of land-plant derived material. The positive correlation between TOC and TOC/TN through the core section reveals that increases in TOC concentrations were caused by the supply of allochthonous carbon-rich plant material into the lake, while low TOC concentrations are related to a high proportion of autochthonous phytoplankton remains (Fig. 5.4). The findings from Rock-Eval Pyrolysis on selected samples from the highly variable interval between 5.8 and 5.0 ka support this interpretation, as the vascular plant-rich samples are characterised by high OI and low HI indices, and vice versa for the phytoplankton-rich materials (Fig. 5.4).

The $\delta^{13}C$ ratio of lacustrine organic matter is controlled by various factors, such as primary productivity, dissolved carbon concentration (CO_{2aq}), sources of organic matter, and post-depositional diagenesis (e.g. Stuiver, 1975; Hollander and McKenzie, 1991; Hodell and Schelske, 1998; Street-Perrott et al., 2004; Teranes and Bernasconi, 2005). However, the large amplitudes in the $\delta^{13}C$ values as exhibited by the sediments of Lake Satagay (up to 12 per mill, Fig. 5.3) can hardly be explained by modifications in lake-water and pore-water chemistry, as there exists no direct river inflow and no significant groundwater infiltration through the lake floor from the underlying shallow talik

(thawed permafrost beneath the lake) that could alter the carbon reservoir. Consequently, the variations in organic-matter $\delta^{13}C$ appear to be related to autochthonous aquatic productivity and sources of organic matter. In boreal high latitudes, the vegetation is predominantly (more than 95 %) composed of C_3 plants (Still et al., 2003), which commonly show $\delta^{13}C$ values around -28 ‰ (Meyers and Lallier-Vergès, 1999). Since phytoplankton usually utilizes dissolved carbon, which is in isotopic equilibrium with the atmosphere, C_3 algal material is isotopically indistinguishable from vascular C_3 plants (Meyers and Lallier-Vergès, 1999). The enriched $\delta^{13}C$ values in the TOC-rich samples (in average -17 ‰ in the lower and -12 ‰ in the upper part of the core section, Fig. 5.3) thus can be attributed to high primary production as a result of a high eutrophic status. High productivity rates in the surface water diminish the availability of the preferential light carbon isotope ($^{12}CO_{2\,aq}$), and instead, dissolved HCO_3^- becomes an important carbon source for photosynthesis, resulting in light $\delta^{13}C$ values of lacustrine organic matter (e.g. Hollander and McKenzie, 1991; Hassan et al., 1997; Teranes and Bernasconi, 2005).

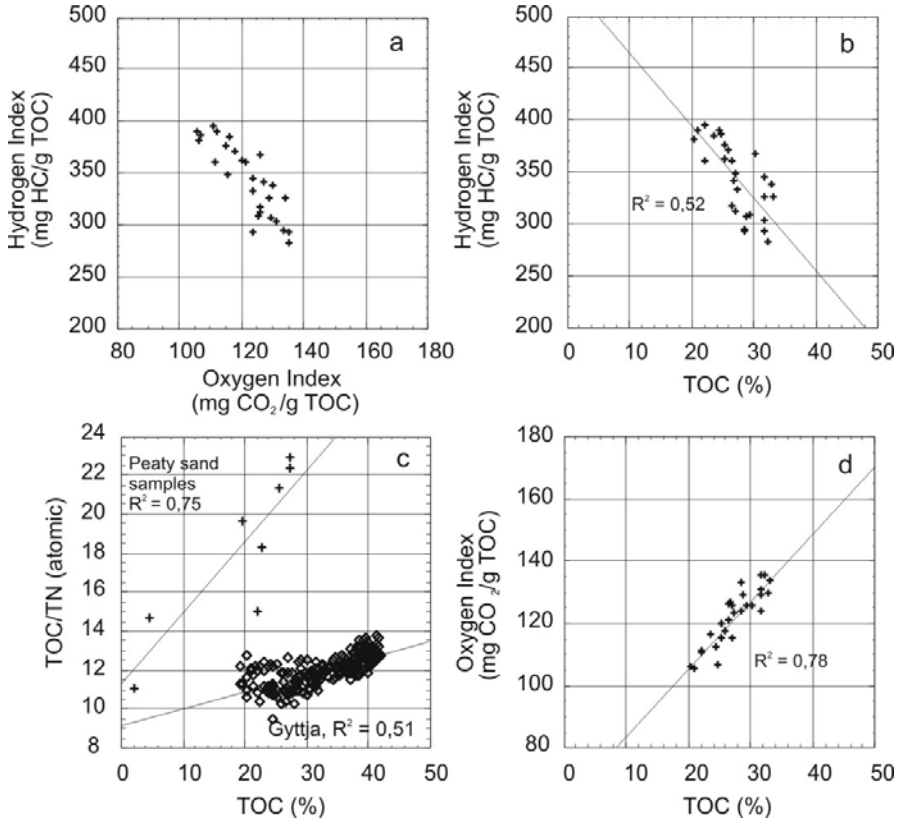

Fig. 5.4: Rock-Eval Pyrolysis data in comparison with other proxies of organic matter composition. The 29 selected samples for Rock-Eval Pyrolysis were taken from the interval between 5.8 and 4.9 cal. ka BP, which is characterised by the highest variability in organic matter composition.
Diagram (a) shows the HI-OI crossplot that indicates a mixture of algae material (high HI, low OI) and vascular-plant organic matter (low HI, high OI), as also indicated by the variability of the TOC/TN rations (Fig. 5.3). High TOC/TN rations indicate the presents of vascular plants and are associated with high TOC concentrations (Diagram b). Low TOC/TN ratios characterise algae-rich sediments with low TOC concentrations (Diagram: b). Also the negative correlation between the HI index and TOC (Diagram c) and the positive correlation between the OI index and TOC (Diagram d) suggests that elevated TOC concentrations are related to a strong supply of vascular plant debris to the lake, and vice versa.

Fossil bioindicators

On the basis of the biological group analysis, the multivariate statistics resulted in the identification of four principal components (PCs), which describe 60% of the variance among the different floral and faunal groups (Fig. 5.5). For the interpretation of the bioindicators, we consider PC1 and PC2, which explain the highest variance. PC1 with 21% variance includes high positive PC loadings for the algae *Scenedesmus*, Desmids, *Lyngbia*, as well as for chaldocera and insects (Fig. 5.5), suggesting that it basically displays the intensity of biological productivity. Palaeolimnological records from the mid- to high-latitudes of Sweden and North America have highlighted particularly the significance of the green alga *Scenedesmus* as biologically indicative for eutrophication and elevated nutrient levels in lakes (Cronberg, 1982; Huber, 1996). The good downcore correlation between elevated PC1 scores with maxima in $\delta^{13}C$ values support the interpretation of PC1 as an indicator of the relative degree of eutrophication through time (Fig. 5.3).

PC2 explains 14% of variance and is dominated by a highly positive PC loading for diatoms and a highly negative PC loading for macrophyte remains (Fig. 5.5). In analogy to the variability of TOC concentrations and TOC/TN ratios, the downcore variability of the loadings of the second principal component reflects the variability in the proportions of autochthonous and allochthonous organic matter (Fig. 5.3).

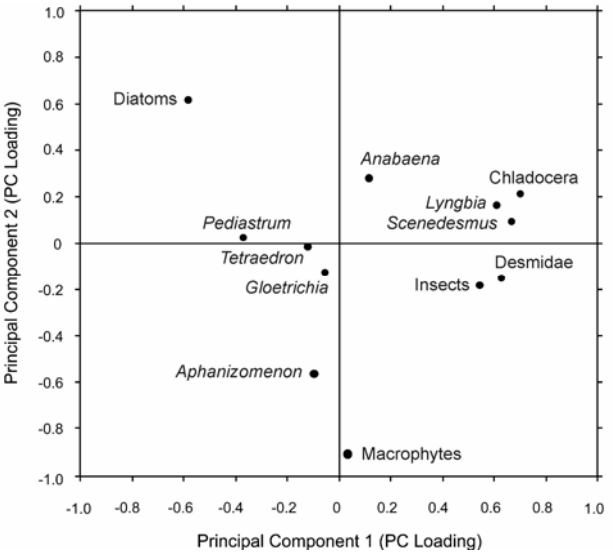

Fig. 5.5: Crossplot of the Principal Component (PC) loadings of PC1 (variance 21 %) and PC2 (variance 14%) derived from biological group analysis and Varimax Principal Component Analysis.

5.4 Discussion

Development of lake status through time

The Lake Satagay record documents a pronounced temporal variability in the sources of organic matter, as indicated by TOC/CN ratios, the HI and OI indices of organic matter composition and the bioindicator assemblages of PC1. As the sediment core was retrieved from the central part of the lake, the relative proportions of autochthonous and allochthonous sediment supply reflect lateral shifts of the shore line that controls the depositional environment in respect to more littoral or open-water conditions at the study site. Evidence for variations in the extension of the lake actually arises from the modern distribution of the three individual lakes and wetlands in the Satagay depression, which in the past were connected to one big lake. The only reasonable way to explain shifts of the shore line are lake-level fluctuations. Thus, high lake levels are indicated by relatively decreased TOC concentrations with dominant autochthonous algal material, whereas opposite values document a stronger supply of vascular-plant

material and indicate low lake-level status (e.g. Talbot and Livingstone, 1989; Meyers and Lallier-Vergès, 1999; Wilkes et al., 1999; Lüniger and Schwark, 2002). The presented proxy data suggest significant lake-level fluctuations to have occurred at different time scales.

After the initiation of thermokarst processes, a shallow lake formed around 7.4 cal. ka and deepened around 6.5 cal. ka BP. This early stage is reflected by the presence of condensed peat-rich and sandy sediments at the base of the gyttja section. Between 6.5 and 3.6 cal. ka BP, marked oscillations in lake level appeared at high amplitudes at centennial time scales, as shown by the factor scores of PC2 and TOC/TN ratio. The interval between 3.7 and 2.7 cal. ka BP was characterised by intermediate to low lake level, followed by a period with mostly high lake level between 2.7 and 1.4 cal. ka BP. The youngest interval between 1.4 and 0.6 cal. ka BP again showed marked lake-level fluctuations.

Changes in lake level apparently were accompanied by changes in lake-trophic level and biological productivity, as indicated by the variability of the bioindicator PC1 scores and $\delta^{13}C$ values of organic matter. The long-term trend suggests enhanced eutrophication after 4.0 cal. ka, overprinted by strong short-term fluctuations in trophy status, particularly in the time interval between 6.5 ka and 4.0 cal. ka, as well displayed by the $\delta^{13}C$ proxy. In most cases, the short-term variations in lake trophy and biological productivity are consistent with lake-level fluctuations, suggesting high trophy status during lake-level lows and vice versa.

The variability of TOC concentrations represents an integrated signal of trophy conditions, biological productivity, and lake-level fluctuations and reveals the clearest pattern of both long-term and short-term variability in lake status. High TOC concentrations reflect low lake level and high biological productivity, particularly after 4.2 cal. ka BP, and pervasive short-term variability during the foregoing time interval, which is also evident at lower amplitude in the younger interval. The significance of short-term variability in lake status is supported by the results of spectral analyses on the different proxy records (Table 5.2). The TOC proxy reveals strong spectral power at the 357-year and 164-year periodicities that are comparable with the lake-level proxy of PC2 that show significant power at the 375-year, 185-year, 115-year, and 84-year periods. The $\delta^{13}C$ productivity proxy reveals strong power at the 370-year and 155-year periods, while the PC1 eutrophy proxy shows periodicities of 420, 195, 160 and 77 years.

Table 5.2: Significant periods (years) for the biogeochemical proxies, the bioindicators represented by the Principle Components, and Sunspots numbers as obtained by the Blackman-Tukey (BT) spectral analysis.

TOC	TOC/TN	$\delta^{13}C$	PC1	PC2	Sunspot
357	381	370	420	375	230
164	159	155	195	185	149
-	81	-	160	115	104
-	-	-	77	84	88

Lake status and climate change

The lake-status record of Lake Satagay matches the development of climate changes in central and eastern Siberia, encompassing the time from the late Holocene climate optimum and following long-term climate deterioration. In the Vilyuy area, which is situated close to Lake Satagay, lacustrine pollen records indicate a thermal maximum with high annual precipitation between roughly 6.8 and 5.1 cal. ka BP, followed by moderate climate conditions through the younger part of the Holocene (Fradkina et al., 2005). The latter authors have also pointed out the presence of short-term climate variability throughout the Holocene, however, without specifying the cyclicity of such events. Unpublished pollen data from Lake Satagay suggest favourable climate conditions to have prevailed until approximately 5.5-5.0 cal. ka BP (Andreev, personal communication, 2005). This is consistent with finding from the Taymyr area in central Siberia, where the regional climate optimum appeared between 9.5 and 5.1 ka cal. ka BP (Andreev and Klimanov, 2000; Andreev et al., 2002a, 2003; Kumke et al., 2004) with highest summer temperatures and precipitation between 7.4 and 5.7 cal. ka BP (Koshkarova, 1995). At present, the most reliable palaeoclimate record for Yakutia is available from Lake Nikolay in the Lena Delta, which is based on quantitative reconstructions on the basis of fossil pollen and chironomids (Andreev et al., 2004a). The findings give evidence of a climate optimum between 9.2 and 5.8 cal. ka BP, followed by unstable climate conditions between 5.8 and 3.7 cal. ka BP.

The comparison of available palaeoclimate data shows that Lake Satagay formed by the end of the climate optimum, possibly in response to enhanced thermokarst activity. The strong cyclicity in lake status between 6.5 and 4.2 cal. ka BP thus reflects regional climate instability during the mid-Holocene climate transition. On a global scale, this phenomenon has been observed in a number of coeval climate records, comprising a high variability in fluvial run-off in western Siberia (Stein et al., 2004), instable monsoon conditions and aridification in NW China (Yu et al., 2006), pronounced lake-level fluctuations in central Europe (Magny et al., 2006), high variability in tropical El-Nino/Southern Oscillation (ENSO, Haug et al., 2001), aridification in northern Africa (deMenocal et al., 2000), and environmental reorganizations in the southern hemisphere (Steig, 1999). The overall driving force of global mid-Holocene climate change can basically be attributed to an enhancement of seasonality in insolation on the northern hemisphere (e.g. Mayewski et al., 2004; Schmidt et al., 2004). The long-term change in the lake status of Lake Satagay after 4.2 cal. ka BP heralds the onset of late Holocene climate deterioration, as also observed in the Lena Delta (Andreev et al., 2004a) and the cited global climate records. Short-term fluctuations in lake status were still present, but at a lower amplitude than during the preceding interval.

The pervasive presence of prominent centennial fluctuations in the entire lake status record of Lake Satagay agree with the prominent 150-180-year variability of lake-level changes in young thermokarst lakes of Central Yakutia, revealed by Bosikov (1991, 1998) and may be explained by responses to changes in solar activity.

Climate variability and solar connections

Some of the short-term periodicities revealed by the lake status data of Lake Satagay coincide with prominent solar cycles. For example, the inferred 77-88-year, the 149-164-year, and the 185-195 year periods are similar to respective periods of the 88-year, 148-year, and 206-year cycles, identified in the residual atmospheric ^{14}C production ($\Delta^{14}C$) data (Stuiver and Braziunas, 1993). Although climatic changes and the partition in the global carbon cycle may affect the $\Delta^{14}C$ pattern, the similarity of ^{14}C and ^{10}Be records suggests that the Holocene $\Delta^{14}C$ variability primarily reflects solar modulation (Beer et al., 1988; Beer, 2000; Muschler et al., 2000). Here, we refer to the latest time series of sunspot numbers, which recently were established for the Holocene (Solanki et al., 2004). Sunspots are directly observable proxies of solar activity, which were formerly available only back to the beginning of the 17th century (Hoyt and Schatten, 1998).

By the use of the sunspot-time series, we performed cross-spectral analyses between the sunspot data of Solanki et al. (2004) and the TOC proxy, which represents the most robust indicator of lake status in our record (Fig. 5.6). Surprisingly, only one significant period of coherency is given in the 357-year domain (Fig. 5.6). However, this period

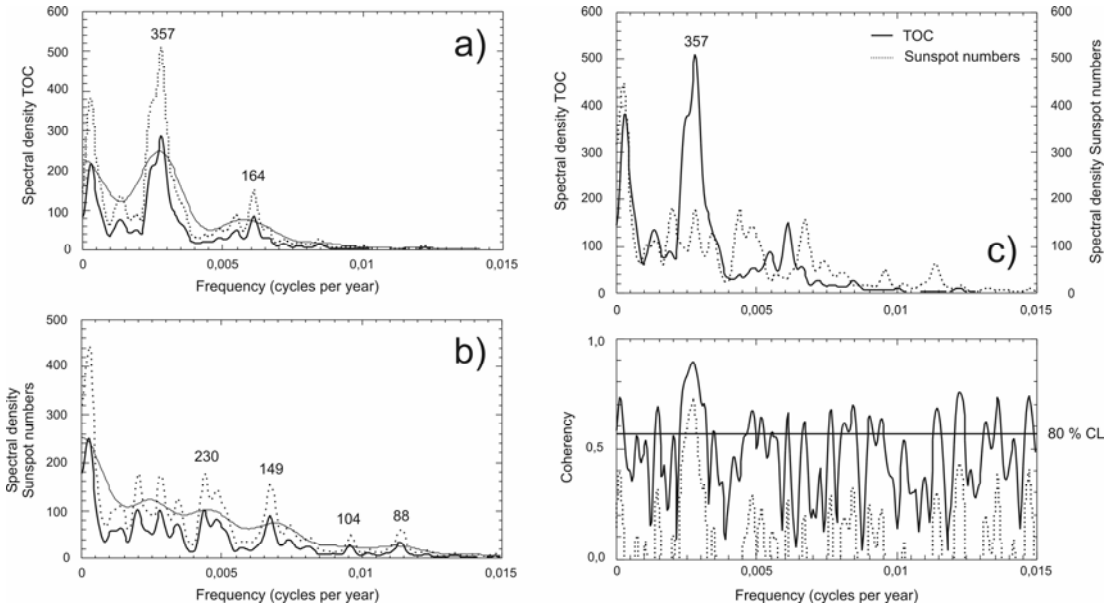

Fig. 5.6: Results of the Blackman-Tuckey (BT) spectral analysis of TOC (a) and Sunspot numbers (b). According to Felis et al. (2000), those peaks of the spectrum (dotted line) that rise above the low-resolution spectrum (thin solid line) by a distance greater than the one-sided confidence interval at the 80 % level (thick solid line) are declared to be significant. The periods of the significant years are shown. The result of the BT cross-spectral analysis between TOC and sunspots are shown in Figure 5.6 (c). The top panel shows the variance spectra of the individual time series, and the bottom panel shows the coherency (the correlation coefficient as a function of frequency) between the two time series (thick solid line). The thin dotted line in the bottom panel indicates the one-sided coherency confidence interval at the 80 % level. Coherency values of >0.8 indicate that over 64 % (0.8^2) of the variance at these periods is linearly correlated between the two time series. The significant period is shown. The criteria for this is that the variance peak is aligned (in the top panel) and that the corresponding coherency exceeds the 80 % confidence level (CL). The significant period of 357 years is shown.

nearly represents the fourfold multiple of the prominent 88-year Gleissberg cycle and multiplied by four approximately produces the prominent 1500-year cycle observed in Holocene climate records of the North Atlantic, which also is supposed to be driven by persistent solar influence (Bond et al., 2001). So the Lake Satagay record, as in the North Atlantic, demonstrates the observation that solar influences on the climate system are mediated through the superposition of short-term periodicities of solar activity.

A better picture of sun-climate linkages arises from the direct comparison of the Lake Satagay TOC record with the sun-spot record of Solanki et al. (2004). Thus, high stands of lake level with more oligotrophic conditions are mainly related to strong minima in sun-spot numbers, such as around 6300, 6200, 5900, 5600, 4800, 4000, 3400, 3100, 2700, and 1300 cal.-yr BP (Fig. 5.7). It also becomes evident that the extreme amplitudes in lake-status fluctuations during the mid-Holocene climate transition are consistent with the dense succession of sun-spot minima during that time. Similar findings were obtained from lake-sediment records in central Europe, where cold climate spells during the mid-Holocene were associated with high lake levels and prominent sun-spot minima (e.g. Magny et al., 2006). In analogy to modern climate and thermokarst lake dynamics in Central Yakutia (Nemichov, 1958; Bosikov, 1991, 1998), the lake-level high stands of Lake Satagay may also be explained by cold and wet episodes with enhanced precipitation and reduced evaporation. Our proxy data favour the assumption of a positive hydrological budget during lake-level high stands, but give no information on palaeotemperature conditions. The correlation of high lake levels with sun-spot minima, however, argues for cold climate conditions. Further support comes from a pilot study of chironomid assemblages of the Lake Satagay sediment record, which tentatively points to decreased July water temperatures during stages of high lake level (Nazarova, personal communication, 2006).

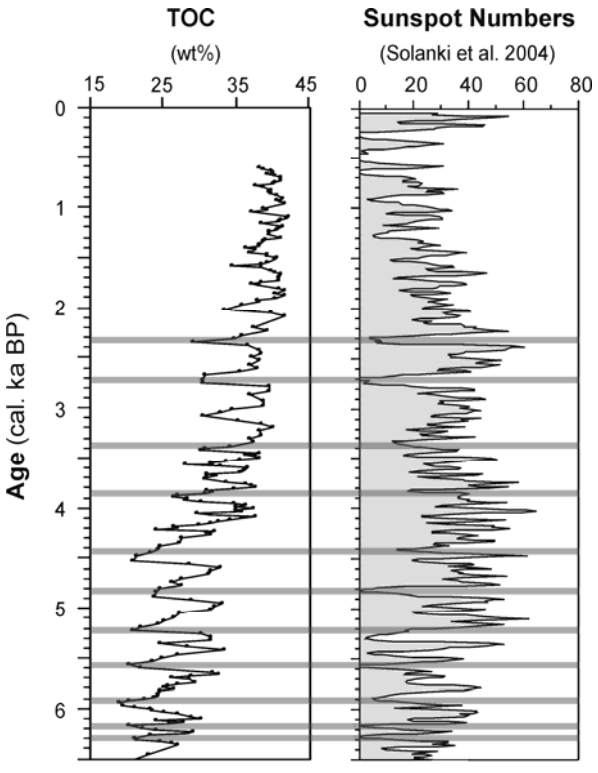

Fig. 5.7: Comparison of the Lake Satagay TOC lake-status record with the sunspot-number record of Solanki et al. (2004) for the mid- to late Holocene time interval. The grey bars indicate distinct episodes of minimum solar activity, closely matching periods of inferred low-lake level and low trophic state of Lake Satagay.

The mechanisms of climate-sun linkages in the Holocene climate system so far are poorly understood. From the fossil climate records it seems that the impact of solar activity on the climate system is more pronounced than predicted by the physical processes underlying solar influences (see review in Schmidt et al., 2004). And it seems that solar influences are transmitted to the climate system at centennial to

millennial time scales rather than on shorter time scales. The influence of solar forcing on climate change apparently is mediated through world-wide atmospheric and oceanic teleconnections with impacts on the operational modes of decadal to sub-decadal climate oscillators, such as Arctic Oscillation/North Atlantic Oscillation (AO/NAO) and El Nino/Southern Oscillation (ENSO) dynamics. On multi-centennial time-scales, Shindell et al. (2001) demonstrated that reduced
solar irradiance during the Maunder Minimum (1645-1715) resulted in surface climatic pattern over the northern hemisphere similar to those of the low index state of the (AO/NAO). The resultant cooling over the northern hemisphere continents, as known from tree-ring and diatom proxies in northeast Siberia (Naurzbaev and Vaganov, 2000; Mackay et al., 2005) presumably reduced the evaporation effects on Yakutian lakes in a similar manner such as during the mid- to late Holocene.

5.5 Conclusions

The Lake Satagay lake status record provides new insights into short- and long-term mid- to late Holocene climate dynamics in eastern Siberia during the last 7500 years. The following conclusions can be drawn:

• The variability in the composition of organic matter and the assemblages of fossil bioindicators give evidence of climate-driven and interrelated changes in biological productivity, lacustrine trophy conditions, and lake-level fluctuations. The lake status record reveals a long-term trend towards lake-level lowering in the course of climate deterioration after 4.2 cal. ka BP and reduced evaporation as well as progressive sediment infill. This long-term trend is overprinted by short-term fluctuations at centennial time scales with high lake levels and decreased biological productivity during cool climate spells with reduced evaporation, as also observed in modern thermokarst lakes of Central Yakutia.

• The short-term climate spells are related to sun-spot variations and are coherent with a 350-yr cycle of solar activity, which represents a multiple of the prominent 88-yr Gleissberg solar cycle. The short-term cycles were most pronounced during the mid-Holocene climate transition between 6.5 and 4.2 cal. ka BP, following the regional climate optimum and heralding late Holocene climate deterioration.

• On a global scale, climate changes in eastern Siberia show affinities to the climate development in central and northern Europe and central Siberia, pointing to prominent teleconnections of atmospheric dynamics within the westerly wind system. Furthermore, the Lake Satagay record shows that climate instability during the mid-Holocene climate transition is of global significance and apparently was mediated by both changes in insolation-driven seasonality and the dense succession of episodes with strongly reduced solar activity.

6. Synthesis

The goal of this thesis was to gain new insights into the development of the late Pleistocene and Holocene environment of Central Yakutia on the basis of different methodical approaches. In general, three different archives were addressed for palaeoenvironmental reconstructions: (1) ground ice enclosed in permafrost sequences, (2) clastic sediments of glacial, fluvial/alluvial, and aeolian origin, and (3) a lacustrine sediment core. Radiocarbon AMS dating provides age constraints for the ice wedges and their host deposits, and the sediment sequence from Lake Satagay. The stratigraphy of glacial and fluvial-terrace sediments mainly follows the classification of the geological map (Prokopiev et al., 1994) and literature data, with the exception of a ^{14}C AMS chronology for a continuous sediment record at the Dyanushka River. In addition, new Infrared-Stimulated Luminecence (IRSL) dates have been used to provide age control on loess-like and fluvio-glacial sediments in the study area (Stauch et al., 2005, in press).

6.1 Relevance of the applied proxy data for the environmental reconstructions

The respective proxy data address different time intervals at various temporal resolutions. Provenance analyses by means of heavy minerals and clay minerals were conducted at low temporal resolution on various periglacial sedimentary deposits of middle to late Pleistocene and subrecent ages. In contrast to previous studies, which mainly dealt with fluvial sediments of the Lena River and its tributaries (Hermel, 1995; Hoops, 1999; Peregrovich, 1999) or were conducted on the Lena Delta region (Schwamborn et al., 2002; Siegert et al., 2002), heavy-mineral analysis in the scope of this thesis were extended to glacial and loess-like sediments in the foreland of the Verkhoyansk Mountains. The distinct differences in heavy-mineral assemblages between Lena River sediments and those originated from the Verkhoyansk Mountains serve as the basis for environmental reconstructions. Relatively high amounts of hornblende, orthopyroxene and garnet characterise the fluvial sediments of the Lena, whereas stable heavy minerals (zircon, tourmaline, rutile) clinopyroxene and apatite dominate the sediments originating in the mountain area (Fig. 4.4). In addition, clay-mineral assemblages give supplementary constraints on sediment sources that may have changed in the course of environmental changes. In summary, a view on the temporal dynamics of fluvial, glacial, and aeolian activity along the middle and lower course of the Lena River was achieved (Chapter 4).

Data on isotopic signals from ground ice were obtained from several time intervals of the late Pleistocene and the Holocene. Given that snow is the primary moisture source, the stable-isotope composition (oxygen and hydrogen isotopes) of ice wedges indicates the prevailing winter conditions at the time of ground-ice formation. Snow melt predominantly fill in the thermal-contraction cracks that have opened during the late winter and thus transmit the isotopic signature of precipitation to the frozen ground (e.g. Mackay, 1983; Vaikmäe, 1989; Lauriol et al., 1995). However, various processes after snow precipitation, such as snow metamorphism, snow melting, and refreezing

may be accompanied by isotopic fractionation that, in the case of non-equilibrium fractionation, alters the original climatic signal of precipitation. The detection of possible non-equilibrium isotopic processes therefore is crucial for the palaeoclimatic interpretation of ice wedges. Deviations from the Global Meteoric Water Line (GMWL; Craig, 1961) in terms of slope and deuterium excess (*d* excess; Dansgaard, 1964) are indicators for those non-equilibrium isotopic processes. The *d* excess parameter provides information on the origin of the moisture-bearing air mass (Dansgaard, 1964). For example, Meyer et al. (2002a) interpreted the shift in *d* excess from low values (on average ~5) for the Pleistocene Ice Complex to high values (on average ~14) in Holocene ice wedges as a change in the main moisture source from higher to lower latitudes in the North Atlantic, owing to the modified oceanic and atmospheric circulation pattern during the last glacial stage. In this study, however, the meaning of *d* excess values was rejected from data interpretation, because of the small number of studied ice wedges and the inconsistent patterns they show in their *d* excess values.

The variability may also be ascribed to several other factors, including the local geomorphological setting and site-specific micro climates that control surface runoff and moisture exchange between the atmosphere and the permafrost ground, respectively. However, if the latter processes does not cause non-equilibrium fractionation, the isotopic composition of ground ice yields a reliable signal of palaeo-winter conditions, as shown in Popp et al. (2006) and presented for time intervals of the middle Weichselian, late Weichselian, and the Holocene (Chapter 3).

The lacustrine sediment core of Lake Satagay provides palaeoenvironmental information in high temporal resolution for the mid and late Holocene. The organic-rich deposits predominantly reflect summer conditions, because the biogeochemical parameters total nitrogen (TN), total organic carbon (TOC), the TOC/TN ratio, and the carbon-isotope ratio ($\delta^{13}C$) indicate the types and amounts of plant and algal materials accumulated during the growing season. Compositional changes of organic matter (Fig. 5.3) thus provide information on environmental changes within the lake and its surroundings (e.g. Meyers and Lallier-Vergès, 1999; Meyers and Teranes, 2001). Rock-Eval pyrolysis, as applied to selected samples, provides a closer look at the organic composition on macromolecule level. On the basis of differences in hydrocarbon and carbonhydrate compositions of algae material and vascular plant organic matter, the pyrolysis data corroborate the inferred implications of the traditional C-N-$\delta^{13}C$ method (e.g. Meyers and Teranes, 2001; Lüniger and Schwark, 2002). Additional bioindicators, such as diatoms and green algae in absolute abundances, demonstrate the sensitive response of the lacustrine system to climatic variability (Chapter 5).

6.2 Late Quaternary to Holocene environmental development in Central Yakutia

In this section, the obtained palaeoenvironmental reconstructions are briefly summarized and compared with former findings of environmental change (see also Figs. 6.1 and 6.2).

In the course of the Mid-Pleistocene Revolution between 0.9 and 0.6 Ma ago (e.g. Berger and Jansen, 1994), which led to an enhanced ice-sheet growth in northern Europe and strengthened glacial and interglacial contrasts at 100-kyr Milankovitch cyclicity, the climate in Central Yakutia changed from temperate to cold conditions.

Sedimentary clues on an incipient periglacial environment were found in sections of the Brunhes normal palaeomagnetic interval (time since 7.2 Ma) at the end of the early Pleistocene along the Lena, Aldan and Vilyuy Rivers (Fradkina et al., 2005). Continuous permafrost has existed since at least 366 to 267 ka BP, as inferred from age determinations of deposits at the archaeological site Diring-Yurakh south of Yakutsk (Waters et al., 1997).

The environment of the middle Pleistocene (corresponding to Marine Isotope Stage 6, 170-130 ka) was characterised by a cold and severe climate in southern and northern Siberia (Chlachula, 2003; Andreev et al., 2004b). Glaciers spread over wide expanses of northern Eurasia (Astakhov, 2004; Svendsen et al., 2004). In the Verkhoyansk Mountains, the corresponding glacier advance around 138 ka ago (Stauch et al., in press) reached far into the mountain foreland, crossing the Lena valley (Fig. 6.1). By this time, the Lena River took a stream course closer to the mountain margin, east of its recent pathway, which is indicated by the provenance of yellowish sands along the lower reaches of Dyanushka River, confirming former findings on the palaeo-stream course (Kind, 1975; Kolpakov, 1986; Alekseev and Drouchits, 2004). The middle Pleistocene glaciers reworked the underlying Lena sediments, but presumably did not initiate a general displacement of the Lena pathway, as assumed by Alekseev and Drouchits (2004). In the vicinity of the Dyanushka River, the Lena influence prevailed until the early Weichselian glaciations, indicated by intercalated layers of hornblende-rich, yellowish sands in sands and tills of otherwise nearby mountain origin (Chapter 4). The glacier ice or glacial deposits presumably caused local damming events in the mountain foreland, as inferred from the occurrence of varved sediments at Menkere River 300 km north of Dyanushka River (Kind, 1975; Kolpakov, 1986; Alekseev and Drouchits, 2004).

The early Weichselian glaciations of the Verkhoyansk Mountains were dated to around 100 ka and 90 ka BP (Stauch et al., in press) and thus correspond well to a maximum early Weichselian ice-sheet extent in northern Eurasia (e.g. Svendsen et al., 2004). After the latter glaciation, no mineralogical clues on an eastern Lena course were found in the mountain foreland (Fig. 6.1). If glacier advances, climatic or tectonic impulses caused the river displacement, remains unclear. Kolpakov (1986) noted that the Lena River was characterised by an unstable hydrological regime during the late Pleistocene, which, in addition to likely increased sediment supply from the mountain region during glacial stages, might have resulted in the aggradation and subsequently displacement of the river valley. However, palaeoclimatic records for the early Weichselian of northeast Siberia are sparse, but surely periglacial conditions with river erosion, deflation, and cryogenesis dominated across the lowlands of Yakutia (Alekseev, 1997; Fradkina et al., 2005). A readvance of glaciers in the Verkhoyansk Mountains occurred during the later early Weichselian before 50 ka BP (Stauch et al., in press), resulting in terminal moraines deposited near the mountain margin or within the mountain valleys. Very likely, these glaciations corresponded to the culminating extent of ice sheets in the Barents-Kara Sea region about 60 to 50 ka BP (Svendsen et al., 2004).

Around this time, 60–50,000 years ago, the formation of the Ice Complex started in places in northern Yakutia (Schirrmeister et al., 2002). In Central Yakutia, the dating of

the oldest Ice-Complex deposits at Mamontova Gora revealed similar ages (Péwé et al., 1977). Analogue to the situation on the Lena Delta (Schwamborn et al., 2002), sands of early to mid-Pleistocene fluvial terraces underlie the Ice Complex in the Lena-Aldan vicinities (e.g. Soloviev, 1973a; Péwé and Journaux, 1983). According to the findings from northern Yakutia, the climate during the middle Weichselian was highly continental with warmer summers and colder winters than today (Meyer et al., 2002a; Schirrmeister et al., 2002; Hubberten et al., 2004; Kienast et al., 2005). However, climatic fluctuations occurred, and towards the late Weichselian, the climate became more severe and dry than in the middle Weichselian across the Laptev Sea region. For the first time, equivalent palaeoclimatic data were obtained from the central Yakutian Ice Complex, showing severe winter conditions for time intervals around 41, 21, and 13 ^{14}C ka BP (Popp et al, 2006). These findings are consistent with those from the Laptev Sea and indicate very cold winter conditions until the onset of initial warming at the end of the late glacial period. Pleistocene ice-wedge growth also took place in the Verkhoyansk Foreland (sites *Tum3* and *Dja2*), but extended Ice-Complex formation was likely prevented through rather unstable surface conditions, such as fluvial activity. For example, ice-wedge site *Dja2* is situated on fluvial-terrace deposits and the isotopic signal of the ice reveals a distinct influence of river water, indicating seasonal flooding of a subaerial exposed surface.

Given that the Ice-Complex development across Yakutia took place under similar climate conditions, a very cold and dry environment prevailed during most intervals of the middle and late Weichselian and gave rise to strong aeolian deflation and dust accumulation. The aeolian accumulation in Central Yakutia, however, was repeatedly interrupted by fluvial activity, which culminated in enhanced river erosion between 37 and 33 ^{14}C ka (Siegert, personal communication, 2006). In contrast, periods of increased aeolian accumulation were IRSL dated to between 33 and 24 ka and between 13 and 9 ka in the Verkhoyansk Foreland (Fig. 6.1) (Stauch et al., in press). Provenance analysis indicates that the wind-drifted material is of primarily Lena origin. Similar findings on the provenance of loess-like sediments were obtained for the Lena-Aldan interstream area (Péwé and Journaux, 1983).

The younger aeolian phase between 13 and 9 ka matches the Pleistocene–Holocene transition that was characterised by a rise in temperature across northeastern Siberia (e.g. Andreev and Klimanov, 2000; Andreev et al., 2002a, 2003; 2004a; Schirrmeister et al., 2002; Demske et al., 2005). In contrast to the other regions, however, the environment of Central Yakutia remained rather dry until about 10 ka BP, indicated by steppe-like vegetation communities (Andreev and Klimanov, in Fradkina et al., 2005).

The warming during the Allerød interstadial apparently ended the Ice-Complex formation and probably interrupted ice-wedge growth during the early Holocene at the Laptev Sea coast (Meyer et al., 2002a; Schirrmeister et al., 2002). Similar conclusions can be drawn from dated ice-wedge sections in Central Yakutia, where the upper horizon of the Ice Complex at *Ulakhan Surdakh* and the subsequent Holocene ice wedge (*Tum1*) was dated to 13 and maximal 8.5 ^{14}C ka BP, respectively. The degradation of permafrost by thermokarst processes and the initial formation of thermokarst lakes also started in the Allerød (Schirrmeister et al., 2002; Velichko et al., 2002).

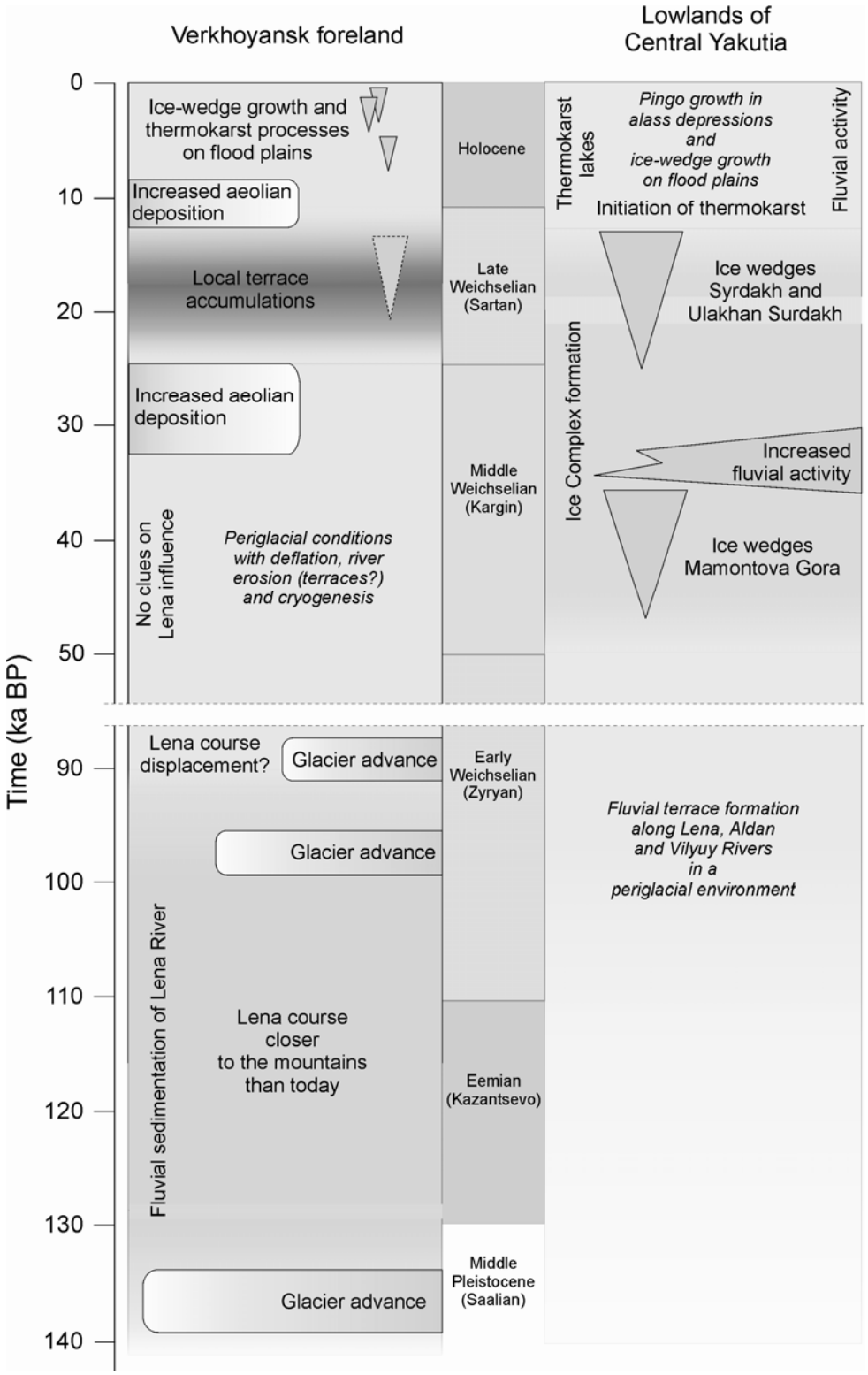

Fig. 6.1: Compilation of environmental development in the Verkhoyansk Foreland (left column) and the lowlands of Central Yakutia. Chronology of glacier advances and periods with increased aeolian accumulation were adopted from Stauch et al. (in press).

In Central Yakutia, the oldest dated lacustrine deposits reach back before 11 ka (Andreev et al., 1997), but it is reasonable to assume that the majority of thermokarst lakes developed during the more favourable Boreal and Atlantic period, when temperature and precipitation values became permanently increased (e.g. Jasinski et al., 1998; Laing et al., 1999; Andreev and Klimanov, 2000; Andreev et al., 2002b, 2002c, 2004). The presence of an early Holocene climate optimum is also supported by the isotopic signals in the studied ice wedges that reveal relatively warm winters in the early Holocene and rather cold winters during intervals of the late Holocene (Chapter 3).

The inference of Holocene climate development in Central Yakutia is mainly based on the reconstruction of vegetation history. Lacustrine pollen records from the Vilyuy area indicate a thermal maximum with high annual precipitation between roughly 6.8 and 5.1 cal. ka BP, followed by moderate climate conditions through the younger part of the Holocene (Fradkina et al., 2005). At present, the most reliable palaeoclimate record for Yakutia is available from Lake Nikolay in the Lena Delta, which is based on quantitative reconstructions on the basis of fossil pollen and chironomids (Andreev et al., 2004a). The findings give evidence of a climate optimum between 9.2 and 5.8 cal. ka BP, followed by unstable climate conditions between 5.8 and 3.7 cal. ka BP. This is consistent with finding from the Taymyr area in central Siberia, where the regional climate optimum appeared between 9.5 and 5.1 ka cal. ka BP (Andreev et al., 2000, 2003; Kumke et al., 2004) with highest summer temperatures and precipitation between 7.4 and 5.7 cal. ka BP (Koshkarova, 1995).

In this thesis, a new approach has been applied to gain insights into Holocene climate variability of the last 7500 years by the reconstruction of lake status variability of Lake Satagay, a typical thermokarst lake situated in the Vilyuy area (Chapter 5). Thermokarst lakes are known to respond sensitively to changes in the regional climate-driven hydrological budget (Gavrilova, 1973; Bosikov, 1991, 1998). Today, marked fluctuations of thermokarst lake levels at sub-decadal time scales indicate repeated changes in summer humidity that are likely related to climate seesaw teleconnections in the global climate system, such as the Arctic Oscillation. Historical data of the last century support the high sensitivity of Siberian lakes to summer climate change. Palaeoenvironmental proxy data inferred from fossil bioindicators and the composition of organic matter of the lacustrine sediment record of Lake Satagay in Central Yakutia reveal distinct variations in lake level, trophic state, and water temperature at centennial time scales during the mid- to late Holocene. A basic and new outcome is that the climate fluctuations recorded in the Lake Satagay sediments apparently show strong affinities to prominent variations in sunspot activity, suggesting an intimate relationship between mediate solar forcing and climate variability in eastern Siberia. It also becomes evident that the short-term climate perturbations were most severe during the transition from the early Holocene climate optimum to late Holocene climate deterioration.

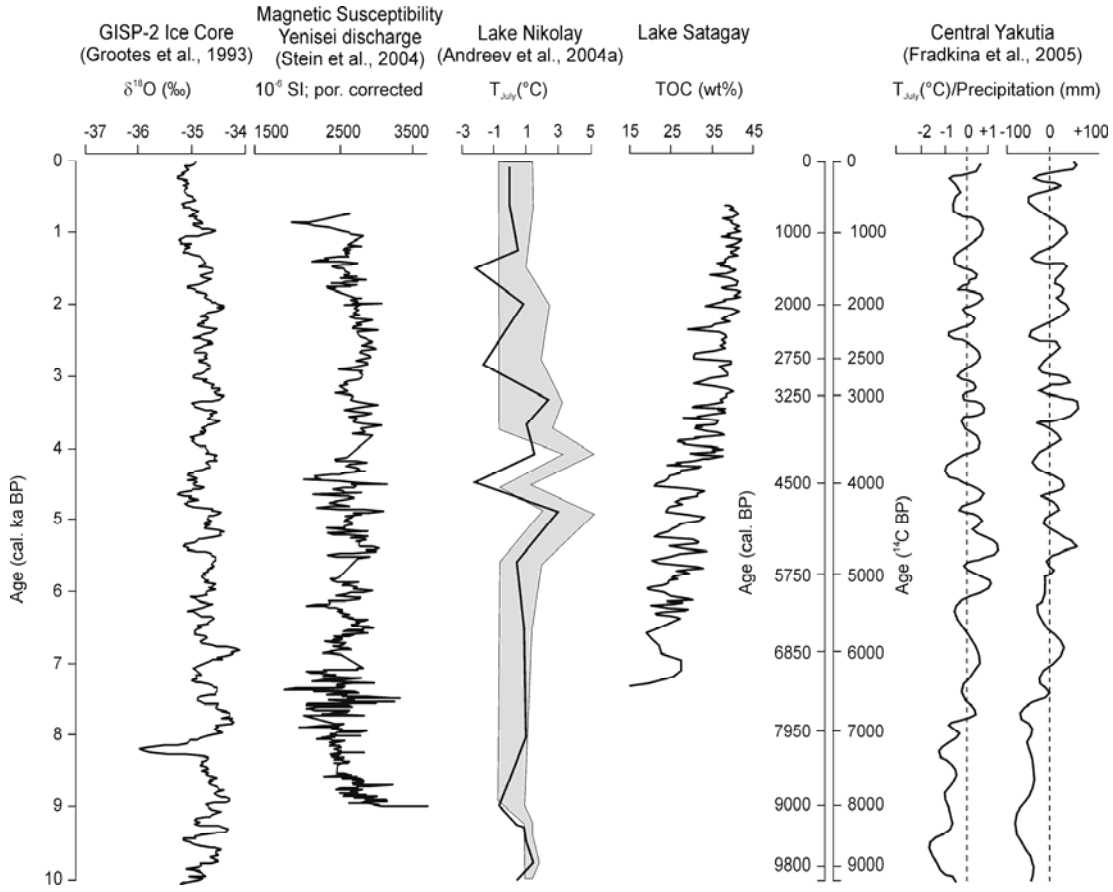

Fig. 6.2: Holocene environmental change as revealed by the GISP2 ice-core record and terrestrial records across Siberia. While the GISP2 isotope record shows a relatively uniform pattern, the Yenisei discharge record as well as the lacustrine records show strong climatic variability, particularly during the transition from the mid to the late Holocene between 6.0 and 4.0 cal. ka BP. Note that the central Yakutian record in the right column is shown at the radiocarbon age scale.

Mid-Holocene climate instability has also been inferred in the Lake Nikolay record of the Lena Delta (Andreev et al., 2004a) and is nicely displayed by marked fluctuations in fluvial run-off in the central Siberian Kara Sea during the same time (Stein et al., 2004) (Fig. 6.2). On a global scale, mid-Holocene climate variability seems to be a world-wide and coeval phenomenon and has also been recognized in NW China, central Europe, as well as in the tropical regions and on the southern hemisphere (Yu et al., 2006; Magny et al., 2006; Haug et al., 2001; deMenocal et al., 2000; Steig, 1999). The overall driving force of global mid-Holocene climate change can basically be attributed to an enhancement of seasonality in insolation on the northern hemisphere following the early Holocene preccessional maximum in insolation (Mayewski et al., 2004; Schmidt et al., 2004). There is growing evidence that the long-term trends in insolation are overprinted by short-term variations in solar activity (e.g. Beer et al., 2000; Bond et al., 2001), as also shown by the Lake Satagay record. The latter also demonstrates that mid-Holocene climate instability besides changing modes in insolation may be attributed to a dense succession of sunspot minima during that time. In conclusion, the eastern Siberian climate system, at least for the Holocene, shows a close linkage to the global

climate system. A future challenge is to gain a better understanding of the driving forces and modes of teleconnections underlying the climatic responses in northeastern Siberia.

7. Outlook

Towards an understanding of environmental change in Central Yakutia, this thesis provides substantial findings on the chronology of periglacial landscape development and climatic variability in the Late Quaternary.

Provenance analysis conducted on Quaternary deposits from exposures along the Dyanushka and Tumara Rivers represented promising case studies for revealing the fluvial and glacial influence in the Verkhoyansk foreland. Although the mid-Pleistocene Lena course east of its recent pathway could be confirmed, no clues were obtained on possible ice-damming events. Nevertheless, such damming events are supposed to have occurred on the basis of marine and terrestrial evidences (e.g. Alekseev and Drouchits, 2004; Spielhagen et al., 2005). For future studies, a suited site for the examination of ice-damming events lies at the Menkere River north of Zhigansk, where outcrops of interfingering fluvial, glacial and lacustrine sediments are described (e.g. Alekseev and Drouchits, 2004). More detailed investigations of terrace deposits in common would provide clues on Lena River dynamics during ancient times and may yield a link to a better understanding of sedimentation processes in the Lena Delta region.

The palaeoclimatic interpretation of isotopic data obtained from ice wedges is a promising technique, but for more precise palaeoclimatic conclusions, the data set should be extended through Yakutia. Excellent archives for this purpose are the Ice Complex formations along the Lena and Aldan Rivers, which represent stratigraphic equivalents of the thick Ice-Complex units in the Laptev Sea region. An ultimate goal should be to obtain palaeo-winter-temperature estimates along a north-south transect of climate gradients from the tundra to the taiga regions. Another perspective is to get more detailed information of boundary conditions that control the depositional environment of the ice-wedge host sediments, and accurate age determinations are needed.

Lake Satagay has shown the potential to infer Holocene fluctuations in environmental and climate conditions at high temporal resolution. In analogy to future ice-wedge studies through a wider area of Yakutia, more of such lake records are needed for a better understanding of climatic variability during the present warm stage. In combination with quantitative summer temperature reconstructions, revealed by the application of transfer functions on fossil chironomid and pollen assemblages, the sensitive climatic response of thermokarst lakes in the continental interior of Yakutia can be better assessed.

The integrated geocryological and limnogeological approach for the reconstruction of both palaeo winter and summer conditions on a wide regional scale will help to unravel the variability of seasonal climate gradients (continentality) through time. In combination with climate modelling the raised data will provide new insights into teleconnections between the eastern Siberian and global climate system.

8. References

ACIA, 2004: Impacts of a warming Arctic: Arctic Climate Impact Assessment. Cambridge University Press, New York, 139 pp.

Agafonov, L., Strunk, H., and Nuber, T., 2004: Thermokarst dynamics in Western Siberia: insights from dendrochronological research. Palaeogeography, Palaeoclimatology, Palaeoecology 209: 183-196.

Agricultural Atlas of the Republic Sakha (Yakutia), 1989: Matveev, I.A. (ed.), Nauk, Moscow, 115 pp. (in Russian).

Alabyan, A.M., Chalov, R.S., Korotaev, V.N., Sidorchuka, A.Y, and Zaitzev, A.A., 1995: Natural and technogenic water and sediment supply to the Lapte Sea. *In*: Kassens, H., Piepenburg, D., Thiede, J., Thimokhov, L., Hubberten, H.-W., and Priamikov, S.M. (eds.), *Russian-German Cooperation: Laptev Sea System*. Reports on Polar Research 176: 265-271.

Alekseev, M.N., 1961: Stratigraphy of continental Neogene and Quaternary deposits in the Vilyuy Depression and the lower Lena River Valley. Akademiya Nauk SSSR, Geologicheskiy Institut, Trudy, v. 51, 199 pp. (in Russian).

Alekseev, M.N., 1997: Paleogeography and geochronology in the Russian eastern Arctic during the second half of the Quaternary. Quaternary International 41/42: 11-15.

Alekseev, M.N. and Drouchits, V.A., 2004: Quaternary fluvial sediments in the Russian Arctic and Subarctic: Late Cenozoic development of the Lena River system, Northeastern Siberia. Proceedings of the Geologists'Association 115: 339-346.

Alekseev, M.N., Kamaletdinov, V.A., Siegert, C., Grinenko, O.V., Gnibidenko, Z.N., Gravis, G.F. and Shamshina, E.A., 1990: *Geological Problems of the Paleolithic Site Diring Yuryakh*, Preprint, Yakutsk, 48 pp. (in Russian).

Anderson, P.M., Lozhkin, A.V., and Brubaker, L.B., 2002: Implications of a 24,000-yr palynological record for a Younger Dryas cooling and for boreal forest development in northeastern Siberia. Quaternary Research 57: 325-333.

Andreev, A.A., Klimanov, V.A., and Sulerzhitsky, L.D., 1997: Younger Dryas pollen records from Central and southern Yakutia. Quaternary International 41/42: 111-117.

Andreev, A.A. and Klimanov, V.A., 2000: Quantitative Holocene climate reconstruction from Artic Russia. Journal of Paleolimnology 24 (1): 81-91.

Andreev, A.A., Siegert, C., Klimanov, V.A., Derevyagin, A.Yu., Shilova, G.N., and Melles, M., 2002a: Late Pleistocene and Holocene vegetation and climate on the Taymyr lowland, northern Siberia. Quaternary Research 57: 138-150.

Andreev, A.A., Schirrmeister, L., Siegert, C., Bobrov, A.A., Demske, D., Seiffert, M., and Hubberten, H.-W., 2002b: Paleoenvironmental changes in northeastern Siberia during the late Quaternary – Evidence from pollen records of the Bykovsky Peninsula. Polarforschung 70: 13-25.

Andreev, A.A., Klimanov, V.A., and Sulerzhitsky, L.D., 2002c: History of vegetation and climate of central Yakutia during the late Glacial and Holocene. Botanicheskiy zhurnal 87 (7): 86-98 (in Russian with English summary).

Andreev, A.A., Tarasov, P.E., Siegert, C., Ebel, T., Klimanov, V.A., Melles, M., Bobrov, A.A., Dereviagin, A.Yu., Lubinski, D.J., and Hubberten, H.-W., 2003: Late Pleistocene

and Holocene vegetation and climate on the northern Taymyr Peninsula, Arctic Russia. Boreas 32: 484-505.

Andreev, A.A., Tarasov, P., Schwamborn, G., Ilyashuk, B., Ilyashuk, E., Bobrov, A., Klimanov, V., Rachold, V., and Hubberten, H.-W., 2004a: Holocene paleoenvironmental records from Nikolay Lake, Lena River Delta, Arctic Russia. Palaeogeography, Palaeoclimatology, Palaeoecology 209: 197-217.

Andreev, A.A., Grosse, G., Schirrmeister, L., Kuzmina, S.A., Novenko, E.Yu., Bobrov, A.A., Tarasov, P.E., Ilyashuk, B.P., Kuznetsova, T.V., Krbschek, M., Meyer, H., and Kunitsky, V.V., 2004b: Late Saalian and Eemian palaeoenvironmental history of the Bol'shoy Lyakhovsky Island (Laptev Sea region, Arctic Siberia). Boreas 33: 319-348.

Astakhov, V., 2004: Middle Pleistocene glaciations of the Russian North. Quaternary Science Reviews 23: 1285-1311.

Atlas of Yakutia, 1981: Bogatova, G.A., Bugrimova, N.P., and Gutzhina, A.G. (eds.), GUGK, Moscow.

Baranova, Yu.P., 1979: Neogene and Pleistocene deposits of Central Yakutia. *In:* Solovjev, P.A., Popov, P.N. (eds.), *Guidebook XIV Pacific Science Congress, Yakutsk, 12-18 August, 1979*. The Yakut Bransh of the Siberian Department of the USSR. Academy of Sciences: Yakutsk, pp. 37-73.

Beer, J., 2000: Long-term indirect indices o solar variability. Space Science Reviews 94: 53-66.

Beer, J., Siegenthaler, U., Bonani, G., Finkel, R.C., Oeschger, H., Suter, M., and Wölfli, W., 1988: Information on past solar activity and geomagnetism from ^{10}Be in the Camp Century ice core. Nature 331: 675-679.

Beer, J., Mende, W., and Stellmacher, R., 2000: The role of the sun in climate forcing. Quaternary Science Reviews 19: 403-415.

Behrends, M., Hoops, E., and Peregovich, B., 1999: Distribution patterns of heavy minerals in Siberian Rivers, the Laptev Sea and the Eastern Arctic Ocean: An approach to identify sources, transport and pathways of terrigenous matter. *In:* Kassens, H., Bauch, H.A., Dmitrenko, I., Eicken, H., Hubberten, H.-W., Melles, M., Thiede, J., Timokhov, L. (eds), *Land-ocean systems in the Siberian Arctic*: *Dynamics and history.* Springer-Verlag, Berlin, pp. 265-286.

Berger, W.H. and Jahnsen, E., 1994: Mid-Pleistocene climate shift – the Nansen connection. *In:* Johannessen, O.M., Muench, R.D. (eds.), *The Polar Oceans and their role in shaping the global environment*. AGU Geophys. Monogr. 85, pp. 295-311.

Biscaye, P.E., 1965: Mineralogy and sedimentation of recent deep-sea clay in the Atlantic Ocean and adjacent seas and oceans. Geol. Soc. Am. Bull. 76: 803-832.

Boenigk, W., 1983: *Schwermineralanalyse*. Enke, Stuttgart, 152 pp. (in German).

Bond, G., Kromer, B., Beer, J., Muscheler, R., Evans, M.N., Showers, W., Hoffmann, S., Lotti-Bond, R., Hajdas, I., and Bonani, G., 2001: Persistent solar influence on North Atlantic climate during the Holocene. Science 294: 2130-2136.

Bosikov, N.P., 1991: *The evolution of alasses in Central Yakutia*. Akademija Nauk SSSR, Permafrost Institute, Yakutsk, 128 pp. (in Russian).

Bosikov, N.P., 1998: Wetness variability and dynamics of thermokarst processes in Central Yakutia. Proceedings of the 7th International Conference on Permafrost, Centre d'etudes nordique, Universite Laval, Quebec: 71-74.

Brigham-Grette, J., Gualtieri, L.M., Glushkova, O.Yu., Hamilton, T.D., Mostoller, D., and Kotov, A., 2003: Chlorine-36 and ^{14}C chronology support a limited last glacial maximum across central Chukotka, northeastern Siberia, and no Beringian ice sheet. Quaternary Research 59: 386-398.

Carslaw, K.S., Harrison, R.G., and Kirkby, J., 2002: Cosmic rays, clouds, and climate. Science 298: 1732-1737.

Chain, V.E. and Koronovskii, N., 1995: *Nordasien*. Enke, Stuttgart, 181 pp. (in German).

Chapin III, F.S., Sturm, M., Serreze, M.C., McFadden, J.P., Key, J.R., Lloyd, A.H., McGuire, A.D., Rupp, T.S., Lynch, A.H., Schimel, J.P., Beringer, J., Chapman, W.L., Epstein, H.E., Euskirchen, E.S., Hinzman, L.D., Jia, G., Ping, C.-L., Tape, K.D., Thompsen, C.D.C., Walker, D.A., and Welker, J.M., 2005: Role of land-surface changes in Arctic summer warming. Science 310: 657-660.

Chapman, W.L. and Walsh, J.E., 1993: Recent variations of sea ice and air temperature in high latitudes. Bull. Am. Meteorol. Soc. 74 (1): 33-47.

Cherdonova, V.S., 1993: Types of circulation processes and its frequency in southern Yakutia. Voprosy geografii Yakutii 7: 17-25 (in Russian).

Chlachula, J., 2003: The Siberian loess record and its significance for reconstruction of Pleistocene climate change in north-central Asia. Quaternary Science Reviews 22: 1879-1906.

Clark, I.D. and Fritz, P., 1997: *Environmental isotopes in hydrology*. Lewis Publishers. Boca Raton, 328 pp.

Craig, H., 1961: Isotopic variations in meteoric waters. Science 133: 1702-1703.

Cronberg, G., 1982: *Pediastrum* and *Scenedesmus* (Chlorococcales) in sediments from Lake Växjösjön, Sweden. Arch. Hydrobiol. Suppl. 60 (4) (or Algological Studies 29): 500-507.

Czudek, T. and Demek, J., 1970: Thermokarst in Siberia and its influence on the development of lowland relief. Quaternary Research 1: 103-120.

Dansgaard, W., 1964: Stable isotopes in precipitation. Tellus 16: 436-468.

Davis, B.A.S., Brewer, S., Stevenson, A.C., Guiot, J., and Data Contributors, 2003: The temperature of Europe during the Holocene reconstructed from pollen data. Quaternary Science Reviews 22: 1701-1716.

deMenocal, P., Ortiz, J., Guilderson, T., and Sarntheim, M., 2000: Coherent high- and low-latitude climate variability during the Holocene warm period. Science 288: 2198-2202.

Demske, D., Heumann, G., Granoszewski, W., Nita, M., Mamakowa, K., Tarasov, P.E., and Oberhänsli, H., 2005: Late glacial and Holocene vegetation and regional climate variability evidenced in high-resolution pollen records from Lake Baikal. Global and Planetary Change 46: 255-279.

Diekmann, B. and Wopfner, H., 1996: Petrographic and diagenetic signatures of climate change in peri- and postglacial Karoo Sediments of SW Tanzania. Palaeogeography, Palaeoclimatology, Palaeoecology 125: 5-25.

Diekmann, B. and Kuhn, G., 1999: Provenance and dispersal of glacial-marine surface sediments in the Weddell Sea and adjoining areas, Antarctica: ice-rafting versus current transport. Marine Geology 158: 209-231.

Dolginow, J. and Kropatschjow, S., 1994: *Abriss der Geologie Russlands und angrenzender Staaten*. E. Schweizerbart'sche Verlagsbuchhandlung (Nägele u. Obermiller), Stuttgart, 174 pp. (in German).

Ehrmann, W.U., Melles, M., Kuhn, G., and Grobe, H., 1992: Significance of clay mineral assemblages in the Antarctic Ocean. Marine Geology 107: 249-273.

Epstein, S. and Mayeda, T., 1953: Variations of O^{18} content of waters from natural sources. Geochimica et Cosmochimica Acta 4: 213-224.

Ershov, E.D., 1995: *Physical and chemical basics of geocryology*. Moscow University press, Moscow, 369 pp. (in Russian).

Esper, J., Cook, E.R., and Schweingruber, F.H., 2002: Low-frequency signals in long tree-ring chronologies for reconstructing past temperature variability. Science 295: 2250-2253.

Felis, T., Pätzold, J., Loya, Y., Fine, M., Nawar, A.H., and Wefer, G., 2000: A coral oxygen isotope record from the northern Red Sea documenting NAO, ENSO, and North Pacific teleconnections on Middle East climate variability since the year 1750. Paleoceanography 15: 679-694.

Fradkina, A.F., Alekseev, M.N., Andreev, A.A., and Klimanov, V.A., 2005: East Siberia (based on data obtained mainly in Central Yakutia). *In*: Velichko, A.A. and Nechaev, V.P. (eds.), *Cenozoic climatic and environmental changes in Russia*. Geological Society of America Special Paper 382: 89-103.

Franz, H.J., 1973: *Physische Geographie der Sowjetunion*. Hermann Haack, Gotha, 535 pp. (in German).

French, H.M., 1996: *The Periglacial Environment*. 2nd edn. Addison-Wesley Longman, London, 341 pp.

Gavrilova, M.K., 1973: *Climate of Central Yakutia*. Yakutknogoizdat, Yakutsk, 120 pp. (in Russian).

Gavrilova, M.K., 1993: Climate and Permafrost. Permafrost and Periglacial Processes 4: 99-111.

Gavrilova, M.K. and Atlasova, V.S., 1969: The frequency of circulation processes in Central Yakutia. Voprosy geografii Yakutii 5: 5-11 (in Russian).

Gavrilov, A.V., Romanovskii, N.N., Romanovsky, V.E., Hubberten, H.-W., and Tumskoy, V.E., 2003: Reconstruction if Ice Complex remnants on the Eastern Siberian Arctic Shelf. Permafrost and Periglacial Processes 14: 187-198.

Glushkova, O.Yu., 2001: Geomorphological correlation of Late Pleistocene glacial complexes of Western and Eastern Beringia. Quaternary Science Reviews 20: 405-417.

Gravenor, C.P., 1979: The nature of the Late Paleozoic glaciation in Gondwana as determined from an analysis of garnets and other heavy minerals. Canadian Journal of Earth Sciences 16: 1137-1153.

Grigoriev, M.N., Davidov, N.M., Kostyukevich, V.V., and Uritsky, Yu.F., 1989: The evolution of the Lena River basin during the late Cenozoic (on the basis of transport processes of clastic material in the cryozone). *In:* Romanov, V.P. (ed.), *Conditions and processes of the cryogene material migration*. Yakutsk, pp. 153-161 (in Russian).

Grootes, P.M., Stuiver, M., White, J.W.C., Johnsen, S., and Jouzel, J., 1993: Comparison of oxygen isotope records from the GISP2 and GRIP Greenland ice cores. Nature 366: 552-554.

Hahne, J. and Melles, M., 1999: Climate and vegetation history of the Taymyr Peninsula since the Middle Weichselian time – palynological evidence from lake sediments. *In:* Kassens, H., H.A. Bauch, I. Dmitrenko, H. Eicken, H.-W. Hubberten, M. Melles, J. Thiede, and L. Timokhov (eds.), *Land-Ocean Systems in the Siberian Arctic: Dynamics and History*. Springer-Verlag, Berlin, pp. 407-424.

Hassan, K.M., Swinehart, J.B., and Spalding, R.F., 1997: Evidence for Holocene environmental change from C/N ratios, and $\delta^{13}C$ and $\delta^{15}N$ values in Swan Lake sediments, western Sand Hills, Nebraska. Journal of Paleolimnology 18: 121-130.

Haug, G.H., Hughen, K.A., Sigman, D.M., Peterson, L.C., and Röhl, U., 2001: Southward migration of the intertropical convergence zone through the Holocene. Science 293: 1304-1308.

Hermel, J., 1995: Sedimentpetrographische Untersuchungen an Flußsedimenten der Lena (Yakutsk – Laptev See), Ostsibirien. Unpublished diploma thesis, TU Braunschweig, 120 pp. (in German).

Hinzman, L.D. et al., 2005: Evidence and implications of recent climate change in northern Alaska and other Arctic regions. Climatic Change 72: 251-298.

Hodell, D.A. and Schelske, C.L., 1998: Production, sedimentation, and isotopic composition of organic matter in Lake Ontario. Limnology and Oceanography 43 (2): 200-214.

Hollander, D.J. and McKenzie, J.A., 1991: CO_2 control on carbon-isotope fractionation during aqueous photosynthesis: A paleo-pCO_2 barometer. Geology 19: 929-932.

Hoops, E., 1999: *Die Charakterisierung von Sedimenten der in die Laptev-See mündenden Flüsse anhand von Schwermineralverteilungen.* PhD thesis, University of Potsdam, 114 pp. (in German).

Houmark-Nielsen, M., Demidov, I., Funder, S., Grøsfjeld, K., Kjær, K.H., Larsen, E., Lavrova, N., Lyså, A., and Nielsen, J.K., 2001: Early and Middle Valdaian glaciations, ice-dammed lakes and periglacial interstadials in northwest Russia: new evidences from the Pyoza River area. Global and Planetary Change 31: 215-237.

Hoyt, D.V. and Schatten, K.H., 1998: Group sunspot numbers: A new solar activity reconstruction: Solar Physics 179: 189-219.

Hu, F.S., Kaufman, D., Yoneji, S., Nelson, D., Shemesh, A., Huang, Y., Tian, J., Bond, G., Clegg, B., and Brown, T., 2003: Cyclic variations and solar forcing of Holocene climate in the Alaskan Subarctic. Science 301: 1890-1893.

Hubberten, H.-W., Andreev, A.A., Astakhov, V.I., Demidov, I., Dowdeswell, J.A., Henriksen, M., Hjorf, C., Houmark-Nielsen, M., Jakobsson, M., Kuzmina, S., Larsen, E., Lunkka, J.P., Lyså, A., Mangerud, J., Möller, P., Saarnisto, M., Schirrmeister, L., Sher, A.V., Siegert, C., Siegert, M.J., and Svendsen, J.I., 2004: The periglacial climate and environment in northern Eurasia during the Last Glaciation. Quaternary Science Reviews 23: 1333-1357.

Huber, J.K., 1996: A postglacial pollen and nonsiliceous algae record from Gegoka Lake, Lake County, Minnesota. Journal of Paleolimnology 16: 23-35.

International Permafrost Association, 1998: *Multi-language glossary of permafrost and related ground-ice terms*. Van Everdingen, R.O. (ed.), The Arctic Institute of North America, Calgary, Canada, 78 pp.

Jasinski, J.P.P., Warner, B.G., Andreev, A.A., Aravena, R., Gilbert, S.E., Zeeb, B.A., Smol, J.P., and Velichko, A.A., 1998: Holocene environmental history of a peatland in the Lena River valley, Siberia. Canadian Journal of Earth Sciences 35: 637-648.

Jean-Baptiste, P., Jouzel, J., Stievenard, M., and Ciais, P., 1998: Experimental determination of the diffusion rate of deuterated water vapor in ice and application to the stable isotopes smoothing of ice cores. Earth and Planetary Science Letters 158: 81-90.

Johnsen, S.J. and White, J.W.C., 1989: The origin of Arctic precipitation under present and glacial conditions. Tellus 41B: 452-468.

Jones, M.H., Fahnenstock, J.T., Walker, D.A., Walker, M.D., and Welker, J.M., 1998: Carbon dioxide fluxes in moist and dry Arctic Tundra during the snow-free season: Responses to increases in summer temperature and winter snow accumulation. Arctic, Antarctic, and Alpine Research 30 (4): 373-380.

Jouzel, J., Alley, R.B., Cuffey, K.M., Dansgaard, W., Grootes, P., Hoffmann, G., Johnson, S.J., Koster, R.D., Peel, D., Shumann, C.A., Stievenard, M., Stuiver, M., and White, J., 1997: Validity of the temperature reconstruction from water isotopes in ice cores. Journal of Geophysical Research 102 (C12): 26.471-26.487.

Kaplan, M.R. and Wolfe, A.B., 2006: Spatial and temporal variability of Holocene temperature in the North Atlantic region. Quaternary Research 65: 223-231.

Katasonov, E.M., 1963: Frozen ground facies analysis of Quaternary deposits in the lower part of the Tumara basin. *In:* Conditions and specific features of the permafrost development in Siberia and North-East. Acad. Nauk, Moscow, pp. 5-25 (in Russian).

Katasonov, E.M., 1975: Frozen-ground and facial analysis of Pleistocene deposits and paleogeography of Central Yakutia. Biuletyn Peryglacjalny 24: 33-40.

Katasonov, E.M., 1979: Structure and absolute geochronology of alas deposits in Central Yakutia. Akad. Nauk SSSR, Moscow, 81 pp. (in Russian).

Katasonov, E.M. and Solovyev, P.A., 1969: *Guide to trip round Central Yakutia - paleogeography and periglacial phenomena*. International Symposium 'Paleogeography and Periglacial Phenomena of Pleistocene', Yakutsk, 91 pp.

Kaufman, D.S., Ager, T.A., Anderson, N.J., Anderson, P.M., Andrews, J.T., Bartlein, P.J., Brubaker, L.B., Coats, L.L., Cwynar, L.C., Duvall, M.L., Dyke, A.S., Edwards, M.E., Eisner, W.R., Gajewski, K., Geirsdóttir, A., Hu, F.S., Jennings, A.E., Kaplan, M.R., Kerwin, M.W., Lozhkin, A.V., MacDonald, G.M., Miller, G.H., Mock, C.J., Oswald, W.W., Otto-Bliesner, B.L., Porinchu, D.F., Rühland, K., Smol, J.P., Steig, E.J., and Wolfe, B.B., 2004: Holocene thermal maximum in the western Arctic (0-180°). Quaternary Science Reviews 23: 529-560.

Kienast, F., Siegert, C., Dereviagin, A., and Mai, D.-H., 2001: Climatic implications of Late Quaternary plant macrofossil assemblages from the Taymyr Peninsula, Siberia. Global and Planetary Change 31: 265-281.

Kienast, F., Schirrmeister, L., Siegert, C., and Tarasov, P., 2005: Palaeobotanical evidence for warm summers in the East Siberian Arctic during the last cold stage. Quaternary Research 63: 283-300.

Kienel, U., Siegert, C., and Hahne, J., 1999: Late Quaternary palaeoenvironmental reconstructions from a permafrost sequence (North Siberian Lowland, SE Taymyr Peninsula) – a multidisciplinary case study. Boreas 28: 181-193.

Kind, N.V., 1975: Glaciations in the Verkhoyansk Mountains and their place in the radiocarbon geochronology of the Siberian Late Anthropogene. Biuletyn Peryglacjalny 24: 41-54.

Kind, N.V., Kolpakov, V.V., and Sulerzhitskiy, L.D., 1971: To the problem of age of the glaciations in the Verkhoyan'ye (upper reaches of the Yana River) district.

Proceedings of the USSR Academy of Sciences, Geological Series, 10, pp. 135-144 (in Russian).

Kolpakov, D.V., 1984: Geomorphology. *In:* Napatov, L.M. (ed.), *Geological mapping report of scale 1:100 000 (Quadrangle Q-52, 53 – Verkhoyansk)*, pp. 92-96.

Kolpakov, V.V., 1979: Glacial and periglacial topography of the Verkhoyansk glacial area and new radiocarbon dates. *In:* Regionalnaya geomorphologiya rayonov novogo osvoeniya. Moscow, pp. 83-98 (in Russian).

Kolpakov, V.V., 1983: Aeolian Quaternary deposits in the Lena area of Yakutia. *In:* Bulletin of the Commission of Quaternary Research, Nauka, Moscow, pp. 123-131 (in Russian).

Kolpakov, V.V., 1986: Effects of glaciations on the rivers in Yakutia. *In:* Velichko, A.A. and Isaeva, L.L. (eds.), *Quaternary glaciations in Middle Siberia*. Nauka, Moscow, pp. 101-108 (in Russian).

Kolpakov, V.V. and Shofman, I.L., 1982: Glacial Isostasy in the Verkhoyansk Highlands Vicinities. *In:* Geology of the Cenozoic of Yakutia. Siberian Branch of the USSR Acad. Sciences, Yakutsk, pp. 150-156 (in Russian).

Koreysha, M.M., 1989: Glaciation. *In:* Yershov, E.D. (ed.), *Geocryology of the SSSR, Eastern Siberia and Far East*. Nedra Publ. Moscow, pp. 160-162 (in Russian).

Koshkarova, V.L., 1995: Vegetation response to global and regional environmental change on the Taymyr Peninsula during the Holocene. Polar Geography and Geology 19: 145-151.

Kossovskaya, A.G., Shutov, V.D., and Murav'ev, V.I., 1960: Mesozoic and upper Palaezoic deposits of the western Verkhoyan and the Vilyuy depression. Trudy Geologicheskogo Instituta (GIN), vyp. 34, Nauka, Moscow, 276 pp. (in Russian).

Kuhn, G. and Diekmann, B., 2002: Late Quaternary variability of ocean circulation in the southeastern South Atlantic inferred from the terrigenous sediment record of a drift deposit in the southern Cape Basin (ODP Site 1089). Palaeogeography, Palaeoclimatology, Palaeoecology 182: 287-303.

Kumke, T., Kienel, U., Weckström, J., Korhola, A., and Hubberten, H.-W., 2004: Inferred Holocene Paleotemperatures from diatoms at Lake Lama, Central Siberia. Arctic, Antarctic, and Alpine Research 36 (4): 624-634.

Kurita, N., Numaguti, A., Sugimoto, A., Ichiyanagi, K., and Yoshida, N., 2003: Relationship between the variation of isotopic ratios and the source of summer precipitation in eastern Siberia. Journal of Geophysical Research 108 (D11): 4339.

Kurita, N., Yoshida, N., Inoue, G., and Chayanova, E.A., 2004: Modern isotope climatology of Russia: A first assessment. Journal of Geophysical Research 109: D03102.

Kuznetsova, L.P., 1997: Atmospheric moisture content and transfer over the territory of the former USSR. *In:* Ohata, T. and Hiyama, T. (eds.), *Second International Workshop on Energy and Water Cycle in GAME-Siberia, 1997*. Research Report of IHAS, Institute for Hydrospheric-Atmospheric Sciences, Nagoya, Japan, pp. 145-151.

Kvasov, D.D., Davydova, N.N., and Rumyantsev, V.A. (eds.), 1986: General relationship of lake genesis and evolution – methods for lake history studies (Obshchie zakonomernosti voznikoveniya i razvitiya ozer – metody izucheniya istorii ozer). Nauka, Leningrad: 146 – 151. (in Russian).

Laing, T.E., Rühland, K.M., and Smol, J.P., 1999: Past environmental and climatic changes related to tree-line shifts inferred from fossil diatoms from a lake near the Lena River Delta, Siberia. The Holocene 9 (5): 547-557.

Lauriol, B., Duchesne, C., and Clark, I.D., 1995: Systématique du Remplissage en Eau des Fentes de Gel: les Résultats d'une Étude Oxygène-18 et Deutérium. Permafrost and Periglacial Processes 6: 47-55.

Lüniger, G. and Schwark, L., 2002: Characterisation of sedimentary organic matter by bulk and molecular geochemical proxies: and example from Oligocene maar-type Lake Enspel, Germany. Sedimentary Geology 148: 275-288.

Mackay, J.R., 1983: Oxygen isotope variations in permafrost, Tuktoyaktuk Peninsula area, Northwest Territories. Current Research, Part B, Geological Survey of Canada, Paper 83-1B, pp. 67-74.

Mackay, J.R., 1990: Some observations on the growth and deformation of epigenetic, syngenetic and anti-syngenetic ice wedges. Permafrost and Periglacial Processes 1: 15-29.

Mackay, A.W., Ryves, D.B., Battarbee, R.W., Flower, R.J., Jewson, D., Rioual, P., and Sturm, M., 2005: 1000 years of climate variability in central Asia: assessing the evidence using Lake Baikal (Russia) diatom assemblages and the application of a diatom-inferred model of snow cover on the lake. Global and Planetary Change 46 (1-4): 281-297.

Magny, M., Leuzinger, U., Bortenschlager, S., and Haas, J.N., 2006: Tripartite climate reversal in central Europe 5600-5300 years ago. Quaternary Research 65: 3-19.

Mange, M.A. and Maurer, H.F.W., 1991: *Schwerminerale in Farbe*. Enke, Stuttgart, 148 pp. (in German).

Mangerud, J., Astakhov, V.I., Murray, A., and Svendsen, J.I., 2001: The chronology of a large ice-dammed lake and the Barents-Kara Ice Sheet advances, Northern Russia. Global and Planetary Change 31: 321-336.

Mangerud, J., Astakhov, V.I., and Svendsen, J.I., 2002: The extent of the Barents-Kara ice sheet during the Last Glacial Maximum. Quaternary Science Reviews 21: 111-119.

Mangerud, J., Jakobsson, M., Alexanderson, H., Astakhov, V., Clarke, G.K.C., Henriksen, M., Hjort, C., Krinner, G., Lunkka, J.P., Möller, P., Murray, A., Nikolskaya, O., Saarnisto, M., and Svendsen, J.I., 2004: Ice-dammend lakes, rerouting of the drainage of Northern Eurasia during the last deglaciation. Quaternary Science Reviews 23: 1313-1332.

Markov, K.K., 1973: Sequences of Late Cenozoic deposits "Mamontova Gora". Moscow University Press, Moscow, 198 pp. (in Russian).

Mayewski, P.A., Rohling, E.E., Stager, J.C., Karlén, W., Maasch, K.A., Meeker, L.D., Meyerson, E.A., Gasse, F., van Kreveld, S., Holmgren, K., Lee-Thorp, J., Rosqvist, G., Rack, F., Staubwasser, M., Schneider, R.R., and Steig, E.J., 2004: Holocene climate variability. Quaternary Research 62: 243-255.

McCabe, G.J., Clark, M.P., and Serreze, M.C., 2001: Trends in northern hemisphere surface cyclone frequency and intensity. Journal of Climate 14 (12): 2763-2768.

McDermott, F., Mattey, D.P., and Hawkesworth, C., 2001: Centennial-scale Holocene climate variability revealed by a high-resolution speleothem $\delta^{18}O$ record from SW Ireland. Science 294: 1328-1331.

Merlivat, L. and Jouzel, J., 1979: Global climatic interpretation of the deuterium-oxygen 18 relationship for precipitation. Journal of Geophysical Research 84 (C8): 5029-5033.

Meyer, H., Schönicke, L., Wand, U., Hubberten, H.-W., and Friedrichsen, H., 2000: Isotope studies of hydrogen and oxygen in ground ice–experiences with the equilibration technique. Isotopes in Environmental and Health Studies 36: 133-149.

Meyer, H., Dereviagin, A.Yu., Siegert, C., and Hubberten, H.-W., 2002a: Paleoclimate studies on Bykovsky Peninsula, North Siberia–Hydrogen and oxygen isotopes in ground ice. Polarforschung 70: 37-51.

Meyer, H., Dereviagin, A.Yu., Siegert, C., Schirrmeister, L., and Hubberten, H.-W., 2002b: Paleoclimate reconstruction on Big Lyakhovsky Island, North Siberia–Hydrogen and oxygen isotopes in ice wedges. Permafrost and Periglacial Processes 13: 91-105.

Meyers, P.A. and Lallier-Vergès, E., 1999: Lacustrine sedimentary organic matter records of Late Quaternary paleoclimates. Journal of Paleolimnology 21: 345-372.

Meyers, P.A. and Teranes, J.L., 2001: Sediment organic matter. *In:* Last, W.M. and Smol, J.P. (eds.), *Tracking environmental change using lake sediments*, Volume 2: Physical and geochemical methods: Kluwer Academic Publishers, Dordrecht, pp. 239-269.

Michel, F.A., 1982: Isotope investigation of permafrost waters in northern Canada. Ph.D. thesis. Department of Earth Scienes, University of Waterloo, Canada, 227 pp.

Moritz, R.E., Bitz, C.M., and Steig, E.J., 2002: Dynamics of recent climate change in the Arctic. Science 297: 1497-1502.

Müller, S., Andreev, A., Zech, W., and Diekmann, B., 2004: Late Pleistocene and Holocene environmental changes in the Verkhoyansk Mountains – a pollen based reconstruction. Geophysikal Research Abstracts, Vol. 6, EGU04-A-00427, EGU 1st General Assembly, 25-30 April 2004, Nice, France.

Murton, J.B. and French, H.M., 1994: Cryostructures in permafrost, Tuktoyaktuk coastlands, western arctic Canada. Canadian Journal of Earth Sciences 31: 737-747.

Muschler, R., Beer, J., Wagner, G., and Finkel, R.C., 2000: Changes in deep-water formation during the Younger Dryas event inferred from ^{10}Be and ^{14}C records. Nature 408: 567-570.

Naidina, O.D. and Bauch, H.A., 2001: A Holocene pollen record from the Laptev Sea shelf, northern Yakutia. Global and Planetary Change 31: 141-153.

Naurzbaev, M.M. and Vaganov, E.A., 2000: Variation of early summer and annual temperature in east Taymir and Putoran (Siberia) over the last two millennia inferred from tree rings. Journal of Geophysical Research 105 (D6): 7317-7326.

Neff, U., Burns, S.J., Mangini, A., Mudelsee, M., Fleitmann, D, and Matter, A., 2001: Strong coherence between solar variability and the monsoon in Oman between 9 and 6 kyr ago: Nature 411: 290-293.

Nemichov, A.G., 1958: About cyclic variations in lake-water levels of lakes in Central Yakutia: Scientific disclosures of the Yakutian branch office of the Academy of Sciences of the SSSR 1, pp. 30-37 (in Russian).

O'Brien, S.R., Mayewski, P.A., Meeker, L.D., Meese, D.A., Twickler, M.S., and Whitlow, S.I., 1995: Complexity of Holocene climate as reconstructed from a Greenland ice core: Science 270: 1962-1964.

Overpeck, J., Hughen, K., Hardy, D., Bradley, R., Case, R., Douglas, M., Finney, B., Gajewski, K., Jacoby, G., Jennings, A., Lamoureux, S., Lasca, A., MacDonald, G., Moore, J., Retelle, M., Smith, S., Wolfe, A., and Zielinski, G., 1997: Arctic environmental change of the last four centuries. Science 278: 1251-1256.

Oxman, V. S., 2003: Tectonic evolution of the Mesozoic Verkhoyansk-Kolyma belt (NE Asia). Tectonophysics 365: 45-76.

Paillard, D., Labeyrie, L., and Yiou, P., 1996: Macintosh program performs time-series analysis. Eos Trans. AGU 77 (39): 379.

Parfenov, L.M., 1991: Tectonics of the Verkhoyansk-Kolyma Mesozoides in the context of plate tectonics. Tectonophysics 199: 319-342.

Parfenov, L.M., 1997: Geological structure and geological history of Yakutia. *In:* Parfenov, L.M. and Spector, V.B. (eds.), *Geological monuments of the Sakha Republic (Yakutia)*, Novosibirsk, pp. 61-77.

Pavlov, A.V., 1994: Current changes of climate and permafrost in the Arctic and Sub-Arctic of Russia. Permafrost and Periglacial Processes 5: 101-110.

Pavlov, A.V. and Ananjeva, G.V., 2004: Assesment of the contemporary air temperature change over the permafrost territory of Russia. Earth Cryoshere 8 (2): 3-9 (in Russian with English abstract).

Peregovich, B., Hoops, E., and Rachold, V., 1999: Sediment transport to the Laptev Sea (Siberian Arctic) during the Holocene – evidence from the heavy mineral composition of fluvial and marine sediments. Boreas 28: 205-214.

Peterson, B.J., Holmes, R.M., McClelland, J.W., Vörösmarty, C.J., Lammers, R.B., Shiklomanov, A.I., Shiklomanov, I.A., and Rahmstorf, S., 2002: Increasing river discharge to the Arctic Ocean. Science 298: 2171-2173.

Petschick, R., Kuhn, G., and Gingele, F., 1996: Clay mineral distribution in surface sediments of the South Atlantic: sources, transport, and relation to oceanography. Marine Geology 130: 203-229.

Péwé, T.L., Journaux, A., and Stuckenrath, R., 1977: Radiocarbon dates and Late-Quaternary stratigraphy from Mamontova Gora, unglaciated Central Yakutia, Siberia, U.S.S.R. Quaternary Research 8: 51-63.

Péwé, T.L. and Journaux, A., 1983: Origin and character of loess-like silt in unglaciated south-central Yakutia, Siberia, U.S.S.R., Geological Survey Professional Paper 1262, Washington, DC, 46 pp.

Popp, S., Diekmann, B., Meyer, H., Siegert, C., Syromyatnikov, I., Hubberten, H.-W., 2006: Palaeoclimate signals as inferred from stable-isotope composition of ground ice in the Verkhoyansk foreland, Central Yakutia. Permafrost and Periglacial Processes 17: 119-132.

Prokopiev, V.S., Ursov, A.S., and Kamaletdinov, V.A., 1994: *Official Geological Map of the Russian Federation, map sheet Q-51-V, G (sheet no. 46) on a scale of 1:500 000*; VSEGEI, St. Petersburg.

Raspopov, O.M., Dergachev, V.A., and Kolström, T., 2004: Periodicity of climate conditions and solar variability derived from dendrochonological and other palaeoclimatic data in high latitudes: Palaeogeography, Palaeoclimatology, Palaeoecology 209: 127-139.

Rind, D., 2002: The sun's role in climate variations. Science 296: 673-677.

Romanovskii, N.N., 1985: Distribution of recently active ice and soil wedges in the USSR. Field and theory. *In:* Church, M. and Slaymaker, O. (eds.), Univ. B.C. Press, Vancuver, BC, Canada, pp. 154-165.

Romanovskii, N.N., 1993: Principles of cryogenesis of the lithozone. Moscow University Press, Moscow, 344 pp. (in Russian).

Rusanov, B.S., Borodenkova, Z.F., Goncharov, V.F., Grinenko, O.V., and Lazarev, P.A., 1967: The geomorphologic region 'Western Verkhoyansk', pp. 56-122 (in Russian).

Schirrmeister, L., Siegert, C., Kuznetsova, T., Kuzmina, S., Andreev, A., Kienast, F., Meyer, H., and Bobrov, A., 2002: Paleoenvironmental and paleoclimatic records from permafrost deposits in the Artic region of Northern Siberia. Quaternary International 89: 97-118.

Schmidt, G.A., Shindell, D.T., Miller, R.L., Mann, M.E., and Rind, D., 2004: General circulation modelling of Holocene climate variability. Quaternary Science Reviews 23: 2167-2181.

Schwamborn, G., Rachold, V., and Grigoriev, M.N., 2002: Late Quaternary sedimentation history of the Lena Delta. Quaternary International 89: 119-134.

Sedenko, S.V., Sedenko, E.G., and Vasil'ev, S.P., 2001: Schematic geological map of the Sakha Republic (Yakutia). *In:* Parfenov, L.M. and Kuzmin, M.I. (eds.), *Tectonics, Geodynamics and Metallogeny of the Sakha Republic (Yakutia)*. Maik Nauka/ Interperiodica, Moscow, 571 pp. (in Russian).

Serreze, M.C., Walsh, J.E., Chapin III, F.S., Osterkamp, T., Dyurgerov, M., Romanovsky, V. Oechel, W.C., Morison, J., Zhang, T., and Barry, R.G., 2000: Observational Evidence of Recent Change in the Northern High-Latitude Environment. Climatic Change 46 (1-2): 159-207.

Sher, A.V., Kuzmina, S.A., Kuznetsova, T.V., and Sulerzhitsky, L.D., 2005: New insights into the Weichselian environment and climate of the East Siberian Arctic, derived from fossil insects, plants and mammals. Quaternary Science Reviews 24: 533-569.

Shindell, D.T., Schmidt, G.A., Mann, M.E., Rind, D., and Waple, A., 2001: Solar forcing of regional climate change during the Maunder Minimum. Science 294: 2149-2152.

Siegert, C., Derevyagin, A.Y., Shilova, G.N., Hermichen, W.-D., and Hiller, A., 1999: Paleoclimatic indicators from permafrost sequences in the eastern Taymyr lowland. *In:* Kassens, H., H.A. Bauch, I. Dmitrenko, H. Eicken, H.-W. Hubberten, M. Melles, J. Thiede and L. Timokhov (eds.), *Land-Ocean Systems in the Siberian Arctic: Dynamics and History*. Springer-Verlag, Berlin, pp. 477-499.

Siegert, C., Schirrmeister, L., and Babiy, O., 2002: The sedimentological, mineralogical and geochemical composition of Late Pleistocene deposits from the Ice Complex on the Bykovsky Peninsula, northern Siberia. Polarforschung 70: 3-11.

Smith, L.C., Sheng, Y., MacDonald, G.M., and Hinzman, L.D., 2005: Disappearing Arctic lakes. Sciences 308: 1429.

Solanki, S.K., Usoskin, I.G., Kromer, B., Schüssler, M., and Beer, J., 2004: Unusual activity of the sun during recent decades compared to the previous 11,000 years. Nature 431: 1084-1087.

Soloviev, P.A., 1959: Cryolithozone of the northern part of the interfluve between the Lena and Amga. Akad. Nauk SSSR, Moscow, 144 pp. (in Russian).

Soloviev, P.A., 1973a: Guidebook: Alass thermokarst relief of Central Yakutia. Second International Conference on Permafrost, Yakutsk 1973. USSR Academy of Sciences, Section of Earth's Sciences, Siberian Division, Yakutsk, 48 pp.

Soloviev, P.A., 1973b: Thermokarst phenomena and landforms due to frost heaving in Central Yakutia. Biuletyn Peryglacjalny 23: 135-155.

Spielhagen, R.F., Erlenkeuser, H., and Siegert, C., 2005: History of freshwater runoff across the Laptev Sea (Arctic) during the last deglaciation. Global and Planetary Change 48: 187-207.

Stauch, G., Lehmkuhl, F., and Frechen, M., 2005: Pleistocene glacial advances in the Verkhoyansk Mountains, North-Eastern Siberia. Geophysical Research Abstracts, Vol. 7, EGU05-A-09061, EGU General Assembly, 24-29 April 2005, Vienna.

Stauch, G., Lehmkuhl, F., and Frechen, M., in press: Luminescence chronology from the Verkhoyansk Mountains, northeastern Siberia. Quaternary Geochronology.

Steig, E.J., 1999: Mid-Holocene climate change. Science 286: 1485-1487.

Stein, R., Dittmers, K., Fahl, K., Kraus, M., Matthiessen, J., Niessen, F., Pirrung, M., Polyakova, Ye., Schoster, F., Steinke, T., and Fütterer, D.K., 2004: Arctic (palaeo) river discharge and environmental change: evidence from the Holocene Kara Sea sedimentary record. Quaternary Science Reviews 23: 1485-1511.

Still, C.J., Berry, J.A., Collatz, G.J., and DeFries, R.S., 2003: Global distribution of C_3 and C_4 vegetation: Carbon cycle implications. Global Biogeochemical Cycles 17 (1): 1006.

Street-Perrott, F.A., Ficken, K.J., Huang, Y., and Eglinton, G., 2004: Late Quaternary changes in carbon cycling on Mt. Kenya, East Africa: and overview of the $\delta^{13}C$ record in lacustrine organic matter. Quaternary Science Reviews 23: 861-879.

Stuiver, M., 1975: Climate versus changes in ^{13}C content of the organic component of lake sediments during the late Quaternary. Quaternary Research 5: 251-262.

Stuiver, M. and Braziunas, T.F., 1993: Sun, ocean, climate and atmospheric $^{14}CO_2$: an evaluation of causal and spectral relationships. The Holocene 3 (4): 289-305.

Stuiver, M., Grootes, P.M., and Braziunas, T.F., 1995: The GISP $\delta^{18}O$ climate record of the past 16,500 years and the role of the sun, ocean, and volcanoes. Quaternary Research 44: 341-354.

Stuiver, M., Reimer, P.J., Bard, E., Beck, J.W., Burr, G.S., Hughen, K.A., Kromer, B., McCormac, G., van der Plicht, J., and Spurk, M., 1998: INTCAL98 radiocarbon age calibration 24,000-0 cal. BP. Radiocarbon 40: 1041-1083.

Svendsen, J.I., Alexanderson, H., Astakhov, V.I., Demidov, I., Dowdeswell, J.A., Funder, S., Gataullin, V., Henriksen, M., Hjort, C., Houmark-Nielsen, M., Hubberten, H.-W., Ingólfsson, Ó., Jakobssen, M., Kjær, K.H., Larsen, E., Lokrantz, H., Lunkka, J.P., Lysså, A., Mangerud, J., Matiouchkov, A., Murray, A., Möller, P., Niessen, F., Nikolskaya, O., Polyak, L., Saarnisto, M., Siegert, C., Siegert, M.J., Spielhagen, R.F., and Stein, R., 2004: Late Quaternary ice sheet history of northern Eurasia. Quaternary Science Reviews 23: 1229-1271.

Swan, A.R.H. and Sandilands, M., 1995: *Introduction to geological data analysis*. Blackwell, Oxford, 446 pp.

Talbot, M.R. and Livingstone, D.A., 1989: Hydrogen index and carbon isotopes of lacustrine organic matter as lake level indicators. Palaeogeography, Palaeoclimatology, Palaeoecology 70: 121-137.

Taylor, S., Feng, X., Kirchner, J.W., Osterhuber, R., Klaue, B., and Renshaw, C.E., 2001: Isotopic evolution of a seasonal snowpack and its melt. Water Resources Research 37 (3): 759-769.

Teranes, J.L. and Bernasconi, S.M., 2005: Factors controlling $\delta^{13}C$ values of sedimentary carbon in hypertrophic Baldeggersee, Switzerland, and implications for interpreting isotope excursions in lake sedimentary records. Limnology and Oceanography 50 (3): 914-922.

Vaikmäe, R., 1989: Oxygen isotopes in permafrost and ground ice–a new tool for paleoclimatic investigations. *In*: 5th Working Meeting Isotopes in Nature, Proceedings. Leipzig, Germany, pp. 543-553.

Vasil'chuk, Yu.K., 1991: Reconstruction of the paleoclimate of the late Pleistocene and Holocene on the basis of isotope studies of subsurface ice and waters of the permafrost zone. Water Ressource (Vodnye Resursy) 17 (6): 640-674.

Vasil'chuk, Yu.K., 1992: Oxygen isotope composition of ground ice. Application to paleogeocryological reconstructions. Vol. 1, Moscow, 420 pp. (in Russian).

Velichko, A.A. and Nechaev, V.P. (eds.), 2005: *Cenozoic climatic and environmental changes in Russia*. Geological Society of America, Special Paper 382, 226 pp.

Velichko, A.A., Catto, N., Drenova, A.N., Klimanov, V.A., Kremenetski, K.V, and Nechaev, V.P., 2002: Climate changes in East Europe and Siberia at the Late glacial–holocene transition. Quaternary International 91: 75-99.

Waters, M.R., Forman, S.L., and Pierson, J.M., 1997: Diring Yuriakh: A lower Paleolithic site in central Siberia. Science 275: 1281-1284.

Werner, K., Andreev, A., Diekmann, B., and Zech, W., 2005: Holocene vegetation history of the Verkhoyansk Mountains foreland, North-Eastern Siberia. 22. Internationale Polartagung, 18-24 September 2005, Jena, Germany, Terra Nostra, pp. 146-147.

Wilkes, H., Ramrath, A., and Negendank, J.F.W., 1999: Organic geochemical evidence for environmental changes since 34,000 yrs BP from Lago di Mezzano, central Italy. Journal of Paleolimnology 22: 349-365.

Wolfe, B.B., Edwards, T.W.D., Aravena, R., Forman, S.L., Warner, B.G., Velichko, A.A., and MacDonald, G.M., 2000: Holocene paleohydrology and paleoclimate at treeline, north-central Russia, inferred from oxygen isotope records in lake sediment cellulose. Quaternary Research 53: 319-329.

Yu, Y., Yang, T., Li, J., Liu, J., An, C., Liu, X., Fan, Z., Lu, Z., Li, Y., and Su, X., 2006: Millennial-scale Holocene climate variability in the NW China drylands and links to the tropical Pacific and the North Atlantic. Palaeogeography Palaeoclimatology Palaeoecology 233: 149-162.

Zamoruyev, V., 2004: Quaternary glaciation of north-east Asia. *In:* Ehlers, J. and Gibbard, P.L. (eds.), *Quaternary glaciations – extent and chronology, part III*. Elsevier, Amsterdam, pp. 321-323.